UNIVERSIDAD COMPLUTENSE DE MADRID

FACULTAD DE CIENCIAS FÍSICAS
Departamento de Física Atómica, Molecular y Nuclear

RATCHETS BROWNIANAS RETROALIMENTADAS E INFORMACIÓN.

MEMORIA PARA OPTAR AL GRADO DE DOCTOR

PRESENTADA POR

Manuel Feito Guzmán

Bajo la dirección del doctor

F. J. Cao

Madrid, 2010

- **ISBN: 978-84-693-3178-1**

Universidad Complutense de Madrid
Facultad de Ciencias Físicas
Departamento de Física Atómica, Molecular y Nuclear

Ratchets brownianas retroalimentadas e información

Manuel Feito Guzmán

Memoria de Tesis Doctoral para optar al grado de
Doctor en Física

Director de tesis: Dr. F. J. Cao

Madrid, 6 de julio de 2009

A CARMEN Y MIGUEL

Agradecimientos

En primer lugar, quiero dar las gracias a mi director de tesis, Francisco Cao, por su guía en todo momento y por sacar siempre tiempo para mí. A lo largo de estos años de investigación he conocido, a través de otros doctorandos, a buenos, notables o excelentes directores de tesis, pero puedo asegurar que en ningún caso mejores que Fran.

Me gustaría agradecer a Hugo Touchette (Queen Mary, University of London) y a José Pablo Baltanás (Universidad de Sevilla) su colaboración y el fructífero intercambio científico mantenido. También quiero dar las gracias a Martin Bier (East Carolina University) por la lectura y discusión de uno de los últimos trabajos.

Deseo señalar el mágnifico trato que he recibido en el Departamento de Física Atómica, Molecular y Nuclear. Especialmente estoy en deuda con Carlos Armenta y José Luis Contreras por su buena predisposición que ha convertido mi trabajo en el Departamento en un verdadero placer.

Abro aquí un bloque de agradecimientos personales dedicado a toda la gente que he tenido cerca durante estos años, con la que he compartido muchos buenos momentos y a la que he procurado no cansar demasiado con asuntos relacionados con esta tesis. Mi familia me ha apoyado en todo momento en este proyecto; las conversaciones telefónicas con Maita de los lunes —que luego nunca eran lunes— son un buen ejemplo. Muchas gracias también a Férez, José María, Jose..., y, cómo no, a Germán, que me ha soportado dentro y fuera de la Facultad (si bien debo decir que yo también he tenido que aguantarlo a él día tras día...)

En este último año en el que he intercalado la investigación con la docencia en el IES Beniaján he aprendido también mucho tanto de mis compañeros como sobre todo de mis alumnos que no se cansan de mostrame cada día lo complejo en lo falsamente sencillo y lo sencillo en lo absurdamente complejo.

Los agradecimientos más especiales son, sin duda, para Maki, por tantas cosas compartidas entre Murcia, Madrid, Albacete y Sevilla (y Barcelona, París, Estambul...)

Me gustaría por último mostrar mi gratitud a todos los profesores que he tenido en la última decada. Ellos son los que, aun a veces sin quererlo, me han abierto las infinitas ventanas de la Física, cuyo paisaje único, también infinito, contemplo siempre maravillado con una mezcla de placer y terror. Para estos profesores es la frase "sin ellos no hubiera sido posible esta tesis."

Publicaciones

- F. J. Cao and M. Feito, *Out of equilibrium quantum field dynamics of an initial thermal state after a change in the external field*, Phys. Rev. D **73**, 045017 (2006).
- M. Feito and F. J. Cao, *Threshold feedback control for a collective flashing ratchet: Threshold dependence*, Phys. Rev. E **74**, 041109 (2006). Véase el capítulo 5.
- M. Feito and F. J. Cao, *Information and maximum power in a feedback controlled Brownian ratchet*, Eur. Phys. J. B **59**, 63 (2007). Véase el capítulo 10.
- M. Feito and F. J. Cao, *Time-Delayed Feedback control of a flashing ratchet*, Phys. Rev. E **76**, 061113 (2007). Véase el capítulo 6.
- M. Feito and F. J. Cao, *Transport reversal in a delayed feedback ratchet*, Physica A **387**, 4553 (2008). Véase el capítulo 7.
- M. Feito and F. J. Cao, *Optimal operation of feedback flashing ratchets*, J. Stat. Mech. P01031 (2009).
- F. J. Cao, M. Feito, and H. Touchette, *Information and flux in a feedback controlled Brownian ratchet*, Physica A **388**, 113 (2009). Véase el capítulo 9.
- F. J. Cao and M. Feito, *Thermodynamics of feedback controlled systems*, Phys. Rev. E **79**, 041118 (2009). Véase el capítulo 11.
- M. Feito, J. P. Baltanás, and F. J. Cao, *Rocking feedback ratchets*, arXiv:0902.3941. Véase el capítulo 8.

Resumen

Las ratchets o motores brownianos pueden verse como controladores que actúan sobre sistemas estocásticos con el objetivo de inducir movimiento neto a través de la rectificación de las fluctuaciones. En la presente tesis investigamos ratchets de ciclo cerrado o retroalimentadas, que son aquellas ratchets cuyo mecanismo de rectificación depende explícitamente del estado del sistema. Hemos analizado la dinámica y el rendimiento de ratchets con control retroalimentado centrándonos en lo que las caracteriza, a saber, el uso de la información sobre el estado del sistema. Hemos mostrado que este uso de la información permite a las ratchets de ciclo cerrado incrementar el rendimiento sobre sus análogas de ciclo abierto. Además, la investigación sobre los efectos del retardo temporal en la retroalimentación nos revela una dinámica rica que exhibe multiestabilidad e inversiones de corriente. Estos estudios que hemos hecho sobre los efectos del retardo temporal junto con los efectos de ruidos en el control retroalimentado nos muestran la viabilidad de realizaciones experimentales de las ratchets retroalimentadas. También hemos encontrado que la combinación de una fuerza oscilante de media cero con el mecanismo de control conduce al máximo flujo que se ha obtenido en una ratchet sin un sesgo a priori. Por otra parte, en esta tesis hemos completado la termodinámica de sistemas generales con control retroalimentado calculando la reducción de entropía cuando el sistema es operado repetidamente por el controlador. Este era el ingrediente que faltaba para establecer la termodinámica de los sitemas con control retroalimentado, y en particular de los demonios de Maxwell. Finalmente, presentamos algunas cuestiones todavía abiertas y futuras perspectivas en el emergente campo de las ratchets retroalimentadas.

Índice general

Parte I

Introducción, estado actual del tema y objetivos

La presente Parte I de la tesis contiene los capítulos introductorios que proporcionan el material necesario para la siguiente Parte II dedicada a los resultados novedosos. En el capítulo 1 discutimos los principales hitos históricos sobre el movimiento browniano y el efecto ratchet. El siguiente capítulo 2 estudia los procesos estocásticos en general, mientras que el capítulo 3 trata de los aspectos básicos de la teoría de la información. Con estos capítulos introductorios en mente comentaremos en el capítulo 4 la situación actual de las ratchets y en particular de las ratchets con control retroalimentado y su relación con el demonio de Maxwell. El capítulo 4 concluye con los objetivos de la tesis, lo que cierra la primera parte.

Capítulo 1

Introducción histórica

En este primer capítulo se resumen los aspectos fundamentales relativos al movimiento browniano y al efecto ratchet. Presentamos una aproximación histórica, enfatizando los trabajos pioneros de Einstein, Langevin, Feynman, y Astumian y Bier entre otros.

1.1 El movimiento browniano

El movimiento browniano toma su nombre del botánico Robert Brown [1], quien en 1827 observó el movimiento desordenado e irregular de granos de polen suspendidos en agua. En realidad este tipo de movimiento ya había sido observado antes pero fue Brown el primero en resaltar su ubicuidad y excluir una explicación vital del mismo tras comprobar que se producía en cualquier suspensión de partículas pequeñas. Diversas explicaciones del movimiento browniano tras la exclusión de las fuerzas vitales hacían referencia a la capilaridad, corrientes de convección, evaporación, interacción con la luz o fuerzas eléctricas. Hasta la aparición de uno de los famosos artículos de Einstein [2,3] en su *annus mirabilis* de 1905 no hubo una teoría satisfactoria del movimiento browniano. Smoluchowsky [4] publicó independientemente un trabajo similar poco después en el que se daba una explicación parecida a la de Einstein. En una serie de experimentos, cuyos primeros resultados fueron publicados en 1908, J. Perrin [5] confirmó con bastante precisión casi todas las predicciones de Einstein. Perrin aplicó los métodos propuestos en el artículo de 1905 para determinar el número de Avogadro. Quedaba así confirmada la naturaleza atómica de la materia. En la década de los veinte N. Wiener abordó la teoría del movimiento browniano desde un punto de vista matemático.

Tres puntos fundamentales aparecen en la explicación de Einstein del movimiento browniano [3, 6]:

- El movimiento de los granos de polen es causado por los incesantes choques de las moléculas de agua sobre él.
- El movimiento de estas moléculas es tan complicado que su efecto sobre los granos de polen debe describirse probabilísticamente en términos de impactos independientes.
- La magnitud observable adecuada es el desplazamiento cuadrático medio de las partículas suspendidas y no la velocidad como se había estudiado sin éxito hasta entonces.

El artículo de Einstein comienza con una deducción del coeficiente de difusión D en función del radio de las partículas suspendidas, de la temperatura y de la viscosidad, que se conoce como relación de Einstein,

$$D = \frac{k_B T}{\gamma}, \tag{1.1}$$

con $\gamma = 6\pi\eta a$, donde η es la viscosidad y a el radio de las partículas de acuerdo a la ley de Stokes. La deducción de la ecuación de difusión se basa en la introducción de una distribución de probabilidad para los desplazamientos. Einstein considera intervalos de tiempo pequeños comparados con los intervalos temporales típicos de observación pero suficientemente grandes para que en dos de estos intervalos sucesivos los movimientos realizados por las partículas pueden considerarse como eventos independientes.

A partir de la dependencia temporal de la distribución de partículas, calculada a través de la distribución de probabilidad para los desplazamientos, Einstein llega a la ecuación de difusión para la densidad de partículas,

$$\frac{\partial \rho}{\partial t} = D\frac{\partial^2 \rho}{\partial x^2}. \tag{1.2}$$

Considerando que hay N partículas situadas en el origen en $t = 0$, la densidad de probabilidad en un tiempo posterior es

$$\rho(x,t) = \frac{N}{\sqrt{4\pi D}}\frac{e^{-x^2/4Dt}}{\sqrt{t}}. \tag{1.3}$$

Finalmente, con esta ecuación se obtiene el desplazamiento cuadrático medio en la dirección X

$$\left\langle x^2(t)\right\rangle - \left\langle x^2(0)\right\rangle = 2Dt. \tag{1.4}$$

El desplazamiento medio es, pues, proporcional a la raíz cuadrada del tiempo, tal y como concluye Einstein en su artículo.

Algún tiempo después, Langevin [7] llegó a los mismos resultados que Einstein (y Smoluchowski) pero usando un tratamiento totalmente distinto. La partícula browniana esférica (el grano de polen) que se mueve en el fluido experimentará una fuerza viscosa proporcional a la velocidad de la forma $-\gamma\frac{dx}{dt}$, donde $\gamma = 6\pi\eta a$. Por otra parte el mecanismo de las colisiones de la partícula browniana se tiene en cuenta a través de una cantidad $\xi(t)$ que oscila muy rápidamente y de forma aleatoria en la escala de tiempos de la dinámica de la partícula browniana. La ecuación que plantea Langevin para la partícula browniana de masa m es

$$m\frac{d^2x}{dt^2} = -\gamma\frac{dx}{dt} + \xi(t). \tag{1.5}$$

Este es el primer ejemplo de ecuación diferencial estocástica. El término de ruido $\xi(t)$ plantea ciertos problemas matemáticos relativos a como interpretar correctamente esta ecuación. Fue Itô [8] quien, en 1951, consiguió dar sentido a la ecuación de Langevin introduciendo formalmente las ecuaciones diferenciales estocásticas. Pero continuemos con algunos puntos clave siguiendo el método original presentado por Langevin. Él multiplica la ecuación (1.5) por x y obtiene así una ecuación para la magnitud relevante x^2.

Con ecuación calcula el promedio (a las realizaciones) de x^2 considerando[1] que $\langle x\xi \rangle = 0$ y haciendo uso del teorema de equipartición. De esta forma Langevin llega al mismo resultado de Einstein para el desplazamiento cuadrático medio. Al asumir que $\langle x\xi \rangle = 0$, Langevin en realidad está haciendo una suposición directamente relacionada con la suposición de Einstein de considerar la independencia de las partículas. Nótese que de nuevo entran en juego los tiempos característicos. De hecho, por simetría ocurrirá que $\langle \xi(t) \rangle = 0$ y además el promedio $\langle \xi(t_1)\xi(t_2) \rangle$ será cero si la diferencia de tiempos $|t_2 - t_1|$ es mucho mayor que el tiempo característico entre colisiones. Este tiempo entre colisiones es mucho menor que el tiempo característico de la dinámica de la partícula browniana porque la masa del grano de polen (partícula browniana) es mucho mayor que la masa de la molécula de agua. Así pues, puede considerarse que $\langle \xi(t_1)\xi(t_2) \rangle$ es proporcional a una función delta de Dirac,

$$\langle \xi(t_1)\xi(t_2) \rangle = \sigma^2 \delta(t_2 - t_1), \tag{1.6}$$

donde la intensidad del ruido, σ, se escribe en términos de constantes físicas como

$$\sigma^2 = 2\gamma k_B T. \tag{1.7}$$

La última ecuación se deduce comparando la velocidad cuadrática media de la partícula browniana con el resultado del teorema de equipartición [9, 10].

Actualmente, un campo de investigación muy activo en relación al movimiento browniano es el estudio de su rectificación a través del llamado efecto racthet.

1.2 Efecto ratchet

En 1912 Smoluchowski [11] ideó un *Gedankenexperiment* en el que mediante un sistema periódico y espacialmente asimétrico (una rueda dentada y trinquete, *ratchet and pawl*) en contacto con un baño térmico era capaz, a primera vista, de rectificar las fluctuaciones térmicas y realizar trabajo. El dispositivo consiste en un eje con unas palas en uno de sus extremos y una rueda dentada con un trinquete en el otro extremo. En el centro del eje hay una rueda de la que cuelga un peso (véase la figura 1.1). Feynman hace un análisis de este efecto en sus *Lectures* [12] (véase también [13]) considerando que la rueda dentada y las palas están inmersas en dos baños térmicos de diferentes temperaturas. Debido a los impactos aleatorios de las moléculas de gas sobre las palas el dispositivo realiza un movimiento browniano rotatorio, que sería rectificado gracias a la presencia del trinquete. Feynman muestra que la diferencia de temperatura es un ingrediente necesario para realmente conseguir rectificación y levantar así el peso.

[1] Esta consideración lleva implícita una interpretación de la ecuación diferencial para x^2 a la manera de Itô, como se verá más adelante (ver sección 2.5.4).

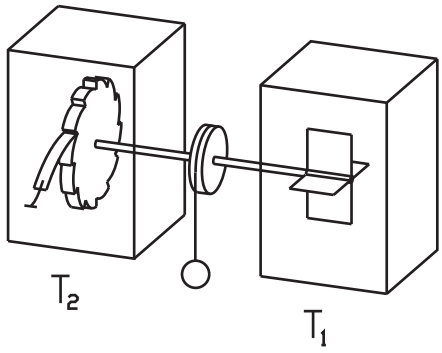

Figura 1.1: Dispositivo ratchet de Feynman. (De Ref. [17]).

Estas reconocidas ideas de rectificar el ruido térmico se usaron de manera explícita en el contexto de transporte dirigido en la década de los 90 por Magnasco [14], Ajdari y Prost [15], y Astumian y Bier [16], entre otros muchos. Precisamente el efecto ratchet consiste en la aparición de un transporte dirigido en un sistema espacialmente asimétrico fuera del equilibrio a través de la introducción de una perturbación externa. Generalmente esto se consigue con un potencial periódico asimétrico (potencial ratchet). El flujo neto puede persistir incluso en presencia de una pequeña fuerza externa opuesta a la corriente, con lo que el sistema realiza trabajo contra esa fuerza. Por esta razón estos sistemas se conocen también como motores brownianos. Véanse [17, 18] para una revisión sobre ratchets o motores brownianos.

Por consiguiente, las ratchets pueden verse como controladores que actúan sobre sistemas estocásticos con el objetivo de inducir un transporte dirigido gracias a la rectificación de las fluctuaciones térmicas. En particular, las flashing ratchets son rectificadores de fluctuaciones térmicas basados en el encendido y apagado de un potencial periódico asimétrico [15, 16].

Podemos explicar el funcionamiento de una flashing ratchet con la ayuda de la figura 1.2. Supongamos que el potencial permanece encendido durante un cierto tiempo, con lo que la densidad de probabilidad de la partícula se concentra en torno a un mínimo del potencial, como ilustramos en la parte superior de la figura 1.2. Después, el potencial se apaga y la partícula comienza un proceso de difusión isotrópica durante el tiempo en que el potencial permanece apagado (gráfica media de la figura 1.2); tras un cierto tiempo encendemos el potencial de nuevo. Si la partícula se encuentra entre los máximos adyacentes al mínimo inicial cuando el potencial se enciende de nuevo entonces la partícula browniana probablemente volverá al mínimo inicial. Si por el contrario la partícula se encontraba más a la derecha que la posición del máximo de la derecha entonces la partícula irá probablemente al mínimo de la derecha, mientras que si se encontraba a la izquierda del

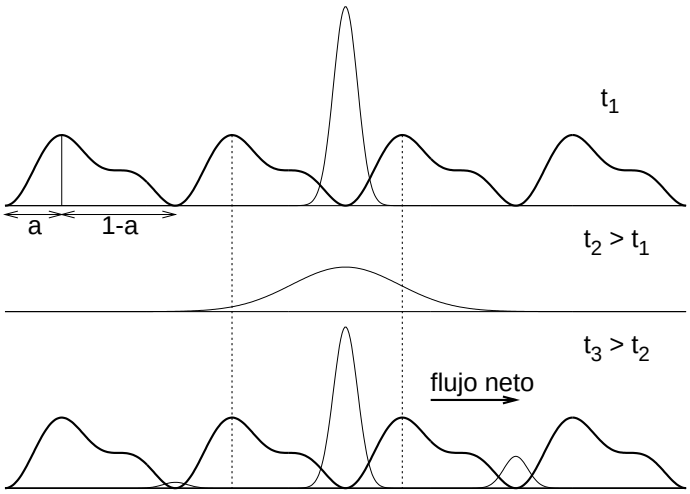

Figura 1.2: Representación esquemática del efecto ratchet en una flashing ratchet. El potencial ratchet pintado tiene periodo 1 y asimetría $a = 1/3$. Las líneas más finas representan la densidad de probabilidad.

máximo de la izquierda probablemente irá al mínimo de la izquierda. La asimetría del potencial ratchet hace que la probabilidad de acabar a la derecha sea mayor que la probabilidad de acabar a la izquierda y consiguientemente aparece un flujo neto no nulo hacia la derecha (gráficas central e inferior de la figura 1.2).

Bibliografía

[1] R. Brown, Philosophical Magazine N.S. **4**, 161 (1828).

[2] A. Einstein, Ann. Phys. **17**, 549 (1905).

[3] J. Stachel (ed), *Einstein 1905: un año maravilloso* (Drakontos, 2001).

[4] M. von Smoluchowski, Ann. Phys. **21**, 756 (1906).

[5] J. Perrin, Ann. Chim. Phys. VIII **18**, 5 (1909).

[6] C. W. Gardiner, *Handbook of stochastic methods* (Springer-Verlag, 1985).

[7] P. Langevin, C. R. Acad. Sci. Paris **146**, 530 (1908).

[8] K. Itô, Mem. Amer. Math. Soc. **4**, 1 (1951).

[9] R. K. Pathria, *Statistical Mechanics, 2nd ed.* (Butterworth-Heinemann, 1996).

[10] H. Risken, *The Fokker-Planck Equation* (Springer-Verlag, 1989).

[11] M. von Smoluchowski, Physik. Z. **13**, 1068 (1912).

[12] R. P Feynman, R. B Leighton, and M. Sands, *The Feynman Lectures on Physics* (Addison-Wesley, Reading, MA, 1963).

[13] J. M. R. Parrondo and P. Español, Am. J. Phys. **64**, 1125 (1996).

[14] M. O. Magnasco, Phys. Rev. Lett. **71**, 1477 (1993).

[15] A. Ajdari and J. Prost, C. R. Acad. Sci. Paris II **315**, 1635 (1993).

[16] R. D. Astumian and M. Bier, Phys. Rev. Lett. **72**, 1766 (1994).

[17] P. Reimann, Phys. Rep. **361**, 57 (2002).

[18] P. Hänggi and F. Marchesoni, Rev. Mod. Phys. **81**, 387 (2009).

Capítulo 2

Procesos estocásticos

Este capítulo aporta las herramientas básicas necesarias para la correcta comprensión de los capítulos siguientes. Se estudian los procesos estocásticos desde un pisto de vista general. Tras algunas definiciones formales introductorias (sección 2.1), describimos el proceso de Wiener y su relación con el ruido blanco (sección 2.2). En las secciones 2.3 y 2.4 se analiza la integración estocástica y se describen y comparan las definiciones de Itô y de Stratonovich. Las integrales estocásticas se usan para dar sentido a las ecuaciones diferenciales estocásticas como por ejemplo la ecuación de Langevin en la sección 2.5. Finalmente, se presenta en la sección 2.6 la llamada ecuación de Fokker-Planck (una ecuación diferencial determinista para la distribución de probabilidad de un proceso estocástico) como un método eficaz que nos permite obtener propiedades relevantes de los procesos estocásticos.

2.1 Definiciones formales

Consideremos un espacio muestral Ω y una colección de eventos o sucesos $\mathcal{A}$ que constituyan una σ-álgebra[1] con una cierta probabilidad $P : \mathcal{A} \to [0, 1]$ de ocurrir (vid. Refs. [1, 2]).

Una variable aleatoria es el resultado de un experimento aleatorio, lo que podemos expresar matemáticamente diciendo que, dado un espacio de probabilidad $(\Omega, \mathcal{A}, P)$, una función $X : \Omega \to \mathbb{R}$ es una *variable aleatoria* si

$$\{\omega \in \Omega : X(\omega) \leq a\} \in \mathcal{A} \text{ para cada } a \in \mathbb{R}. \tag{2.1}$$

La función de probabilidad del conjunto anterior es la función distribución de la variable X,

$$F(x) \equiv P(\{\omega \in \Omega : X(\omega) \leq x\}) = P(X \leq x). \tag{2.2}$$

Si existe una función integrable $\rho(x)$ tal que

$$F(x) = \int_{-\infty}^{x} \rho(x')\, dx', \tag{2.3}$$

entonces se dice que $\rho(x)$ es la densidad de probabilidad asociada a la distribución de X.

Un proceso estocástico $X = \{X(t), t \in T\}$ es una función de dos variables $X : T \times \Omega \to \mathbb{R}$ donde $X(t) = X(t, \cdot)$ es una variable aleatoria para cada $t \in T$. Para cada $\omega \in \Omega$ decimos que $X(\cdot, \omega) : T \to \mathbb{R}$ es una *realización* o una *trayectoria* del proceso estocástico. En otras palabras, un proceso estocástico $X = \{X(t), t \in T\}$ es una colección de variables aleatorias en un espacio de probabilidad $(\Omega, \mathcal{A}, P)$ indexado por un parámetro $t \in T \subset \mathbb{R}$, que podemos interpretar como el tiempo. Es frecuente la notación $X_t \equiv X(t)$. Aquí trataremos procesos estocásticos continuos (tanto X_t como su argumento t son continuos).

[1] Es decir, $\mathcal{A}$ es una familia no vacía de subconjuntos de Ω que contiene al propio Ω y es cerrada bajo complementación y unión numerable.

2.2 Proceso de Wiener

Decimos que una variable aleatoria X es una variable aleatoria gaussiana de media μ y varianza σ^2 si su función densidad de probabilidad viene dada por

$$\rho(x) = \frac{1}{\sqrt{2\pi}\sigma} \exp\left(\frac{-(x-\mu)^2}{2\sigma^2}\right). \tag{2.4}$$

Se suele representar abreviadamente mediante la notación $X \sim \mathcal{N}(\mu, \sigma^2)$.

Un proceso de Wiener $W = \{W(t), t \geq 0\}$ es un proceso estocástico que verifica

1. $W(0) = 0$ con probabilidad 1.
2. $W(t) - W(s) \sim \mathcal{N}\left(0, \sigma^2(t-s)\right)$ para todo $t \geq s \geq 0$.
3. $W(t_{j+1}) - W(t_j)$ con $j = 0, 1, \ldots, n-1$ son independientes para cualquier combinación finita de instantes de tiempo $t_0 < t_1 < \cdots < t_n$ de T.

De esta definición se tiene en particular que $\langle W(t) \rangle = 0$ y $\langle W(t)^2 \rangle = \sigma^2 t$ para todo $t \geq 0$.

2.2.1 Propiedades

- $W(t+\tau) - W(t)$ es independiente de $W(t)$ para todo $\tau > 0$. Esta afirmación se sigue directamente de la definición de proceso de Wiener.
- $\langle W(t)W(s) \rangle = \sigma^2 \,\text{mín}(t, s)$. La demostración es la siguiente. Tomemos $t \geq s \geq 0$, entonces

$$\begin{aligned} \langle W(t)W(s) \rangle &= \langle [W(s) + W(t) - W(s)]W(s) \rangle \\ &= \langle W(s)^2 \rangle + \langle [W(t) - W(s)]W(s) \rangle \\ &= \sigma^2 s + \langle W(t) - W(s) \rangle \langle W(s) \rangle \\ &= \sigma^2 s + 0 \cdot 0 = \sigma^2 \,\text{mín}(t, s). \end{aligned} \tag{2.5}$$

- Para casi todo ω, la trayectoria $t \mapsto W(t, \omega)$ no es diferenciable en ningún punto (no es diferenciable salvo en conjuntos de medida nula) y es de variación infinita en cada subintervalo. La demostración es complicada (Dvoretzky, Erdös y Kakutani) [3].

2.2.2 Ruido blanco y proceso de Wiener

El ruido de la ecuación (1.5) tiene las características razonables de que su media es cero y además sus valores estás descorrelacionados para cualesquiera instantes de tiempo por muy próximos que estén (obviamente esto es una

idealización matemática, justificada por la diferencia de orden de magnitud de las dos escalas de tiempo ya comentadas). Esto nos lleva a definir el ruido blanco gaussiano como un proceso gaussiano $\xi(t)$ estacionario[2] de media cero y correlación proporcional a una delta de Dirac,

$$\langle \xi(t) \rangle = 0, \qquad \langle \xi(t)\xi(s) \rangle = \sigma^2 \delta(t-s). \tag{2.6}$$

Entonces, la varianza de este ruido blanco es independiente del tiempo y puede ser interpretada como una intensidad media y escribirse como

$$\left\langle \xi(t)^2 \right\rangle = \int_{-\infty}^{+\infty} S(\nu) d\nu, \tag{2.7}$$

donde $S(\nu)$ es la densidad espectral, que mide la intensidad media por unidad de frecuencia a frecuencia ν. Por el teorema de Wiener-Khintchine [6, 9] la densidad espectral puede encontrarse a partir de la transformada de Fourier de la correlación,

$$S(\nu) = \int_{-\infty}^{+\infty} \langle \xi(t+\tau)\xi(t) \rangle \, e^{-2\pi i \nu \tau} d\tau, \tag{2.8}$$

y de acuerdo a (2.6)

$$S(\nu) = \sigma^2, \tag{2.9}$$

es decir, la densidad espectral es plana (constante) como ocurre con la luz blanca, que contiene todas las frecuencias del visible uniformemente distribuidas. Esta es la razón por la que se habla de ruido blanco. Como ya se comentó en la sección 1, físicamente la intensidad del ruido σ se relaciona con la temperatura a través de

$$\sigma^2 = 2\gamma^2 D = 2\gamma k_B T. \tag{2.10}$$

En contraposición se habla de ruido de color cuando la densidad espectral es dependiente de la frecuencia, lo que equivale a considerar correlaciones no nulas entre tiempos distintos.

Notemos que en la definición de ruido blanco aparece una delta de Dirac. Esto hace que el ruido blanco no sea en realidad un proceso estocástico y debe pensarse en él como en un proceso estocástico generalizado [2], de la misma forma que la delta de Dirac es una función generalizada. En cualquier caso, el ruido blanco no existe tampoco físicamente, aunque puede aproximarse tanto como se quiera mediante un proceso estocástico bien definido con densidad espectral suficientemente ancha. En este sentido generalizado

[2]Decimos que un proceso estocástico $X(t)$ con $\langle X^2(t) \rangle < \infty \; \forall t \geq 0$ es estacionario (en sentido amplio) si su función de autocorrelación, $C(t,s) \equiv \langle X(t)X(s) \rangle$ con $t, s \geq 0$ sólo depende de la diferencia de tiempos [la llamamos entonces $C(t-s)$] y además $\langle X(t) \rangle = \langle X(s) \rangle$ para todo $t, s \geq 0$.

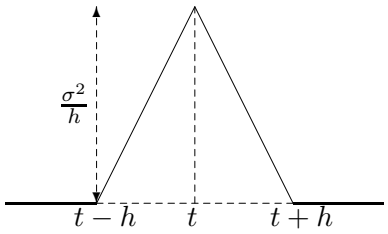

Figura 2.1: Gráfica de $\phi_h(s)$ [ecuación (2.15).]

puede interpretarse formalmente el ruido blanco como la derivada del proceso de Wiener (que como ya comentamos no es realmente diferenciable),

$$\dot{W}(t) \equiv \xi(t), \tag{2.11}$$

o alternativamente,

$$W(t) = \int_0^t \xi(s)ds. \tag{2.12}$$

Esta derivada formal tiene sentido por lo siguiente. Por una parte, de las propiedades del proceso de Wiener es inmediato que

$$\lim_{h\to 0} \left\langle \frac{W(t+h) - W(t)}{h} \right\rangle = 0. \tag{2.13}$$

Por otra parte, consideremos las funciones $\phi_h(s)$ dadas por [3]

$$\phi_h(s) \equiv \left\langle \left(\frac{W(t+h) - W(t)}{h} \right) \left(\frac{W(s+h) - W(s)}{h} \right) \right\rangle, \tag{2.14}$$

con $t > 0$ fijo y distinto de s y $h > 0$. Usando de nuevo las propiedades del proceso de Wiener resulta

$$\phi_h(s) = \frac{\sigma^2}{h^2} \left[\text{mín}(t+h, s+h) - \text{mín}(t+h, s) - \text{mín}(t, s+h) + \text{mín}(t, s) \right]. \tag{2.15}$$

Esta función está representada en la figura 2.1. Vemos que

$$\lim_{h\to 0} \phi_h(s) = 0, \tag{2.16}$$

mientras que

$$\lim_{h\to 0} \int \phi_h(s)ds = \sigma^2. \tag{2.17}$$

Por tanto podemos decir que $\phi_h(s) \to \sigma^2\delta(s-t)$ cuando $h \to 0$. La interpretación del ruido blanco como la derivada del proceso de Wienner queda ahora justificada a la vista de las ecuaciones (2.6), (2.13), (2.16), y (2.17).

2.3 Integración estocástica

2.3.1 La integral de Itô $\int_{t_0}^{t} G(t')dW(t')$

Sea $G(t)$ una función arbitraria del tiempo[3] y sea $W(t)$ el proceso de Wiener. Consideremos la partición del intervalo $[t_0, t]$

$$t_0 < t_1 < \cdots < t_n = t \tag{2.18}$$

y unos puntos intermedios τ_i tales que $t_{i-1} \leq \tau_i \leq t_i$. Podemos construir las sumas parciales

$$S_n = \sum_{i=1}^{n} G(\tau_i) \left[W(t_i) - W(t_{i-1})\right] \tag{2.19}$$

y dar una definición general de *integral estocástica* como el límite de estas sumas parciales (refinamiento de la partición) de manera análoga a la definición de integral de Riemman-Stieljes. Ahora bien, dadas las características del proceso de Wiener (no es de variación acotada, por ejemplo), el resultado dependerá de los puntos intermedios τ_i. Una posible elección que elimina esta arbitrariedad es tomar

$$\tau_i = t_{i-1} \qquad \text{(prescripción de Itô)}. \tag{2.20}$$

Así, definimos la *integral estocástica de Itô* como

$$\int_{t_0}^{t} G(t')dW(t') = \underset{n\to\infty}{\text{ms-lim}} \sum_{i=1}^{n} G(t_{i-1}) \left[W(t_i) - W(t_{i-1})\right], \tag{2.21}$$

donde ms-lim es el límite en media cuadrática.[4]

La integral de Itô $\int_{t_0}^{t} G(t')dW(t')$ existe siempre que la función $G(t)$ sea continua y no anticipativa[5] en el intervalo $[t_0, t]$ (vid. [2, 4]).

2.3.2 La integral de Stratonovich $\mathcal{S}\int_{t_0}^{t} G(X(t'), t')dW(t')$

Definimos la *integral estocástica de Stratonovich* como

$$\mathcal{S}\int_{t_0}^{t} G(X(t'), t')dW(t') = \underset{n\to\infty}{\text{ms-lim}} \left\{ \sum_{i=1}^{n} G\left(\frac{X(t_i) + X(t_{i-1})}{2}, t_{i-1}\right) \left[W(t_i) - W(t_{i-1})\right] \right\}, \tag{2.22}$$

[3] En particular $G(t)$ puede depender de un proceso estocástico $X(t)$. Cuando sea conveniente especificar esta dependencia hablaremos explícitamente de $G(X(t), t)$.

[4] Dada una secuencia de variables aleatorias X_n sobre un espacio muestral Ω decimos que $\underset{n\to\infty}{\text{ms-lim}}\, X_n = X$ si $\lim_{n\to\infty} \langle (X_n - X)^2 \rangle = 0$.

[5] Decimos que $G(t)$ es una función no anticipativa de t si para todos s y t tales que $t < s$, $G(t)$ es estadísticamente independiente de $W(s) - W(t)$. Es decir, $G(t)$ es independiente del comportamiento del proceso de Wiener en el futuro de t.

Es también frecuente la notación $\int_{t_0}^{t} G(t') \circ dW(t') \equiv \mathcal{S} \int_{t_0}^{t} G(t') dW(t')$.

Una definición más naïve común en la literatura es la correspondiente a calcular las sumas parciales mediante la evaluación de la función $G(X(t), t)$ en los puntos $\tau_i = \frac{t_{i-1}+t_i}{2}$. Aunque puede dar los mismos resultados que la definición de Stratonovich para ciertos integrandos, no se puede probar la convergencia de esta última definición en general [4].

2.3.3 Un ejemplo: $\int_{t_0}^{t} W(t')dW(t')$ (Itô y Stratonovich)

Este ejemplo puede calcularse exactamente [4] y es bastante clarificador para entender las definiciones de integral de Itô y Stratonovich. Muestra también el uso de las propiedades del proceso de Wiener. Para una mayor claridad usaremos la notación abreviada $W_i \equiv W(t_i)$.

Calculamos en primer lugar el valor de la integral de Itô. Comencemos calculando las sumas parciales (2.19) que aparecen en (2.21),

$$\begin{aligned} S_n =& \sum_{i=1}^{n} W_{i-1}(W_i - W_{i-1}) \equiv \sum_{i=1}^{n} W_{i-1}\Delta W_i \\ =& \frac{1}{2}\sum_{i=1}^{n}[(W_{i-1} + \Delta W_i)^2 - (W_{i-1})^2 - (\Delta W_i)^2] \\ =& \frac{1}{2}[W(t)^2 - W(t_0)^2] - \frac{1}{2}\sum_{i=1}^{n}(\Delta W_i)^2, \end{aligned} \tag{2.23}$$

donde se ha realizado la suma telescópica. Basta calcular el límite en media cuadrática del término $\sum_{i=1}^{n}(\Delta W_i)^2$. Nótese que

$$\left\langle \sum_i (\Delta W_i)^2 \right\rangle = \sum_i \left\langle (W_i - W_{i-1})^2 \right\rangle = \sum_i \sigma^2(t_i - t_{i-1}) = \sigma^2(t - t_0), \tag{2.24}$$

de acuerdo a la definición del proceso de Wiener. Vamos a ver que además $\underset{n\to\infty}{\text{ms-lim}} \sum_i (\Delta W_i)^2 = \sigma^2(t - t_0)$.

$$\begin{aligned} &\left\langle \left[\sum_i (W_i - W_{i-1})^2 - \sigma^2(t - t_0) \right]^2 \right\rangle \\ &\quad = \left\langle \sum_i (W_i - W_{i-1})^4 + 2\sum_{i>j} (W_i - W_{i-1})^2 (W_j - W_{j-1})^2 \right. \\ &\qquad \left. - 2\sigma^2(t - t_0)\sum_i (W_i - W_{i-1})^2 + \sigma^4(t - t_0)^2 \right\rangle. \end{aligned} \tag{2.25}$$

Por otra parte, $W_i - W_{i-1}$ es independiente de $W_j - W_{j-1}$ y entonces

$$\left\langle (W_i - W_{i-1})^2 (W_j - W_{j-1})^2 \right\rangle = \left\langle (W_i - W_{i-1})^2 \right\rangle \left\langle (W_j - W_{j-1})^2 \right\rangle, \tag{2.26}$$

y por ser $W_i - W_{i-1}$ una variable gaussiana,

$$\left\langle (W_i - W_{i-1})^4 \right\rangle = 3 \left\langle (W_i - W_{i-1})^2 \right\rangle^2 . \tag{2.27}$$

Como además para el proceso de Wiener sabemos que $\left\langle (W_i - W_{i-1})^2 \right\rangle = \sigma^2(t_i - t_{i-1})$, nos queda para la ec. (2.25)

$$\begin{aligned}
&\left\langle \left[\sum_i (W_i - W_{i-1})^2 - \sigma^2(t - t_0) \right]^2 \right\rangle \\
&= 2\sigma^4 \sum_i [(t_i - t_{i-1})]^2 + \sigma^4 \sum_{i,j} \left[(t_i - t_{i-1}) - (t - t_0) \right] \left[(t_j - t_{j-1}) - (t - t_0) \right] \\
&= 2\sigma^4 \sum_i (t_i - t_{i-1})^2 .
\end{aligned} \tag{2.28}$$

Como el refinamiento de una partición P_n hace decrecer la norma de la partición (la longitud del mayor de sus intervalos: $|P_n| = \text{máx}_{1 \le i \le n} |t_i - t_{i-1}|$) entonces la expresión anterior tiende a cero cuando $n \to \infty$,

$$\begin{aligned}
\left\langle \left[\sum_i (W_i - W_{i-1})^2 - \sigma^2(t - t_0) \right]^2 \right\rangle &= 2\sigma^4 \sum_i (t_i - t_{i-1})^2 \\
&\le 2\sigma^4 |P_n| \sum_i (t_i - t_{i-1}) = 2\sigma^4 |P_n| (t - t_0) \to 0.
\end{aligned} \tag{2.29}$$

Por tanto, $\underset{n\to\infty}{\text{ms-lim}} \sum_i (\Delta W_i)^2 = \sigma^2(t - t_0)$ y finalmente

$$\int_{t_0}^{t} W(t') dW(t') = \frac{1}{2} \left[W(t)^2 - W(t_0)^2 - \sigma^2(t - t_0) \right] . \tag{2.30}$$

Nótese que este resultado difiere del cálculo ordinario de Riemann-Stieljes, en el que no estaría presente el último término. La razón es que los incrementos del proceso de Wiener son de orden $\sqrt{t}$ y por consiguiente los términos de segundo orden en $\Delta W(t)$ no se anulan al tomar el límite.

Por otra parte, siguiendo el cálculo de Stratonovich sí que recuperamos el resultado que se obtiene integrando formalmente como si se tratara de una integral de Riemman-Stieljes ya que las sumas parciales a evaluar en la definición de Stratonovich son

$$\sum_i \frac{W_i + W_{i-1}}{2} (W_i - W_{i-1}) = \frac{1}{2} \sum_i (W_i^2 - W_{i-1}^2) = \frac{1}{2} [W(t)^2 - W(t_0)^2], \tag{2.31}$$

donde de nuevo ha aparecido una suma telescópica.

Por lo tanto, las definiciones de Itô y Stratonovich para la integral estocástica llevan a resultados distintos [véanse las ecuaciones (2.30) y (2.31)].

2.4 Reglas del cálculo de Itô

Usando razonamientos similares a los usados en la Sec. 2.3.3 puede verse que

$$\begin{aligned}\int_{t_0}^{t} G(t')[dW(t')]^{2+N} &\equiv \underset{n\to\infty}{\text{ms-lim}} \sum_i G_{i-1}\Delta W_i^{2+N} \\ &= \begin{cases} \int_{t_0}^{t} G(t')\sigma^2 dt' & \text{si } N=0, \\ 0 & \text{si } N>0 \end{cases}\end{aligned} \tag{2.32}$$

y que

$$\int_{t_0}^{t} G(t')dt'dW(t') \equiv \underset{n\to\infty}{\text{ms-lim}} \sum_i G_{i-1}\Delta W_i \Delta t_i = 0. \tag{2.33}$$

Con este sentido preciso podemos escribir formalmente

$$(dt)^{1+N} \to 0 \text{ (con } N>0) \tag{2.34}$$

$$dtdW(t) \to 0 \tag{2.35}$$

$$[dW(t)]^2 \to \sigma^2 dt \tag{2.36}$$

$$[dW(t)]^{2+N} \to 0 \text{ (con } N>0) \tag{2.37}$$

La idea que subyace es que $dW(t)$ es un infinitésimo de orden $1/2$ y en cálculos diferenciales los infinitésimos de orden uno o menor hay que tenerlos en cuenta mientras que los de orden superior se desprecian.

2.5 Ecuaciones diferenciales estocásticas

Un proceso estocástico $X(t)$ satisface la ecuación diferencial estocástica de Itô (SDE)

$$dX(t) = a(X(t),t)dt + b(X(t),t)dW(t) \tag{2.38}$$

si para todo t y t_0 se satisface

$$X(t) = X(t_0) + \int_{t_0}^{t} a(X(t'),t')dt' + \int_{t_0}^{t} b(X(t'),t')dW(t') \tag{2.39}$$

Análogamente, si la integral estocástica se interpreta como de Stratonovich hablaremos de ecuación diferencial estocástica de Stratonovich.

2.5.1 Existencia y unicidad

Las condiciones suficientes para la existencia de una solución única no anticipativa $X(t)$ en un intervalo cerrado $[t_0, T]$ a la SDE son

i) Condición de Lipschitz: Existe K tal que

$$|a(x,t) - a(y,t)| + |b(x,t) - b(y,t)| \leq K|x - y| \tag{2.40}$$

para todo x e y y para todo $t \in [t_0, T]$

ii) Condición de crecimiento: Existe K tal que

$$|a(x,t)|^2 + |b(x,t)|^2 \leq K^2(1 + |x|^2) \tag{2.41}$$

para todo x y para todo $t \in [t_0, T]$.

La condición de Lipschitz es esencialmente una condición de suavidad y prácticamente todas las SDE de interés la satisfacen. La segunda condición evita que la solución explote a infinito bajo condiciones iniciales concretas, análogamente a lo que ocurre para ecuaciones diferenciales ordinarias [4].

2.5.2 Fórmula de Itô

Sea $X(t)$ solución de la SDE

$$dX(t) = a(X(t), t)dt + b(X(t), t)dW(t). \tag{2.42}$$

Sea $Y(t) = u(X(t), t)$, con u continua y con derivadas $\frac{\partial u}{\partial t}$, $\frac{\partial u}{\partial x}$ y $\frac{\partial^2 u}{\partial x^2}$ continuas. Entonces, $Y(t)$ es solución de

$$dY(t) = \left\{ \frac{\partial u}{\partial t} + a\frac{\partial u}{\partial x} + \frac{\sigma^2}{2} b^2 \frac{\partial^2 u}{\partial x^2} \right\} dt + b\frac{\partial u}{\partial x} dW(t). \tag{2.43}$$

Los argumentos de u, $\frac{\partial u}{\partial t}$, etc. son $(X(t), t)$. A este importante resultado se le conoce como fórmula de Itô o regla de la cadena de Itô [4].

Nótese que la fórmula de Itô difiere en la regla de la cadena del cálculo ordinario (Stratonovich) en el término proporcional a σ^2.

La comprobación de la fórmula de Itô se sigue fácilmente expandiendo $Y(t)$ hasta segundo orden en $dW(t)$ de acuerdo a las reglas vistas en 2.4:

$$dY = \frac{\partial u}{\partial t} dt + \frac{\partial u}{\partial x} dX + \frac{1}{2} \frac{\partial^2 u}{\partial x^2} (dX)^2. \tag{2.44}$$

Si ahora sustituimos dX por su expresión (2.42) y usamos que de acuerdo a lo visto en 2.4 se tiene $(adt + bdW)^2 = a^2(dt)^2 + b^2(dW)^2 + 2abdtdW = \sigma^2 b^2 dt$ obtenemos la regla de la cadena de Itô. La fórmula de Itô puede generalizarse para SDE en varias dimensiones [1] usando en ese caso $dW_i(t)dW_j(t) = \sigma_i^2 \delta_{ij} dt$.

La fórmula de Itô puede utilizarse inteligentemente para resolver SDE's. Por ejemplo, nos permite demostrar fácilmente que

$$Y(t) = e^{W(t) - \sigma^2 t/2} \tag{2.45}$$

es la solución de la SDE

$$dY = YdW \tag{2.46}$$

con la condición inicial $Y(0) = 1$. Para ello basta considerar un proceso estocástico $X(t)$ que satisfaga la SDE correspondiente a tomar en (2.42) los coeficientes constantes $a(X(t), t) = -\frac{\sigma^2}{2}$ y $b(X(t), t) = 1$, esto es,

$$dX = -\frac{\sigma^2}{2}dt + dW, \tag{2.47}$$

y tomar como condición inicial $X(0) = 0$. La ecuación (2.43) con $u(x, t) = e^x$ nos da precisamente la ecuación (2.46):

$$dY = \left[-\frac{\sigma^2}{2}e^{X(t)} + \frac{\sigma^2}{2}e^{X(t)}\right]dt + e^{X(t)}dW(t) = YdW(t). \tag{2.48}$$

Así pues, $Y(t) = e^{X(t)}$. Por otra parte, la ecuación (2.47) es directamente integrable dando

$$X(t) = -\frac{\sigma^2}{2}t + W(t). \tag{2.49}$$

En conclusión,

$$Y(t) = e^{X(t)} = e^{W(t)-\sigma^2 t/2}. \tag{2.50}$$

2.5.3 Relación Itô-Stratonovich

La relación Itô-Stratonovich afirma lo siguiente. Si $X(t)$ es un proceso estocástico que verifica la SDE (de Itô)

$$dX(t) = a(X(t), t)dt + b(X(t), t)dW(t), \tag{2.51}$$

entonces $X(t)$ verifica la SDE (de Stratonovich)

$$dX = \left\{a - \frac{1}{2}\sigma^2 b\frac{\partial b}{\partial x}\right\}dt + b \circ dW, \tag{2.52}$$

donde la dependencia de a, b y $\frac{\partial b}{\partial x}$ en $(X(t), t)$ está implícita. La demostración de este importante resultado se basa en la igualdad

$$\int_{t_0}^{t} f[X(t'), t'] \circ dW(t') = \int_{t_0}^{t} f(X(t'), t')dW(t') + \frac{\sigma^2}{2}\int_{t_0}^{t} b(X(t'), t')\partial_x f(X(t'), t')dt', \tag{2.53}$$

que se puede obtener a partir de las definiciones de integrales de Itô y Stratonovich junto con la aplicación de la fórmula de Itô (2.43). Es importante resaltar que la ec. (2.53) no da una relación general entre las integrales de Itô

y de Stratonovich para funciones arbitrarias, sino que sólo es válida cuando $X(t)$ es solución de la ec. (2.51).

Nótese que la equivalencia de las ecs. (2.51) y (2.52) implica en particular que las SDE de Itô y Stratonovich coinciden si la función $b(X_t, t)$ es independiente de X_t, es decir, para ruidos aditivos.

Usando la relación Itô-Stratonovich y la regla de la cadena de Itô es fácil obtener la regla de la cadena de Stratonovich, que coincide con el resultado del cálculo ordinario [4].

2.5.4 Dilema Itô-Stratonovich

Dada una SDE en el sentido de Itô podemos convertirla en una SDE de Stratonovich y viceversa, tal y como hemos visto en la sección anterior. Ahora bien, la pregunta clave es cuál de las dos interpretaciones es la más útil. La ventaja de la interpretación de Stratonovich es que conserva las reglas básicas del cálculo ordinario como la regla de la cadena. Esto hace que los cálculos se simplifiquen en algunos casos. Por ejemplo, la SDE de Itô

$$dX(t) = \sigma^2 dt + 2\sqrt{X(t)}dW(t) \tag{2.54}$$

Se expresa en el sentido de Stratonovich de la forma simple

$$dX(t) = 2\sqrt{X(t)} \circ dW(t), \tag{2.55}$$

o bien, usando la regla de la cadena ordinaria

$$d(\sqrt{X(t)}) = \circ dW(t). \tag{2.56}$$

La resolución, dada una condición inicial $X(0) = X_0 > 0$, aparece ahora inmediatamente: $X(t) = (\sqrt{X_0} + W(t))^2$.

Por tanto, para realizar ciertos cálculos la interpretación de Stratonovich puede ser más útil. Sin embargo, desde un punto de vista fundamental la interpretación de Itô tiene mejores propiedades matemáticas (la integral de Itô es una martingala [5]), lo que facilita enormemente la demostración rigurosa de propiedades matemáticas. Por ejemplo, sólo en la integral de Itô tenemos fórmulas simples del tipo $\langle \int_0^t G dW \rangle = 0$ para funciones G no anticipativas. Estas integrales contienen sumas parciales de términos del tipo $G_{i-1}\Delta W_i$. Para integrales de Itô, G_{i-1} está evaluada en t_{i-1} y por tanto el intervalo del proceso de Wiener es independiente de G_{i-1}, mientras que en Stratonovich G_{i-1} se evalúa también en el tiempo t_i, lo que ya no garantiza la independencia con ΔW_i aunque G sea no anticipativa.

En cualquier caso lo dicho hasta el momento no plantea ningún dilema real sobre qué interpretación debe usarse, puesto que existe una equivalencia matemática entre ambos tipos de SDE. El verdadero problema surge un paso antes, cuando se trata de modelizar un fenómeno físico con ruido mediante una ecuación diferencial estocástica. Ecuaciones tipo Langevin con ruido no

aditivo (ruido multiplicativo) surgen naturalmente como modelizaciones de procesos físicos [4,6,7]. Estas ecuaciones no están bien definidas hasta que no se interpretan como SDE de Itô o de Stratonovich. Una u otra interpretación llevan a soluciones distintas de las magnitudes físicas del problema. Ese es el dilema real.

Finalmente, comentamos algunos aspectos relacionados con la interpretación física correcta de una SDE, aunque esto no soluciona totalmente el dilema. Si se aproxima el ruido blanco por un proceso suave con correlación no nula a tiempos finitos y diferenciable a trozos, de manera que las ecuaciones diferenciales que aparecen son ecuaciones diferenciales ordinarias (ODE) de las que obtenemos soluciones regularizadas sobre esa partición en la que el ruido es suave y luego tomamos el límite sobre las soluciones de las ODE's haciendo tender a cero la escala de descorrelación del ruido y refinando la partición, se obtiene la solución de Stratonovich [1, 2]. Sin embargo, si el límite de ruido blanco se toma en la propia ODE se obtiene una SDE de Itô.

2.5.5 Ecuación de Langevin

La velocidad de una partícula browniana de masa unidad moviéndose en un modelo unidimensional[6] es un proceso estocástico, digamos $Y(t)$, que satisface la ecuación de Langevin (véase Sec. 1.1)

$$\dot{Y}(t) = -\gamma Y(t) + \xi(t), \tag{2.57}$$

donde $-\gamma Y(t)$ da cuenta de la fuerza viscosa y $\xi(t)$ es un ruido blanco gaussiano relacionado con las fluctuaciones térmicas. De acuerdo a lo visto en 2.2.2 podemos interpretar el ruido blanco como la derivada del proceso de Wiener y entonces debe entenderse la ecuación de Langevin como la SDE siguiente

$$\begin{cases} dY = -\gamma Y dt + dW \\ Y(0) = Y_0, \end{cases} \tag{2.58}$$

con Y_0 la velocidad inicial.

La posición de la partícula browniana es un proceso estocástico $X(t)$ tal que $Y(t) = \dot{X}(t)$. En el régimen sobreamortiguado la ecuación (2.57) se lee $\gamma Y(t) = \xi(t)$, con lo que la posición está gobernada por $\gamma \dot{X}(t) = \xi(t)$. Si se añade una fuerza externa $F(X(t))$ entonces la ecuación que describe el movimiento de la partícula browniana sobreamortiguada es

$$\gamma \dot{X}(t) = F(X(t)) + \xi(t), \tag{2.59}$$

que se conoce como ecuación de Langevin sobreamortiguada. (En ocasiones las SDE's de esta forma se llaman simplemente ecuaciones de Langevin).

[6] La generalización a varias dimensiones puede verse en [8].

2.5.6 Simulaciones numéricas: el algoritmo de Euler

La aproximación de Euler (o de Euler-Maruyama) [1] da una aproximación discreta del proceso estocástico. Proporciona un método numérico estable con una convergencia adecuada [1] para simular procesos estocásticos en un ordenador.

El proceso estocástico $X = \{X(t),\ t_0 \leq t \leq T\}$ que satisface la SDE

$$dX(t) = a(X(t), t)dt + b(X(t), t)dW(t) \tag{2.60}$$

puede aproximarse por el proceso estocástico $Y(t) = \{Y(t),\ t_0 \leq t \leq T\}$ que satisface el esquema de iteración

$$Y_{n+1} = Y_n + a(Y_n, t_n)(t_{n+1} - t_n) + b(Y_n, t_n)(W_{n+1} - W_n), \tag{2.61}$$

donde el subíndice n indica que el proceso se evalúa en los instantes discretos t_n, con $t_0 < t_1 < \cdots < t_n < \cdots < t_N = T$. Consideraremos instantes de tiempos discretos equiespaciados, i.e.,

$$t_n = t_0 + n\Delta; \quad \Delta = \frac{T - t_0}{N}. \tag{2.62}$$

Los incrementos del proceso de Wiener, $W_{n+1} - W_n$, son variables aleatorias gaussianas independientes de media cero, $\langle W_{n+1} - W_n \rangle = 0$, y varianza $\left\langle (W_{n+1} - W_n)^2 \right\rangle = \sigma^2(t_{n+1} - t_n) = \sigma^2\Delta$; véase Sec. 2.2. Por lo tanto, el esquema de Euler puede implementarse en un ordenador como

$$Y_{n+1} = Y_n + a(Y_n, t_n)\Delta + b(Y_n, t_n)\sigma\sqrt{\Delta}\ z_n, \tag{2.63}$$

donde z_n son números (pseudo)aleatorios independientes distribuidos gaussianamente tales que $\langle z_n \rangle = 0$ y $\langle z_n z_m \rangle = \delta_{nm}$.

2.6 La ecuación de Fokker-Planck

2.6.1 Formalismo general

La ecuación de Fokker-Planck (FPE) es una ecuación diferencial en derivadas parciales para la evolución temporal de la densidad de probabilidad de un proceso estocástico. El nombre de Fokker-Planck viene de los trabajos de Fokker [9] y más tarde de Planck [10], aunque también es común referirse a esta ecuación como ecuación de Smoluchowski o como ecuación de Kolmogorov hacia delante. A continuación derivamos la FPE para una SDE de la forma general (2.38).

Sea $X(t)$ un proceso estocástico que satisface la SDE de Itô (2.38) y que tiene una densidad de probabilidad

$$\rho(x, t) \equiv \rho_{X_t}(x). \tag{2.64}$$

Estudiemos la evolución temporal de una función analítica del tiempo de la forma $Y(t) = u[X(t)]$. Promediando sobre la fórmula de Itô (2.43) tenemos

$$\left\langle \frac{dY}{dt} \right\rangle = \left\langle au' + \frac{\sigma^2}{2} b^2 u'' \right\rangle, \tag{2.65}$$

donde se ha usado que el proceso de Wiener es independiente de $X(t)$ y por tanto de cualquier función analítica de $X(t)$. Nótese que este punto sólo es válido en la interpretación de Itô. Si ahora expresamos los promedios usando la densidad de probabilidad $\rho(x,t)$ tenemos

$$\left\langle \frac{dY}{dt} \right\rangle = \int a(x,t) u'(x) \rho(x,t) dx + \frac{\sigma^2}{2} \int b^2(x,t) u''(x) \rho(x,t) dx. \tag{2.66}$$

Integrando por partes y considerando condiciones de contorno tales que $\rho(x,t)$ se anula en la frontera de integración,

$$\left\langle \frac{dY}{dt} \right\rangle = - \int u(x) \partial_x [a(x,t)\rho(x,t)] dx + \frac{\sigma^2}{2} \int u(x) \partial_x^2 [b^2(x,t)\rho(x,t)] dx. \tag{2.67}$$

Por otra parte,

$$\left\langle \frac{dY}{dt} \right\rangle = \int u(x) \partial_t \rho(x,t) dx. \tag{2.68}$$

Finalmente, igualando las ecuaciones (2.67) y (2.68) y teniendo en cuenta que $u(x)$ es una función arbitraria se obtiene la ecuación de Fokker-Planck

$$\partial_t \rho(x,t) = -\partial_x [a(x,t)\rho(x,t)] + \frac{\sigma^2}{2} \partial_x^2 [b^2(x)\rho(x,t)]. \tag{2.69}$$

El proceso estocástico descrito por esta ecuación de Fokker-Planck es equivalente al proceso de difusión de Itô con coeficiente de arrastre $a(x,t)$ y coeficiente de difusión $b(x,t)$ [es decir, la SDE (2.38)], tal y como acabamos de mostrar.

Análogamente podemos construir una ecuación de Fokker-Planck equivalente a la SDE de Stratonovich $dX = adt + b \circ dW$. Usando la relación Itô-Stratonovich se obtiene la siguiente ecuación en derivadas parciales para la densidad de probabilidad del proceso estocástico que satisface $dX = adt + b \circ dW$,

$$\partial_t \rho(x,t) = -\partial_x [a(x,t)\rho(x,t)] + \frac{\sigma^2}{2} \partial_x \left\{ b(x,t) \partial_x [b(x,t)\rho(x,t)] \right\}. \tag{2.70}$$

Conviene aquí destacar algunos puntos importantes:

- La FPE es una ecuación diferencial en derivadas parciales de segundo orden de tipo parabólico. Por tanto, precisa de una condición inicial del tipo $\rho(x,t_0) = f(x)$ y condiciones de contorno sobre la frontera del dominio de x (e.g. condiciones de contorno periódicas o condiciones de regularidad en el infinito [6]).

- Si $b(x,t) = 0$ la FPE es una ecuación de Liouville.
- Si $a(x,t) = 0$ y $b(x,t)$ es constante la FPE es una ecuación de difusión.
- Si sólo hay ruido aditivo las ecuaciones (2.69) y (2.70) coinciden, como ya ocurría con las SDE's homólogas de Itô y Stratonovich.

Finalmente, señalamos que la FPE (2.69) se puede escribir en forma de ecuación de continuidad como

$$\partial_t \rho(x,t) = -\partial_x J(x,t), \tag{2.71}$$

donde la corriente $J(x,t)$ vale

$$J(x,t) = a(x,t)\rho(x,t) - \frac{\sigma^2}{2}\partial_x[b^2(x,t)\rho(x,t)]. \tag{2.72}$$

2.6.2 Soluciones estacionarias

Vamos a considerar ahora la ecuación de Fokker-Plank en una variable con coeficientes $a(x)$ y $b(x)$ independientes del tiempo. Las soluciones estacionarias verifican que $\partial_t \rho = 0$, con lo que la ecuación (2.71) implica $\partial_x J = 0$ dando una corriente constante J, y la ecuación (2.72) queda

$$J = a(x)\rho(x) - \frac{\sigma^2}{2}\partial_x[b^2(x)\rho(x)]. \tag{2.73}$$

Esta última ecuación es directamente integrable dando la solución general para la densidad de probabilidad estacionaria [6],

$$\rho(x) = \mathcal{N} e^{-\Phi(x)} - J e^{-\Phi(x)} \frac{2}{\sigma^2} \int^x \frac{e^{\Phi(x')}}{b^2(x')}\, dx', \tag{2.74}$$

con

$$\Phi(x) \equiv \ln\left(\frac{\sigma^2}{2} b^2(x,t)\right) - \frac{2}{\sigma^2}\int^x \frac{a(x')}{b^2(x')}\, dx'. \tag{2.75}$$

Las constantes $\mathcal{N}$ y J se determinan a partir de la normalización de la densidad de probabilidad y de las condiciones de contorno.

Aplicación: Soluciones estacionarias para la ecuación de Langevin

La ecuación de Fokker-Planck puede ser una herramienta adecuada para tratar ecuaciones diferenciales estocásticas. Una cuestión de gran interés es obtener la velocidad estacionaria de una partícula browniana que obedece la ecuación de Langevin (2.59). Este proceso es equivalente a la FPE [ecuaciones (2.71) y (2.72)] con coeficientes

$$\begin{aligned} a(x) &= \frac{1}{\gamma} F(x) = -\frac{1}{\gamma}\frac{dV(x)}{dx}, \\ \frac{\sigma^2}{2} b^2(x) &= D = \frac{k_B T}{\gamma}. \end{aligned} \tag{2.76}$$

Vamos a considerar una fuerza periódica tal que $F(0) = F(L)$, lo que nos permite asumir que la posición $x(t)$ está acotada en el intervalo $[0, L]$ y tenemos condiciones de contorno $\rho(0) = \rho(L)$. Esta condición de contorno, más la normalización $\int_0^L \rho(x) = 1$, fijan el problema (2.73)–(2.75). Tras un cálculo simple, aunque laborioso, se obtiene para la corriente estacionaria (2.73) [11, 12]

$$J = \frac{DA}{B_+ B_- - AC} \tag{2.77}$$

con

$$\begin{aligned} A &\equiv 1 - e^{\frac{V(L)-V(0)}{k_B T}}, \\ B_\pm &\equiv \int_0^L dx\, e^{\pm\frac{V(x)}{k_B T}}, \\ C &\equiv \int_0^L dx \int_0^x dy\, e^{\frac{V(y)-V(x)}{k_B T}}. \end{aligned} \tag{2.78}$$

De forma alternativa, la corriente estacionaria puede escriberse como [11]

$$J = \frac{D\left[1 - e^{(V(L)-V(0))/k_B T}\right]}{\int_0^L dx \int_x^{x+L} dy\, e^{(V(y)-V(x))/k_B T}}. \tag{2.79}$$

Este resultado es válido para potenciales totalmente generales siempre y cuando $V'(x + L) = V'(x)$. Más adelante usaremos estos resultados en el estudio de las ratchets, donde hemos encontrado potenciales efectivos que satisfacen esta condición. Finalmente, la velocidad estacionaria media se calcula como

$$\langle \dot{x} \rangle_{\mathrm{st}} = JL. \tag{2.80}$$

De hecho, vamos a probar la relación más general

$$\langle \dot{x}(t) \rangle = \int_0^L J(x, t) dx. \tag{2.81}$$

En efecto, promediando sobre el ruido de media cero en la ecuación de Langevin (2.59),

$$\gamma \langle \dot{x}(t) \rangle = \langle F(x(t)) \rangle, \tag{2.82}$$

mientras que por otra parte si integramos la corriente (2.73) [con coeficiente dados por la ecuación (2.76)] en el intervalo $[0, L]$ con condiciones de contorno periódicas $\rho(L, t) = \rho(0, t)$ obtenemos

$$\int_0^L J(x, t) dx = \frac{1}{\gamma} \langle F(x(t)) \rangle. \tag{2.83}$$

Estas dos últimas ecuaciones dan el resultado buscado (2.81).

Usaremos los conceptos y técnicas introducidos en este capítulo 2 (cálculo de Itô, ecuaciones de Langevin, algoritmo de Euler, ecuación de Fokker-Planck...) a lo largo de esta tesis.

Bibliografía

[1] P.E. Kloeden and E. Platen, *Numerical Solution of Stochastic Differential Equations* (Springer, 1992).

[2] L. Arnold, *Stochastic differential equations* (Wiley, 1974).

[3] L. C. Evans, *An introduction to stochastic differential equations* (Departament of Mathematics, UC Berkeley).

[4] C. W. Gardiner, *Handbook of stochastic methods* (Springer-Verlag, 1985).

[5] S. Karlin and H. M. Taylor, *A first course in stochastic processes* (Academic Press, 1975).

[6] H. Risken, *The Fokker-Planck Equation* (Springer-Verlag, 1989).

[7] Van Kampen, *Stochastic process in physics and chemistry, 2nd ed.* (North Holland, 2001).

[8] J. Keizer, *Statistical thermodynamics of nonequilibrium processes* (Springer-Verlag, 1987).

[9] A. D. Fokker, Ann. der Phys. **348**, 810 (1914).

[10] M. Planck, Sitzungsber. Preuss. Akad. Wiss. Phys. Math. Kl. **24**, 324 (1917).

[11] P. Reimann, Phys. Rep. **361**, 57 (2002).

[12] L. Dinis, *Optimización y control de juegos de azar y motores brownianos colectivos, Ph.D Thesis* (Universidad Complutense de Madrid, 2005).

Capítulo 3

Teoría de la información

En este capítulo revisamos algunos de los conceptos fundamentales de la teoría de la información [1–6]. Tras una breve introducción desde una perspectiva histórica (Sec. 3.1) presentaremos las principales magnitudes de la teoría de la información: la entropía y la información mutua (Sec. 3.2), y también algunos aspectos básicos sobre canales de comunicación (Sec. 3.3).

3.1 Introducción

Los primeros intentos de definir una medida de la información se remontan a los trabajos de Nyquist [7,8] y Hartley [9] en la década de los veinte, pero fue en 1948 cuando se sentaron las bases de lo que se conocería como teoría de la información, a raíz de dos trabajos seminales de Claude E. Shannon [10–12]. El concepto de *entropía* introducido por Shannon constituye la idea central de la teoría de la información. La entropía de una variable aleatoria se define en términos de su distribución de probabilidad y da una medida de su aleatoriedad o incertidumbre. Además, esta entropía está directamente relacionada con la máxima compresión que se puede conseguir de un mensaje. Según cuenta Feynman [13], Shannon utilizó el término 'entropía' aconsejado por von Neumann, que le dijo que le daría "mucho juego en los debates, porque nadie sabe realmente lo que es la entropía" Shannon utilizó la letra H para referirse a esta entropía por la similitud de su expresión con la función H del teorema H de Boltzmann [12].

Los trabajos de Shannon culminan con los teoremas centrales de Shannon. El *teorema de codificación en ausencia de ruido* muestra cuán compresible puede ser un mensaje, o equivalentemente, qué redundancia tiene. El *teorema de codificación en un canal ruidoso* halla cuánta redundancia hay que añadir a un mensaje comunicado a través de un canal con ruido para que sea comprensible por el receptor.

Aunque la teoría de la información surgió del estudio de sistemas de comunicaciones, posteriormente la relación entre la teoría de la información y la termodinámica ha sido tratada en detalle, destacando los trabajos de Brillouin [14] y Jaynes [15]. La afirmación de Landauer "Information is physical" [16] es una consecuencia de que la información es registrada por sistemas físicos (transistores, neuronas, cadenas de ADN...) y que los sistemas de procesamiento de la información (computadores, cerebros, células...) están gobernados por leyes físicas. Así, problemas físicos fundamentales como el demonio de Maxwell [17] pueden entenderse interpretando las magnitudes físicas en términos de la teoría de la información.

En los últimos años, la teoría cuántica se ha convertido en un nuevo campo de aplicación de la información y la computación, dando lugar a todo una nueva rama del conocimiento conocidada como información y computación cuántica [18–20].

3.2 Entropía e información mutua

Para introducir los conceptos básicos de entropía e información mutua consideraremos una variable aleatoria discreta X con espacio muestral o alfabeto $\mathscr{X}$, de cardinal finito $|\mathscr{X}|$, y distribución de probabilidad $p(x) = p_X(x) = \Pr\{X = x\}$, i.e., $X \sim p(x)$.

3.2.1 Entropía, entropía conjunta y entropía condicional

Se define entonces la entropía $H(X)$ de esta variable X como

$$H(X) = -\sum_{x\in\mathscr{X}} p(x)\log p(x), \tag{3.1}$$

con el convenio $0\log 0 = 0$, como corresponde por continuidad. La base del logaritmo es 2 y se dice que la entropía se mide en *bits*. Si el logaritmo se expresa en base e la entropía se dice que está expresada en *nats*. Salvo que se especifique lo contrario entenderemos en lo sucesivo que log es la función logaritmo en base 2.

Nótese que esta entropía así definida puede interpretarse como el valor esperado (esperanza matemática) de $\log \frac{1}{p(X)}$,

$$H(X) = E_p \log \frac{1}{p(X)}. \tag{3.2}$$

La cantidad $h(x) = \log \frac{1}{p(x)}$ se conoce como *contenido de información de Shannon*. Por ejemplo, la letra 'm' tiene una probabilidad de aparición (frecuencia) de 0.0235 en el idioma inglés [21] y por tanto su contenido de información es de 5.4 bits. Promediando sobre las 26 letras del alfabeto inglés más el espacio en blanco (27 posibles salidas) se obtiene para la entropía un valor de aproximadamente 4.1 bits. Ahora bien, esta no es la entropía del inglés verdadero, sino de un inglés ficticio en el que no hubiese correlaciones. Por ejemplo, en inglés real es mucho más probable que después de una 't' vaya una 'h' que una 'q' y eso no se ha tenido en cuenta en el cálculo anterior.

Dadas un par de variables aleatorias discretas $(X, Y) \sim p(x, y)$ se define su *entropía conjunta* como

$$H(X,Y) = -\sum_{x\in\mathscr{X}}\sum_{y\in\mathscr{Y}} p(x,y)\log p(x,y). \tag{3.3}$$

(La generalización a una variable vectorial N-dimensional es directa).

Por otra parte, se define la *entropía condicional* de una variable aleatoria dada otra como el valor esperado de las entropías de las distribuciones

condicionadas, promediadas sobre la variable que condiciona, es decir, dado $(X,Y) \sim p(x,y)$,

$$\begin{aligned} H(Y|X) &= \sum_{x\in\mathscr{X}} p(x) H(Y|X=x) \\ &= -\sum_{x\in\mathscr{X}} p(x) \sum_{y\in\mathscr{Y}} p(y|x) \log p(y|x) \\ &= -\sum_{x\in\mathscr{X}} \sum_{y\in\mathscr{Y}} p(x,y) \log p(y|x). \end{aligned} \tag{3.4}$$

La entropía $H(X)$ es una buena medida de la incertidumbre del resultado del experimento probabilístico correspondiente a la variable estocástica X, como lo justifican las siguientes propiedades:

1. La entropía siempre es positiva: $H(X) \geq 0$, con la igualdad si y sólo si $p(x_0) = 1$ y $p(x) = 0\ \forall x \in \mathscr{X} - \{x_0\}$. Por tanto, cuando el experimento es determinista no hay incertidumbre alguna y viceversa.

2. $H(X) \leq \log|\mathscr{X}|$, con la igualdad si y sólo si $p(x) = 1/|\mathscr{X}|\ \forall x \in \mathscr{X}$. La máxima entropía se produce, pues, para variables uniformemente distribuidas. Además, en este caso, si el número de posibles resultados aumenta (aumenta $|\mathscr{X}|$) entonces la entropía aumenta (mayor incertidumbre).

3. El condicionamiento reduce la entropía: $H(X|Y) \leq H(X)$, con la igualdad si y sólo si X e Y son independientes.

4. Regla de la cadena: $H(X,Y) = H(X) + H(Y|X)$. Esto es, la entropía (incertidumbre) de un par de variables es la entropía de una de ellas más la entropía de la otra cuando ya se conoce la primera.

5. Acotamiento independiente: $H(X,Y) \leq H(X)+H(Y)$, con la igualdad si y sólo si X e Y son independientes.

Las demostraciones de las propiedades 1 y 4 son inmediatas a partir de las definiciones de entropía, entropía conjunta y entropía condicional; la propiedad 5 es consecuencia inmediata de 3 y 4 y para demostrar 2 y 3 basta usar la desigualdad $\log x \leq x - 1$ (con igualdad si y sólo si $x = 1$).[1]

[1] Dem.: $f(x) = \log(x) - (x-1)$ es cóncava $\frown$ (su segunda derivada es negativa en todo su dominio) y $f(1) = f'(1) = 0$.

Por ejemplo, para la propiedad 3,

$$\begin{aligned} H(X|Y) - H(X) &= -\sum_{x\in\mathscr{X}}\sum_{y\in\mathscr{Y}} p(x,y)\log p(x|y) + \sum_{x\in\mathscr{X}} p(x)\log p(x) \\ &= \sum_{x\in\mathscr{X}}\sum_{y\in\mathscr{Y}} p(x,y)\left(-\log p(x|y) + \log p(x)\right) \\ &= \sum_{x\in\mathscr{X}}\sum_{y\in\mathscr{Y}} p(x,y)\log\frac{p(x)}{p(x|y)} \\ &\leq \sum_{x\in\mathscr{X}}\sum_{y\in\mathscr{Y}} p(x,y)\left(\frac{p(x)}{p(x|y)} - 1\right) \\ &= \sum_{x\in\mathscr{X}}\sum_{y\in\mathscr{Y}} p(x)p(y) - \sum_{x\in\mathscr{X}}\sum_{y\in\mathscr{Y}} p(x,y) \\ &= 1 - 1 = 0. \end{aligned} \tag{3.5}$$

Estas propiedades de la entropía son generalizables de forma natural a variables N-dimensionales. Las fórmulas resultantes se demuestran trivialmente por inducción.

El experimento estocástico más simple no trivial corresponde a una proceso de Bernoulli $X = \{0, 1\}$, con $p(0) = p$ y por tanto $p(1) = 1 - p$. Para este caso, la entropía vale

$$H(X) = -p\log p - (1-p)\log(1-p) \equiv H_b(p) \tag{3.6}$$

Esta función $H_b(p)$ se llama entropía binaria[2]. Nótese que $H_b(p)$ es simétrica en torno a $p = 1/2$, donde toma su valor máximo de 1 bit (véase fig. 3.1). Otra característica importante es que $H_b(p)$ es cóncava $\frown$.

Finalmente, conviene definir una magnitud importante para secuencias de n variables aleatorias. Dado un proceso estocástico discreto X_t con $t = 1, 2, \ldots, n$, se define la *tasa de entropía* como

$$\bar{H}(\mathscr{X}) = \lim_{n\to\infty} \frac{1}{n} H(X_1, X_2, \ldots, X_n) \tag{3.7}$$

cuando el límite existe. Es una medida de la entropía por símbolo. Para variables independientes $\bar{H}(\mathscr{X}) = \lim_{n\to\infty} \frac{1}{n}\sum_{i=1}^{n} H(X_i)$, siempre que el límite exista. Si además de independientes son idénticamente distribuidas $\bar{H}(\mathscr{X}) = H(X)$, donde $H(X)$ es el valor común de la entropía de cada X_i, y si además son uniformemente distribuidas entonces $\bar{H}(\mathscr{X}) = \log|\mathscr{X}|$.

Otra magnitud importante es

$$H' = \lim_{n\to\infty} H(X_n|X_{n-1}, X_{n-2}, \ldots, X_1), \tag{3.8}$$

[2]El subíndice b se omite con frecuencia puesto que la entropía binaria tiene por argumento un número (letras minúsculas) y no ha lugar a confusión con la entropía $H(X)$ cuyo argumento es un proceso estocástico (letras mayúsculas).

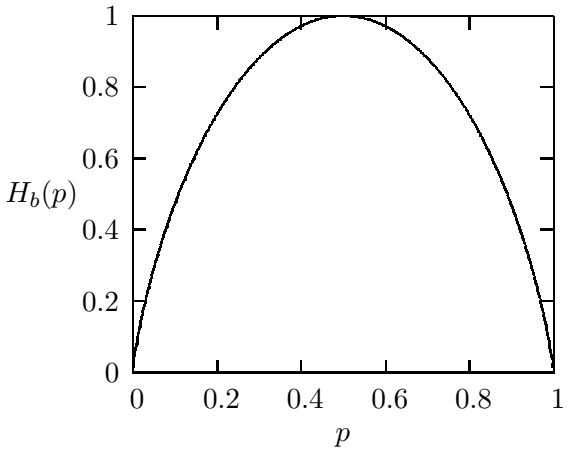

Figura 3.1: $H_b(p)$ versus p.

que es la entropía condicionada de la última variable aleatoria dado el pasado completo. Puede demostrarse [1] que para un proceso estocástico estacionario los límites (3.7) y (3.8) existen y además coinciden.

3.2.2 Entropía relativa e información mutua

Se define la *entropía relativa* o *divergencia de Kullback Leibler* entre dos distribuciones de probabilidad $p(x)$ y $q(x)$ por

$$D(p||q) = \sum_{x \in \mathscr{X}} p(x) \log \frac{p(x)}{q(x)}. \tag{3.9}$$

Puede interpretarse como una medida de la "distancia" entre distribuciones ya que es no negativa (desigualdad de Gibbs)[3] y cumple que $D(p||q) = 0 \Leftrightarrow p = q$. Sin embargo no es una distancia en sentido matemático (no es simétrica y no cumple la desigualdad triangular).

Dadas dos variables aleatorias $(X, Y) \sim p(x, y)$ se define la *información mutua* $I(X;Y)$ como la entropía relativa entre la función de distribución conjunta $p(x, y)$ y el producto de las distribuciones marginales, $p(x)p(y)$, es decir,

$$I(X;Y) = \sum_{x \in \mathscr{X}} \sum_{y \in \mathscr{Y}} p(x, y) \log \frac{p(x, y)}{p(x)p(y)}. \tag{3.10}$$

Nótese que como $I(X;Y) = D(p(x, y)||p(x)p(y))$ entonces $I(X;Y) \geq 0$, con la igualdad si y sólo si $p(x, y) = p(x)p(y)$, i.e., X e Y son independientes.

[3] Dem.: $D(p||q) = \sum p(x) \log \frac{p(x)}{q(x)} \geq (\sum p(x)) \log \frac{\sum p(x)}{\sum q(x)} = 1 \log \frac{1}{1} = 0$.

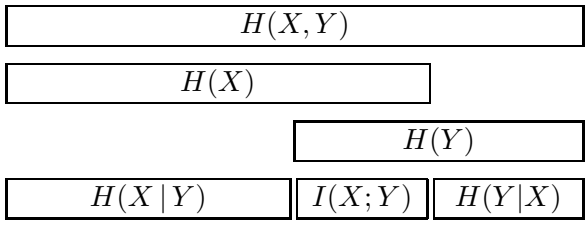

Figura 3.2: Relaciones entre información y entropía. (Tomado de [21]).

Es fácil ver que la información mutua puede definirse de forma equivalente a ec. (3.10) en términos de entropía como

$$I(X;Y) = H(X) - H(X|Y), \tag{3.11}$$

lo que permite interpretar la información mutua $I(X;Y)$ como la reducción de incertidumbre en X gracias al conocimiento de Y. En particular,

$$I(X;X) = H(X), \tag{3.12}$$

es decir, la información mutua de una variable consigo misma es su entropía y por ello $H(X)$ se denomina a veces *autoinformación*. Por otra parte, usando la equación (3.11) junto con el resultado ya visto $H(X,Y) = H(X) + H(Y|X)$, obtenemos la relación

$$I(X;Y) = H(X) + H(Y) - H(X,Y), \tag{3.13}$$

que refleja la simetría $I(X;Y) = I(Y;X)$. En la figura 3.2 se muestran esquemáticamente las diversas relaciones entre la información mutua, la entropía y las entropías conjuntas y condicionadas.

Siguiendo la definición (3.11), definimos la *información mutua condicionada* entre X e Y dado Z por

$$I(X;Y|Z) = H(X|Z) - H(X|Y,Z). \tag{3.14}$$

Partiendo de la definición de la información mutua (3.11) y usando la regla de la cadena de la entropía (véase propiedad 4 en sección 3.2.1) obtenemos la regla de la cadena para la información mutua:

$$\begin{aligned} I(X,Y;Z) &= H(X,Y) - H(X,Y|Z) \\ &= H(X) + H(Y|X) - H(X|Z) - H(Y|X,Z) \\ &= I(X;Z) + I(Y;Z|X) \end{aligned} \tag{3.15}$$

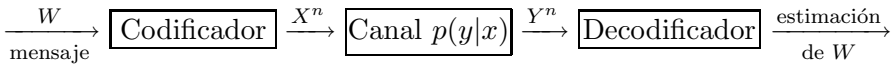

Figura 3.3: Esquema de un sistema de comunicación.

3.3 Canales

Un sistema de comunicación consta de los ingredientes esquematizados en la figura 3.3. En un sistema físico real, la transferencia de información estará sujeta a ruido de manera que puede ocurrir que la estimación del mensaje transmitido no sea correcta. Si el emisor y el receptor están de acuerdo en cuál fue el mensaje transmitido entonces la comunicación ha sido exitosa.

Un *canal discreto* es una terna $(\mathscr{X}, p(y|x), \mathscr{Y})$ consistente en un alfabeto finito de entrada $\mathscr{X}$, un alfabeto finito de salida $\mathscr{Y}$ y una matriz de probabilidades de transición $p(y|x)$ que expresan la probabilidad de tener una salida $Y = y$ cuando la entrada es $X = x$. Las probabilidades de transición $p(y|x)$ dan cuenta de este hecho y determinan el tipo de canal del sistema de comunicación. Por convenio x indexa las filas e y las columnas. Se dice que el canal discreto es *sin memoria* si la probabilidad de obtener una secuencia de salida y^n dada una secuencia de entrada x^n verifica

$$p(y^n|x^n) = \prod_{i=1}^{n} p(y_i|x_i). \tag{3.16}$$

Un canal se dice que es *simétrico* si las filas de la matriz de transición $p(y|x)$ son permutaciones unas de otras y lo mismo para las columnas.

Un importante tipo de canal simétrico sin memoria es el llamado canal binario simétrico. En este canal se transmite un 0 ó un 1 y se recibe un 0 ó un 1 con una probabilidad de error p como se muestra en la figura 3.4, de manera que la matriz de transición es

$$p(y|x) = \begin{pmatrix} 1-p & p \\ p & 1-p \end{pmatrix}. \tag{3.17}$$

Estos conceptos básicos sobre teoría de la información que han sido introducidos en este capítulo van a ser de utilidad para la correcta comprensión de algunos de los cálculos y resultados de esta tesis.

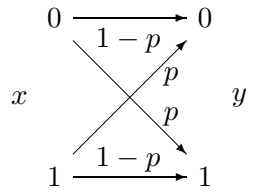

Figura 3.4: Canal binario simétrico.

Bibliografía

[1] T. Cover and J. Thomas, *Elements of Information Theory* (John Wiley & Sons, New York, 1991).

[2] R. G. Gallager, *Information Theory and Reliable Communication* (John Wiley & Sons, 1968).

[3] R. E. Blahut, *Principles and practice of information theory* (Addison-Wesley, 1987).

[4] M. Mansuripur, *Introduction to information theory* (Prentice-Hall, 1987).

[5] A. M. Yaglom and I. M. Yaglom, *Probability and information* (D. Reidel Publishing Company, 1983).

[6] R. Ash, *Information theory* (John Wiley and Sons, 1965).

[7] H. Nyquist, Bell Sys. Tech. J. **3**, 324 (1924).

[8] H. Nyquist, A.I.E.E. Trans. **47**, 617 (1928).

[9] R. V. L. Hartley, Bell Sys. Tech. J. **7**, 535 (1928).

[10] C. E. Shannon, Bell Sys. Tech. J. **27**, 379 and 623 (1948).

[11] C. E. Shannon, Bell Sys. Tech. J. **28**, 656 (1949).

[12] C. E. Shannon and W. Weaver, *The mathematical Theory of Communication* (University of illinois Press, 1949).

[13] R. P. Feynman, *Lectures on computation* (Addison-Wesley, 1998). R. P. Feynman, *Conferencias sobre computación* (Drakontos, 2003).

[14] L. Brillouin, *Science and information theory* (Academic Press, New York, 1962).

[15] R. D. Rosenkrantz (ed.), *E. T. Jaynes, Papers on probability, statistics and statistical Physics* (D. Reidel Publishing Company, 1983).

[16] R. Landauer, Phys. Today **44**, 23 (1991).

[17] H. S. Leff and A. F. Rex, *Maxwell's Demon 2: Entropy, Classical and Quantum Information, Computing* (Institute of Physics, Bristol, 2003).

[18] A. Galindo, *Del bit al qubit* (Universidad Complutense de Madrid, Lección inagural del Curso Académico 2001-2002).
http://teorica.fis.ucm.es/∼agt/conferencias/leccionweb.pdf

[19] A. Galindo and M. A. Martín-Delgado, Rev. Mod. Phys. **74**, 347 (2002).

[20] M. A. Nielsen and I. L. Chuang, *Quantum Computation and Quantum Information* (Cambridge University Press, 2000).

[21] David J. C. MacKay, *Information Theory, Inference, and Learning Algorithms* (Cambridge University Press, 2003).
http://www.inference.phy.cam.ac.uk/mackay/itila/

Capítulo 4

Estado actual del tema y objetivos

Este capítulo completa la parte introductoria que precede a la siguiente Parte II, en la que expondremos nuestros nuevos resultados. Aquí discutimos las principales cuestiones sobre las ratchets (sección 4.1) y su relación con la teoría de la información y el demonio de Maxwell (sección 4.2). Concluiremos esta primera parte exponiendo los objetivos de la presente tesis (sección 4.3).

4.1 Ratchets

En esta sección vamos a introducir las ratchets como rectificadores de las fluctuaciones térmicas. Tras discutir sucintamente las diferentes clases de racthets nos centraremos en las llamadas flashing ratchets. Por otra parte, la teoría de control [1,2] nos permite clasificar las ratchets en dos categorías: ratchets de ciclo abierto y ratchets de ciclo cerrado. En las primeras la operación de control es independientemente del estado del sistema, mientras que en las segundas el controlador usa información sobre el estado del sistema para operar. Daremos algunos ejemplos de estas ratchets de ciclo abierto y cerrado, y compararemos sus rendimientos.

4.1.1 Introducción

Las ratchets o motores brownianos son rectificadores de las fluctuaciones térmicas. Esta rectificación se consigue habitualmente mediante una perturbación externa determinista o estocástica en un sistema que es o se convierte en asimétrico bajo inversión espacial [3]. En los últimos años ha habido un gran interés por las ratchets debido a su relevancia tanto a nivel teórico como experimental. Desde un punto de vista práctico el efecto ratchet tiene potencialmente multitud de aplicaciones en biología, materia condensada y nanotecnología [3–5].

Una prescripción básica para tener el efecto ratchet es sacar al sistema fuera del equilibrio térmico (lo que tiene un coste energético). Esto puede conseguirse de distintas maneras. Feynman comprendió este punto y propuso considerar la ratchet de Smoluchowski en contacto con dos baños térmicos de diferentes temperaturas (véase el capítulo 1). Ello constituye la base de las llamadas ratchets térmicas o ratchets de Feynman.

Otro ejemplo típico de un dispositivo ratchet es una partícula browniana de masa m a temperatura T y con coeficiente de fricción γ que evoluciona en una dimensión con coordenada $x(t)$ de acuerdo a la SDE

$$m\ddot{x}(t) = F(x(t), g(t)) + h(t) + F_{\text{ext}} - \gamma\dot{x}(t) + \xi(t), \tag{4.1}$$

con

$$\left\langle \xi(t)\xi(t')\right\rangle = 2\gamma k_B T\delta(t-t'). \tag{4.2}$$

En esta modelización $g(t)$ y $h(t)$ pueden ser funciones deterministas o estocásticas del tiempo t, mientras que F_{ext} es una fuerza externa constante. Las fluctuaciones térmicas se han modelado a través del ruido blanco

$\xi(t)$, de media cero y descorrelacionado, con intensidad $2\gamma k_B T$. La fuerza $F(x,g) = -\partial_x V(x,g)$ deriva de un potencial espacialmente periódico, i.e., $V(x+L, g(t)) = V(x, g(t))$ para todo t y x.

Las ratchets que incluyen un término de masa [véase ecuación (4.1)] se conocen como ratchets inerciales y se ha mostrado que exhiben comportamiento caótico [6, 7] incluso en ausencia de ruido. El término de inercia juega un papel relevante en ciertos dispositivos como por ejemplo en los SQUIDS [3]. Por contra, en muchas otras situaciones, como en los sistemas biológicos, el término de inercia puede despreciarse. En este régimen sobreamortiguado la ecuación (4.1) pasa a ser

$$\gamma \dot{x}(t) = F(x(t), g(t)) + h(t) + F_{\text{ext}} + \xi(t). \tag{4.3}$$

Una magnitud de gran interés en las ratchets es la corriente media de partículas o velocidad media $\langle \dot{x}(t) \rangle$. El efecto ratchet consiste precisamente en la aparición de una corriente no nula para fuerza externa cero y el resto de fuerzas y gradientes también nulos tras promediar sobre el espacio, el tiempo y las colectividades [3]. La fuerza externa F_{ext} de la ecuación (4.1) no debería considerarse como parte del sistema sino más bien como una perturbación externa que permite estudiar la respuesta del sistema. De hecho, es incluso posible tener una corriente neta de partículas en contra de la fuerza externa, siempre que ésta sea suficientemente pequeña, con lo que el motor browniano realiza trabajo contra la fuerza [8–10].

Hay dos clases fundamentales de ratchets [3]: *pulsating ratchets*, en los que $h(t) = 0$, y *tilting ratchets*, en los que $g(t) = 0$. El ejemplo paradigmático de una tilting ratchet es la rocking ratchet, en la cual una perturbación de media cero y periódica $h(t)$ se aplica al sistema para 'balancear' (rock) el potencial ratchet que la partícula siente [11]. Por otra parte, una flashing ratchet [12] es una pulsating ratchet en la que el potencial es encendido y apagado alternativamente. Estudiaremos con más detalle estas flashing ratchets en la sección siguiente.

4.1.2 Flashing ratchet

Descripción

Una ratchet de una partícula puede modelizarse como una partícula browniana que satisface la ecuación de Langevin sobreamortiguada

$$\gamma \dot{x}(t) = \alpha(x(t), t) F(x(t)) + \xi(t). \tag{4.4}$$

Aquí, $F(x) = -V'(x)$, con $V(x)$ el potencial ratchet, que es normalmente periódico, $V(x) = V(x+L)$, y tiene ruptura de simetría bajo $x \to -x$. La función α implementa la acción del controlador que enciende ($\alpha = 1$) o apaga ($\alpha = 0$) el potencial racthet. Gracias a este encendido y apagado se rompe el balance detallado y el sistema trabaja como un motor browniano.

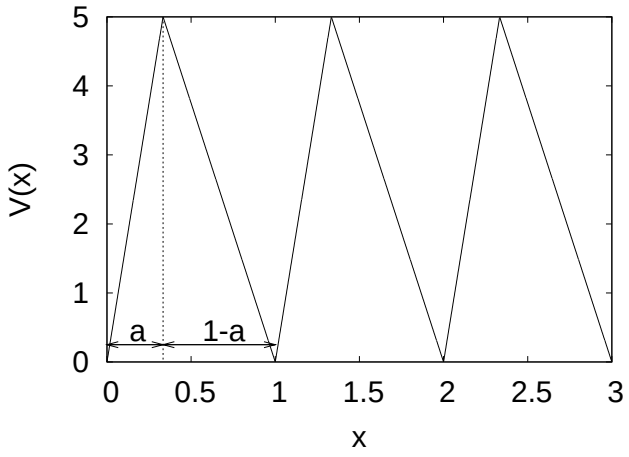

Figura 4.1: Potencial ratchet de diente de sierra con periodo $L = 1$, altura $V_0 = 5$ y parámetro de asimetría $a = 1/3$.

Un ejemplo típico de potencial ratchet es el potencial de diente de sierra mostrado en la figura 4.1. Otro ejemplo puede ser

$$V(x) = \frac{2V_0}{3\sqrt{3}} \left[\sin\left(\frac{2\pi x}{L}\right) + \frac{1}{2}\sin\left(\frac{4\pi x}{L}\right) \right]. \tag{4.5}$$

Este potencial se ha usado en la fig. 1.2 para ilustrar el efecto ratchet en una flashing ratchet (véase el capítulo 1).

La ecuación (4.4) se puede generalizar para describir flashing ratchets colectivas compuestas por N partículas brownianas con posiciones $\{x_j(t)\}$:

$$\gamma \dot{x}_i(t) = \alpha(\{x_j(t)\}, t)F(x_i(t)) + \xi_i(t); \qquad i = 1, \ldots, N, \tag{4.6}$$

donde $\xi_i(t)$ son ruidos blancos gaussianos de media cero y varianza $\langle \xi_i(t)\xi_j(t')\rangle$ $= 2\gamma k_B T \delta_{ij}\delta(t-t')$, como corresponde a la relación de fluctuación-disipación.

Fashing ratchets de ciclo abierto

En las ratchets de ciclo abierto el controlador no usa ninguna información sobre el estado del sistema para operar sobre él. En el marco de las flashing ratchets esto se traduce en que el valor del parámetro de control $\alpha(t)$ no depende del estado de la partícula browniana, como ocurre, por ejemplo, con un encendido y apagado aleatorio o periódico. Estas dos posibilidades dan corrientes no nulas si los ritmos de encendido-apagado son apropiados. Conviene señalar que en las flashing ratchets colectivas con control de ciclo abierto las N ecuaciones de Langevin (4.6) están desacopladas y por consiguiente la velocidad del centro de masas es independiente del número N de partículas.

Estudiemos con más detalle el protocolo periódico. Siguiendo [13], vamos a considerar un potencial de diente de sierra periódico con parámetro de asimetría a y periodo L (vid. fig. 4.1), y con una altura suficientemente grande (comparada con k_BT) para poder aproximar la densidad de probabilidad por una función delta en cada uno de los mínimos del potencial encendido. Cuando el potencial se apaga en el instante $t = 0$ cada uno de los picos empieza a difundir, al satisfacer la densidad de probabilidad una FPE con coeficientes $a(x,t) = 0$ y $\sigma^2 b^2(x,t)/2 = D$, que es una ecuación de difusión. Para la delta centrada en el origen la solución de esta ecuación es

$$\rho(x,t) = \frac{e^{-x^2/4Dt}}{\sqrt{4\pi Dt}}. \tag{4.7}$$

Durante un tiempo T_{off} el potencial permanece encendido y la partícula difunde. A continuación, el potencial se apaga durante un tiempo T_{on} y así sucesivamente. En uno de estos ciclos on-off una fracción de partículas $\int_{aL}^{\infty} \rho(x, T_{\text{off}})dx$ avanza un periodo espacial L, mientras que una fracción $\int_{-\infty}^{-(1-a)L} \rho(x, T_{\text{off}})dx$ retrocede L, como se explicó en el capítulo 1.2 (véase también la fig. 1.2). Por lo tanto, en un ciclo completo de duración $T_{\text{on}} + T_{\text{off}}$ la posición de la partícula avanza en media

$$\langle \Delta x \rangle = L \int_{aL}^{\infty} \rho(x, T_{\text{off}})\, dx - L \int_{-\infty}^{-(1-a)L} \rho(x, T_{\text{off}})\, dx, \tag{4.8}$$

y la velocidad estacionaria es

$$\langle \dot{x} \rangle = \frac{\langle \Delta x \rangle}{T_{\text{on}} + T_{\text{off}}}. \tag{4.9}$$

Sin más que operar se obtiene [13]

$$\langle \dot{x} \rangle = \frac{L}{2(T_{\text{on}} + T_{\text{off}})} \left[\operatorname{erfc}\left(\frac{aL}{\sqrt{4DT_{\text{off}}}} \right) - \operatorname{erfc}\left(\frac{(1-a)L}{\sqrt{4DT_{\text{off}}}} \right) \right], \tag{4.10}$$

donde erfc es la función error complementaria. Como puede verse en la fig. 4.2, el flujo neto tiende a cero para periodos cortos o largos. En efecto, para periodos cortos el sistema no tiene tiempo suficiente para difundir durante el tiempo de potencial apagado, con lo que el desplazamiento medio por ciclo es despreciable; para periodos largos la mayor del tiempo el sistema está muy cerca del equilibrio y el flujo va a cero también.

Flashing ratchets de ciclo cerrado

Las ratchets de ciclo cerrado, también llamadas ratchets retroalimentadas, usan información sobre el estado del sistema para operar sobre él. El uso de esta información por parte del controlador para decidir cómo opera sobre

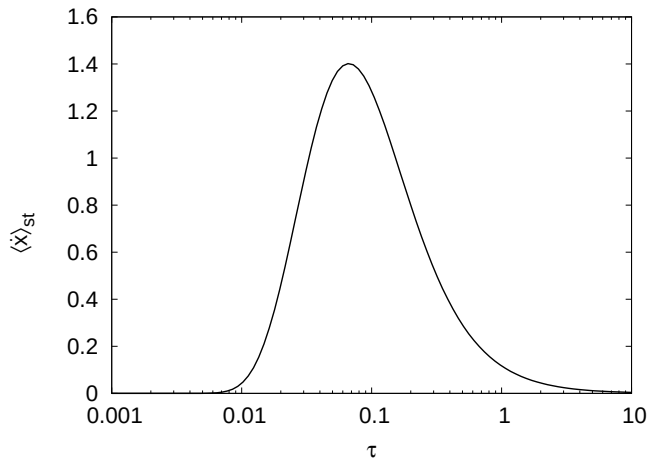

Figura 4.2: Velocidad estacionaria (4.10) para los parámetros $a = 1/3$, $L = 1$ y $D = 1$. Hemos tomado $T_{\rm on} = T_{\rm off} = \tau/2$.

el sistema puede mejorar el rendimiento máximo alcanzable en las ratchets de ciclo cerrado en comparación con las correspondientes ratchets de ciclo abierto. Para ratchets colectivas con más de una partícula, el control retroalimentado usando información puede inducir un acoplamiento efectivo de las partículas brownianas, lo que lleva a la dependencia del flujo con el número de partículas. Hay varios protocolos o estrategias de retroalimentación que dan un aumento del rendimiento en el flujo.

En el *protocolo de maximización instantánea de la velocidad* la política de control depende del signo de la fuerza neta por partícula,

$$f(t) = \frac{1}{N}\sum_{i=1}^{N} F(x_i(t)), \tag{4.11}$$

en cada instante de tiempo. Más concretamente, el parámetro de control está dado por $\alpha(t) = \Theta(f(t))$, con Θ la función de Heaviside [$\Theta(x) = 1$ si $x > 0$, en caso contrario $\Theta(x) = 0$]. Ésta es la mejor estrategia (da la máxima velocidad media) para una sola partícula; véase Ref. [14]. Sin embargo, para un número grande de partículas la dinámica del sistema queda atrapada con el potencial encendido o apagado (fig. 4.3a) y entonces la corriente asintótica media tiende a cero cuando N aumenta [15]. Este efecto indeseado se corrige en el *protocolo de umbrales*, propuesto por primera vez en [16] (cf. fig. 4.3b), en el que se fuerza el encendido-apagado del potencial si la fuerza neta por partícula f cruza ciertos valores umbrales. En la figura 4.4 mostramos la dependencia de la velocidad del centro de masas con el número de partículas para el protocolo de maximización, el protocolo de umbrales y el protocolo de ciclo abierto periódico con periodos óptimos.

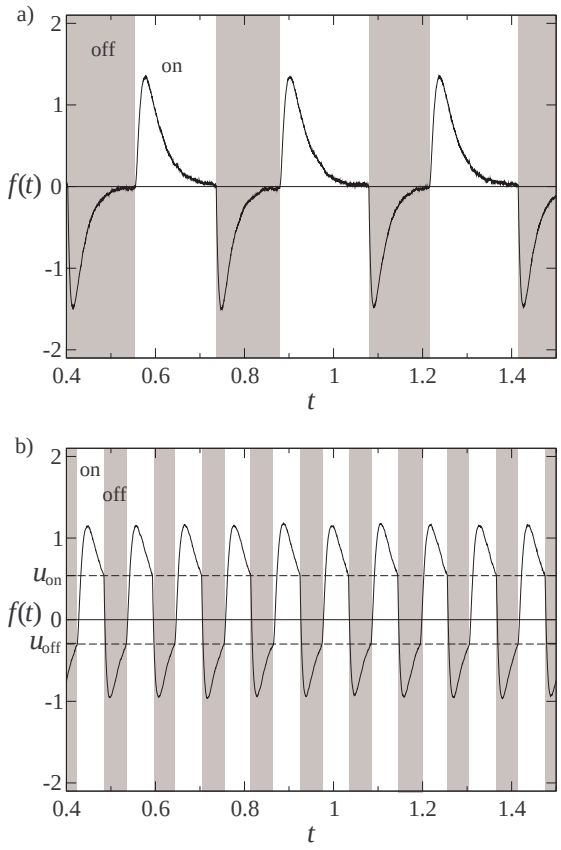

Figura 4.3: Dependencia temporal de la fuerza neta por partícula (4.11) en simulaciones con $N = 10^6$ partículas para a) el protocolo de maximización de la velocidad del centro del masas y b) el protocolo de umbrales. Se ha usado el potencial ratchet de la ecuación (4.5) con $V_0 = 5$. Unidades: $k_B T = 1, L = 1, D = 1$. (Cf. Ref. [16]).

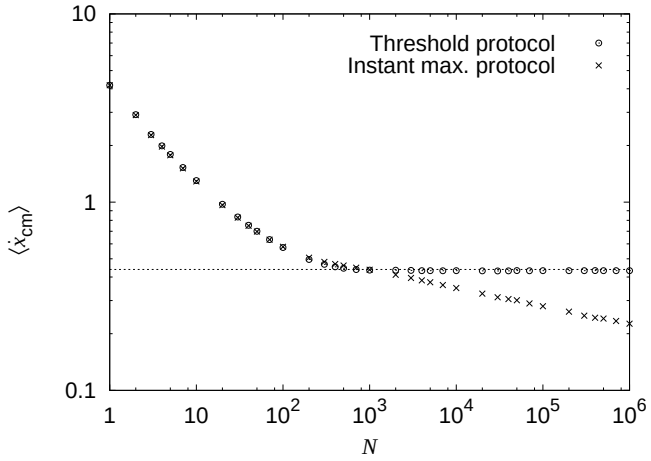

Figura 4.4: Velocidad asintótica media del centro de masas frente al número de partículas N para el protocolo de maximización de la velocidad del centro de masas (aspas), el protocolo de umbrales con umbrales óptimos (círculos) y el protocolo periódico con periódos óptimos para los tiempos de encendido y apagado (línea discontinua). Se ha usado el potencial ratchet de la ecuación (4.5) con $V_0 = 5$. Unidades: $k_B T = 1, L = 1, D = 1$. Véase Ref. [14].

Tanto el protocolo de maximización instantánea de la velocidad del centro de masas como el protocolo de umbrales están basados en la distribución de las fuerzas $\{F(x_i)\}$. Pero otras elecciones son también posibles. Por ejemplo, en el llamado *protocolo de maximización del desplazamiento neto* [17] el parámetro de control depende de la distribución de partículas como sigue:

$$\alpha(t) = \Theta(d(t)); \quad d(t) = \sum_{i=1}^{N} (x_i(t) - x_0), \tag{4.12}$$

donde x_0 es la media de una distribución gaussiana en equilibrio en el potencial ratchet. Se ha encontrado numéricamente [17] que este protocolo mejora al protocolo de maximización instantánea para ratchet colectivas de dos y tres partículas y potenciales de altura $\gtrsim 30 k_B T$. Sin embargo, funciona peor para un número elevado de partículas o potenciales más bajos.

4.2 Información y demonio de Maxwell

El control sobre sistemas físicos por parte de un agente externo aparece frecuentemente en física con objetivos tales como estabilizar dinámicas inestables o aumentar el rendimiento de esos sistemas. El estudio de las propie-

dades de los sistemas con control es una tarea fundamental para la ingeniería y para la física fundamental [2].

Es obvio que la operación del controlador modifica la dinámica del sistema, pero también el estado del sistema puede influir en las decisiones del controlador sobre el propio sistema. El sistema se dice retroalimentdo o con control de ciclo cerrado cuando está presente esta influencia del sistema sobre el controlador. Por el contrario, el sistema tiene un control de ciclo abierto si las decisiones del controlador se toman independientemente del estado del sistema. Ya hemos introducido previamente esta clasificación en la sección anterior en el contexto de las flashing ratchets.

Resulta claro e intuitivo que el uso de información sobre el estado del sistema puede ser potencialmente útil para que el controlador actúe sobre el sistema y mejore el rendimiento del sistema (e.g. la potencia o la eficiencia). Está claro también que, con una determinada cantidad de información sobre el sistema, el rendimiento puede ser mejorado sólo hasta cierto punto. Sin embargo, cómo cuantificar estos límites fundamentales al control de los sistemas con retroalimentación no está tan claro. La interrelación entre la información y el control retroalimentado ha constituido una tarea difícil desde el nacimiento del demonio de Maxwell [18], un ser que recogiendo información sobre el sistema es capaz de reducir la entropía del sistema sin realizar trabajo sobre él. Szilard [19] estudia un demonio de Maxwell sencillo que le sirve para señalar por primera vez la interrelación entre la adquisición de la información y la termodinámica. En este trabajo pionero la idea de bit de información está ya presente y es clave para entender el demonio. Landauer [20] establece formalmente esta interrelación en el siguiente principio: El borrado de un bit de información a temperatura T implica un coste energético de al menos $k_B T \ln 2$ [20]. Tal y como Bennett [21] señaló, el controlador (demonio) debe borrar su memoria —que almacena la información recogida— después de cada ciclo para permitir al sistema y al controlador operar de manera realmente cíclica. Así pues, el principio de Landauer puede verse como la clave para preservar la segunda ley de la termodinámica en los sistemas con control retroalimentado. Desde un enfoque basado en la complejidad algorítmica, Zurek [22, 23] establece cómo alcanzar la descripción más corta para el contenido de la memoria del demonio que permita minimizar el coste energético. Él propone comprimir el contenido de la memoria del demonio antes de borrarla. Esta compresión de la memoria puede realizarse, en principio, sin gasto nergético, es decir, puede realizarse reversiblemente [24]. Ello implica que la mínima energía requerida para borrar la memoria del demonio no viene dada por el número de bits almacenados, sino por el mínimo número de bits en los que puede almacenarse la información contenida en la memoria tras ser comprimida. Este resultado importante llama la atención sobre la relevancia de considerar si la información es redundante o no.

Estos límites fundamentales del control de los sistemas físicos pueden

estudiarse desde una perspectiva de la teoría de la información [25–27]. Recientemente, se ha establecido que la máxima cantidad de entropía ΔH_{closed} que se puede extraer de cualquier sistema dinámico con una actuación de ciclo cerrado está acotada superiormente por la disminución de entropía máxima que se puede alcanzar con un control de ciclo abierto ΔH_{open} más la información mutua entre el controlador C y el estado del sistema X [26,27]:

$$\Delta H_{\text{closed}} \leq \Delta H_{\text{open}} + I(X;C). \tag{4.13}$$

4.3 Objetivos de la tesis

Las ratchets retroalimentadas constituyen un importante campo de trabajo en la actualidad (véase por ejemplo el reciente artículo de revisión [17]). Dispositivos experimentales que implementan el llamado protocolo de maximización [15] se han propuesto y realizado recientemente [28]. Véase también las referencias [29,30] sobre máquinas moleculares sintéticas operando como ratchets retroalimentadas (o ratchets de información). Además, las ratchets retroalimentadas se han sugerido como un mecanismo capaz de explicar el movimiento de pasos de la kinesina de doble cabeza [31], y están también presentes en otros motores moleculares activados químicamente [32–34]. Por lo tanto, las ratchets con retroalimentación son relevantes no sólo como sistemas que nos permiten profundizar en los procesos fuera del equilibrio sino también como sistemas con potenciales aplicaciones en nanotecnología y biología.

Una vez que hemos introducido en esta Parte I de la tesis el material básico, estamos en condiciones de presentar nuestros resultados originales. En esta tesis presentamos un estudio de las ratchets con retroalimentación, y también de sistemas generales con control retroalimentado. Más específicamente, los objetivos de esta tesis son los siguientes:

1. Estudiar en detalle protocolos de control relevantes, centrándonos en su capacidad para incrementar el rendimiento (e.g. flujo y potencia). Este estudio permite además profundizar en los fenómenos no lineales y fuera del equilibrio. Ver capítulos 5, 6, 7, 8, 9 y 10 de la Parte II.

2. Investigar, desde una perspectiva teórica, la viabilidad de dispositivos ratchets experimentales con control retroalimentado que muestren un mejor rendimiento que los dispositivos de ciclo abierto. En particular, se estudian los efectos de retardos temporales y ruidos en la retroalimentación. Ver capítulos 6, 7, 9 y 10 de la Parte II.

3. Establecer relaciones entre el rendimiento de las ratchets con retroalimentación y la información que el controlador usa. Esto permite cuantificar el aumento del rendimiento de las ratchets de ciclo cerrado sobre sus homólogas de ciclo abierto en términos de la información,

que es lo que explícitamente diferencia unas de otras. Ver capítulos 9 y 10 de la Parte II.

4. Calcular la reducción de entropía en un sistema general con un control retroalimentado que se aplica repetidamente por parte del controlador externo. El cálculo de esta reducción de entropía era, hasta ahora, el ingrediente que faltaba para establecer la termodinámica de los sistemas con control retroalimentado. Ver capítulo 11 de la Parte II.

Presentamos en la siguiente Parte II nuestros resultados originales tal como fueron publicados en revistas internacionales. Estos resultados proporcionan respuestas a los objetivos de la tesis planteados arriba. Además de la discusión y conclusiones en cada artículo de la Parte II, incluimos en la Parte III una discusión general y las conclusiones finales.

Bibliografía

[1] R. F. Stengel, *Optimal Control and Estimation* (Dover, 1994).

[2] J. Bechhoefer, Rev. Mod. Phys. **77**, 783 (2005).

[3] P. Reimann, Phys. Rep. **361**, 57 (2002).

[4] H. Linke, Appl. Phys. A **75**, 167 (2002).

[5] P. Hänggi and F. Marchesoni, Rev. Mod. Phys. **81**, 387 (2009).

[6] P. Jung, J. G. Kissner, and P. Hänggi, Phys. Rev. Lett. **76**, 3436 (1996).

[7] J. L. Mateos, Phys. Rev. Lett. **84**, 258 (2000).

[8] K. Sekimoto, J. Phys. Soc. Jpn. **66**, 1234 (1997).

[9] J. M. R. Parrondo, J. M. Blanco, F. J. Cao, and R. Brito, Europhys. Lett. **43**, 248 (1998).

[10] A. Parmeggiani, F. Jülicher, A. Ajdari, and J. Prost, Phys. Rev. E **60**, 2127 (1999).

[11] M. O. Magnasco, Phys. Rev. Lett. **71**, 1477 (1993).

[12] A. Ajdari, and J. Prost, C. R. Acad. Sci. Paris II **315**, 1635 (1993).

[13] R. D. Astumian, and M. Bier, Phys. Rev. Lett. **72**, 1766 (1994).

[14] M. Feito and F. J. Cao, J. Stat. Mech. P01031 (2009).

[15] F. J. Cao, L. Dinis, and J. M. R. Parrondo, Phys. Rev. Lett. **93**, 040603 (2004).

[16] L. Dinis, J. M. R. Parrondo, and F. J. Cao, Europhys. Lett. **71**, 536 (2005).

[17] E. M. Craig, N. J. Kuwada, B. J. López, and H. Linke, Ann. Phys. **17**, 115 (2008).

[18] H. S. Leff and A. F. Rex, *Maxwell's Demon 2: Entropy, Classical and Quantum Information, Computing* (Institute of Physics, Bristol, 2003).

[19] L. Szilard, Z. Phys. **53**, 840 (1929).

[20] R. Landauer, IBM J. Res. Dev. **5**, 183 (1961).

[21] C. H. Bennett, Int. J. Theor. Phys. **21**, 905 (1982).

[22] W. H. Zurek, Phys. Rev. A **40**, 4731 (1989).

[23] W. H. Zurek, Nature **341**, 119 (1989).

[24] C. H. Bennett, IBM J. Res. Dev. **17**, 525 (1973).

[25] S. Lloyd, Phys. Rev. A **39**, 5378 (1989).

[26] H. Touchette and S. Lloyd, Phys. Rev. Lett. **84**, 1156 (2000).

[27] H. Touchette and S. Lloyd, Physica A **331**, 140 (2004).

[28] B. J. López, N. J. Kuwada, E. M. Craig, B. R. Long, and H. Linke, Phys. Rev. Lett. **101**, 220601 (2008).

[29] V. Serreli, C.-F. Lee, E. R. Ray, and D. Leigh, Nature (London) **445**, 523 (2007).

[30] E. R. Kay, D. Leigh, and F. Zerbetto, Angew. Chem. Int. Ed. **46**, 72 (2007).

[31] M. Bier, BioSystems **88**, 301 (2007).

[32] H. X. Zhou and Y. D. Chen, Phys. Rev. Lett., **77**, 194 (1996).

[33] R. D. Astumian and I. Derényi, Eur. Biophys. J **27**, 474 (1998).

[34] M. Álvarez-Pérez, S. M. Goldup, D. A. Leigh, and A. M. Z. Slawin, J. Am. Chem. Soc. **130**, 1836 (2008).

Parte II

Resultados

La estructura de esta Parte II es como sigue. En el siguiente capítulo 5 tratamos sobre el llamado protocolo de umbrales en ratchets de control retroalimentado. En los capítulos 6 y 7 llevamos a cabo un estudio analítico y numérico de la presencia de retardos temporales en el control de ratchets, que es una cuestión relevante para fines experimentales. En el capítulo 8 investigamos los efectos de añadir una fuerza oscilante periódica a una flashing ratchet colectiva de ciclo cerrado. En los siguientes capítulos presentamos nuestros resultados relacionados con la teoría de la información y la cuantificación del rendimiento. Es este sentido, los capítulos 9 y 10 se centran en la relación entre información y rendimiento (flujo y potencia máxima) en ratchets con control de ciclo cerrado. Finalmente, en el capítulo 11 establecemos la termodinámica de sistemas generales con control retroalimentado calculando la reducción de entropía en estos sistemas cuando son operados repetidamente por el controlador externo.

Chapter 5

Threshold feedback control for a collective flashing ratchet: Threshold dependence

PHYSICAL REVIEW E **74**, 041109 (2006)

Threshold feedback control for a collective flashing ratchet: Threshold dependence

M. Feito[1] and F. J. Cao[1,2]

[1] *Departamento de Física Atómica, Molecular y Nuclear, Universidad Complutense de Madrid, Avenida Complutense s/n, 28040 Madrid, Spain.*
[2] *LERMA, Observatoire de Paris, Laboratoire Associé au CNRS UMR 8112, 61, Avenue de l'Observatoire, 75014 Paris, France.*

We study the threshold control protocol for a collective flashing ratchet. In particular, we analyze the dependence of the current on the values of the thresholds. We have found analytical expressions for the small threshold dependence both for the few and for the many particle case. For few particles the current is a decreasing function of the thresholds, thus, the maximum current is reached for zero thresholds. In contrast, for many particles the optimal thresholds have a nonzero finite value. We have numerically checked the relation that allows to obtain the optimal thresholds for an infinite number of particles from the optimal period of the periodic protocol. These optimal thresholds for an infinite number of particles give good results for many particles. In addition, they also give good results for few particles due to the smooth dependence of the current up to these threshold values.

PACS numbers: 05.40.-a, 02.30.Yy

5.1 Introduction

Ratchets or Brownian motors are rectifiers of thermal fluctuations. This rectification is usually achieved through the introduction of an external deterministic or stochastic perturbation in a system that is or becomes asymmetric under spatial inversion [1]. Over the last years ratchets have been studied due to their theoretical and experimental relevance. From a practical point of view the ratchet effect has many potential applications in biology, condensed matter and nanotechnology [1, 2].

Ratchets can be viewed as controllers that act on stochastic systems with the aim of inducing directed motion through the rectification of the fluctuations. In particular, flashing ratchets are thermal fluctuation rectifiers based on switching on and off a periodic potential [3, 4]. Several studies deal with the problem of optimizing the particle current [5] or the efficiency [6] in these systems. However, they all consider only open-loop controllers (as that obtained with a periodic or random switching). Recently, feedback control protocols have been introduced in the context of collective ratchets [7, 8].

In the feedback control protocols the action of the controller depends on the state of the system. This feedback control, or closed-loop control, can be implemented in systems where the state of the system is monitored (as occurs in some experimental setups with colloidal particles [9]).

In this paper we study one of these closed-loop controls, the *threshold control*, previously introduced in Ref. [8]. The structure of the paper is as follows. In the next Section we present the mathematical model of the collective flashing ratchet with the threshold control protocol and we discuss briefly other protocols that have been studied in recent articles. Later, in Sec. 5.3, we analyze the dependence of the average center-of-mass velocity on the thresholds, obtaining analytical approximated expressions that are compared with the numerical results. In Subsec. 5.3.1 we study the small thresholds dependence (distinguishing the many particles case and the few particles case), while in Subsec. 5.3.2 we discuss the dependence of the average center-of-mass velocity for any thresholds and any number of particles. Finally, we present our conclusions in Sec. 5.4.

5.2 The model

We consider N Brownian particles with positions $x_i(t)$ at temperature T within a ratchet potential $V(x)$, and whose dynamics is described by the overdamped Langevin equations

$$\gamma \dot{x}_i(t) = \alpha(t) F(x_i(t)) + \xi_i(t); \qquad i = 1, \ldots, N, \tag{5.1}$$

with γ the friction coefficient (related to the diffusion coefficient D through Einstein's relation $D = k_B T/\gamma$) and $\xi_i(t)$ Gaussian white noises of zero mean satisfying the fluctuation-dissipation relation $\langle \xi_i(t)\xi_j(t')\rangle = 2\gamma k_B T \delta_{ij}\delta(t - t')$. The force is given by $F(x) = -V'(x)$ and α is a control parameter that can take only two possible values, $\alpha = 0$ (potential 'off') or $\alpha = 1$ (potential 'on').

Several control strategies have been studied in order to maximize the particle current in this system. The *optimal periodic switching* [7,8] consists on switching the potential on during a time period $\mathcal{T}_{\text{on}}$ and switching it off during $\mathcal{T}_{\text{off}}$. Note that it is an open-loop control protocol and therefore the results are independent of N. This protocol is the periodic flashing ratchet, that has been widely studied both theoretically and experimentally [1, 2]. The *maximization of the center-of-mass instant velocity* protocol has been introduced and studied in Ref. [7]. It consists on switching the potential on only if the net force would be positive. Therefore, it is a closed-loop control protocol, because it needs information about the state of the system in order to operate. This is the best strategy for a single particle. However, for a large number of particles the system gets trapped with the potential 'on' or 'off' and then the average steady state current tends to zero as N

increases [7]. Another closed-loop control protocol, the *threshold control*, was proposed in [8] to avoid this effect. In this paper we analyze it further.

The net force per particle is

$$f(t) = \frac{1}{N}\sum_{i=1}^{N} F(x_i(t)). \tag{5.2}$$

On the other hand, given the state of the system $x_i(t)$, a good estimator for the time derivative of $f(t)$ can be obtained using Langevin equation (5.1) and Ito calculus (see Ref. [8]),

$$\dot{f}_{\rm exp} \equiv \frac{1}{\gamma N}\sum_i \alpha(t)F(x_i(t))F'(x_i(t)) + \frac{k_B T}{\gamma N}\sum_i F''(x_i(t)). \tag{5.3}$$

The *maximization of center-of-mass instant velocity* protocol has $\alpha(t) = \Theta(f(t))$, with Θ the Heaviside function [$\Theta(x) = 1$ if $x > 0$, else $\Theta(x) = 0$]. In contrast, the *threshold control* policy has two thresholds $u_{\rm on} \geq 0$ and $u_{\rm off} \leq 0$ which induce earlier switchings that permit to avoid the trapping. When $f(t)$ decreases below $u_{\rm on}$ we switch off the potential, although the net force is still positive, in order to avoid the trapping. Analogously the potential is switched on if the net force per particle increases above $u_{\rm off}$, so we induce the flipping of the system before $f(t)$ is positive. Therefore, the *threshold control* is given by

$$\alpha(t) = \begin{cases} 1 & \text{if } f(t) \geq u_{\rm on}, \\ 1 & \text{if } u_{\rm off} < f(t) < u_{\rm on} \text{ and } \dot{f}_{\rm exp}(t) \geq 0, \\ 0 & \text{if } u_{\rm off} < f(t) < u_{\rm on} \text{ and } \dot{f}_{\rm exp}(t) < 0, \\ 0 & \text{if } f(t) \leq u_{\rm off}. \end{cases} \tag{5.4}$$

This scheme removes the long decaying tails in the evolution of the net force preventing the trapping. Note that this protocol and the maximization of the center-of-mass instant velocity protocol are feedback controls or closed-loop controls. The threshold control protocol in the zero thresholds limit gives the maximization of the center-of-mass instant velocity protocol.

5.3 Threshold control strategy

5.3.1 Small thresholds

In this subsection we analyze the threshold control strategy improving and extending the analytic expressions found for the maximization of the center-of-mass instant velocity protocol [7].

Many particles: quasideterministic approximation

For many particles (large N) the net force has a quasideterministic behavior. It can be described in terms of two contributions, a deterministic contribution f^∞ (given by the behavior for an infinite number of particles) plus a small stochastic contribution

$$f(t) = f^\infty(t) + \text{fluctuations}. \tag{5.5}$$

This approximate description has proven to be fruitful in order to understand the behavior of these ratchets in the many particle case [7].

The deterministic contribution, that reflects the behavior of the system for an infinite number of particles ($N \to \infty$), can be described through a particle distribution $\rho(x,t)$ that evolves according to the mean-field Fokker-Planck equation $\gamma\partial_t\rho(x,t) = \left[-\alpha(t)\partial_x F(x) + k_B T\partial_x^2\right]\rho(x,t)$. The net force per particle is a deterministic function $f^\infty(t) = \langle F(x)\rangle_\rho \equiv \int_0^L dx\,\rho(x,t)F(x)$, with L the period of the ratchet potential. The net force is zero for the equilibrium distribution when the potential is on and also when it is off. We denote by $f_\nu^\infty(t)$ with $\nu =$ on,off the value of the deterministic part of the net force when the system has been evolving with the potential on or off respectively a time t after a switching. After a certain time τ_ν it can be approximately described by [7]

$$f_\nu^\infty(t) = C_\nu e^{-\lambda_\nu(t-\tau_\nu)}. \tag{5.6}$$

C_ν and λ_ν are constants that are obtained by fitting the net force obtained with the Fokker-Planck equation. In order to obtain $f_{\text{on}}^\infty(t)$ we evolve the equilibrium distribution for the off potential with the Fokker-Planck equation with the potential on, i.e., we assume that the system was close to the equilibrium state for the off potential before the off-on switching. We proceed analogously for $f_{\text{off}}^\infty(t)$.

On the other hand, the amplitude of the fluctuations of the net force f can be estimated as [7]

$$\Sigma = \sqrt{\langle f^2(t)\rangle - \langle f(t)\rangle^2} \simeq \sqrt{\frac{\langle F^2\rangle_\rho - \langle F\rangle_\rho^2}{N}} \sim \frac{V_0}{L\sqrt{a(1-a)N}}. \tag{5.7}$$

This simple result is a good estimation of the amplitude of the fluctuations for potentials with characteristic height V_0 and asymmetry a. For example, the potential

$$V(x) = \frac{2V_0}{3\sqrt{3}}\left[\sin\left(\frac{2\pi x}{L}\right) + \frac{1}{2}\sin\left(\frac{4\pi x}{L}\right)\right], \tag{5.8}$$

that we have used for the figures of this article, has characteristic height V_0 and characteristic asymmetry $a = 1/3$ (where aL is defined as the minimum

distance between a minimum and a maximum of the potential, with L being the period of the potential).

We have already provided estimations for both the deterministic part of the net force per particle and the amplitude of its fluctuations. This will allow us to calculate the average current.

First, we compute the characteristic times during which the potential remains on, $t_{\rm on}$, and off, $t_{\rm off}$. In the threshold control protocol the switching happens when the force crosses the threshold value with the appropriate slope [see Eq. (5.4)]. When the threshold is crossed the equality $u_\nu = f_\nu(t_\nu)$ is satisfied, with $f_\nu(t)$ the value of the net force a time t after a switching. Therefore, using the quasideterministic approximation (5.5) we obtain for the characteristic times

$$|f_\nu^\infty(t_\nu)| - \Sigma = |u_\nu|. \tag{5.9}$$

Using Eq. (5.6) we get the following explicit equations for the characteristic times

$$t_\nu = \tau_\nu + \frac{1}{\lambda_\nu} \ln \frac{|C_\nu|}{|u_\nu| + \Sigma}, \tag{5.10}$$

with Σ given by Eq. (5.7). Moreover, Eq. (5.6) implies that this approximation is valid for $t_\nu \gtrsim \tau_\nu$, where τ_ν are the transient times for each dynamics (afterwards, Eq. (5.6) is a good approximation). This implies $|u_\nu| + \Sigma \ll |C_\nu|$, that can be expressed as $|u_\nu| + \Sigma \ll \max_t |f_\nu^\infty(t)|$ by using $|C_\nu| \sim \max_t |f_\nu^\infty(t)|$. As $\Sigma \sim 1/\sqrt{N}$, we see that this approximation is valid for small thresholds and large number of particles.

We now compute the average displacement of the center-of-mass during an on-off period. Note that the center-of-mass moves only when the potential is 'on', because when it is 'off' the dynamics is purely diffusive. Therefore, as the center-of-mass position is $x_{\rm cm} = \sum_i x_i/N$, its average displacement during an on-off cycle in the many particle case is given by using the evolution equations (5.1) as

$$\Delta x_{\rm cm}(t_{\rm on}) = \frac{1}{\gamma} \int_0^{t_{\rm on}} f_{\rm on}^\infty(t)\, dt. \tag{5.11}$$

The integration of the late time expression (5.6) with $\nu =$ on suggests a functional form

$$\Delta x_{\rm cm}(t_{\rm on}) = \Delta x_{\rm on} \left(1 - e^{-t_{\rm on}/\Delta t_{\rm on}}\right). \tag{5.12}$$

This functional form fits well the function $\Delta x_{\rm cm}(t_{\rm on})$ obtained from the numerical integration of the Fokker-Planck equation, and this fit is used to determine $\Delta x_{\rm on}$ and $\Delta t_{\rm on}$. We have seen that the inclusion of the characteristic time $\Delta t_{\rm on}$ improves the analytical results obtained in Ref. [7] (there

it was assumed $\Delta x_{\rm cm}(t_{\rm on}) = \Delta x_{\rm on}$). This better estimation of the average displacement improves the results for the intermediate regime of not-so-large number of particles. Furthermore, the whole expression (5.12) is also necessary to improve the results for nonzero thresholds. When thresholds are enlarged the frequency of switching increases and therefore the times $t_{\rm on}$ decrease. This implies a shorter displacement, as Eq. (5.12) predicts.

The previous results allows us to give an approximate expression for the average center-of-mass velocity in the stationary regime,

$$\begin{aligned}\langle \dot{x}_{\rm cm}\rangle_{\rm st} &\equiv \lim_{t\to\infty}\frac{x_{\rm cm}(t)-x_{\rm cm}(0)}{t} = \frac{\Delta x_{\rm on}}{t_{\rm on}+t_{\rm off}}\left(1-e^{-t_{\rm on}/\Delta t_{\rm on}}\right)\\ &= \frac{\Delta x_{\rm on}\left[1-A\,(u_{\rm on}+\Sigma)^{1/(\lambda_{\rm on}\Delta t_{\rm on})}\right]}{B-\frac{1}{\lambda_{\rm on}}\ln(u_{\rm on}+\Sigma)-\frac{1}{\lambda_{\rm off}}\ln(|u_{\rm off}|+\Sigma)},\end{aligned} \tag{5.13}$$

with Σ given by Eq. (5.7), and A and B given by

$$A = e^{-\tau_{\rm on}/\Delta t_{\rm on}} C_{\rm on}^{-1/(\lambda_{\rm on}\Delta t_{\rm on})}\,, \qquad B = \tau_{\rm on}+\tau_{\rm off}+\frac{1}{\lambda_{\rm on}}\ln C_{\rm on}+\frac{1}{\lambda_{\rm off}}\ln|C_{\rm off}|\,.$$

The final expression in Eq. (5.13) shows the explicit dependence on the thresholds $u_{\rm on}$, $u_{\rm off}$, and on the amplitude of the force fluctuations Σ; all the other parameters are determined by the dynamics for an infinite number of particles with zero thresholds. Eq. (5.13) has been obtained in the quasideterministic approximation and therefore is valid when the number of particles N is large and the thresholds are small as discussed after Eq. (5.10). We have verified that it gives good estimations inside its regime of validity. In particular, for zero thresholds Eq. (5.13) is better than the formula obtained in Ref. [7] thanks to the introduction of the characteristic time $\Delta t_{\rm on}$. (The formula in Ref. [7] is recovered for $u_{\rm on} = u_{\rm off} = 0$ and $\Delta t_{\rm on} = 0$.)

Figs. 5.1-5.3 compare the predictions of the quasideterministic approximation, Eq. (5.13), with the numerical results for the threshold control protocol applied with the potential (5.8) and $V_0 = 5k_BT$. For this potential the fit to the Fokker-Planck evolution gives $C_{\rm on} = 0.67k_BT/L$, $\tau_{\rm on} = 0.058L^2/D$, $\lambda_{\rm on} = 28D/L^2$, $C_{\rm off} = -0.74k_BT/L$, $\tau_{\rm off} = 0.037L^2/D$, $\lambda_{\rm off} = 39D/L^2$, and $\Delta x_{\rm on} = 0.08L$, $\Delta t_{\rm on} = 0.05L^2/D$.

In Fig. 5.1 we plot the current as a function of the threshold $u_{\rm on}$ (with $u_{\rm off} = -u_{\rm on}$) comparing the quasideterministic approximation (5.13) and the numerical results obtained from the Langevin evolution equations (5.1). We see that the quasideterministic approximation gives a good estimation of the current. However, it fails to predict the minimum located at low threshold values. This minimum is caused by a secondary effect that has not been accounted in the deduction of the analytic formula. This secondary effect is due to the fact that nonzero thresholds have the disadvantage of not being instantly optimal, because they imply switching on the potential when the force is still negative and switching off the potential when the force

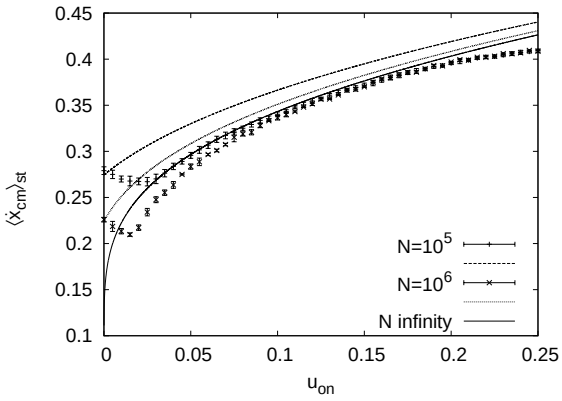

Figure 5.1: Average of the center-of-mass velocity $\langle \dot{x}_{\rm cm} \rangle_{\rm st}$ as a function of the threshold $u_{\rm on}$ for numbers of particles $N = 10^5, 10^6$ and the limit $N \to \infty$ for the potential (5.8) with $V_0 = 5k_BT$. Analytical quasideterministic approximation (5.13) (lines) and numerical results from Langevin equations (5.1) (points with error bars). We have taken $u_{\rm off} = -u_{\rm on}$. (Units: $L = 1$, $D = 1$, $k_BT = 1$.)

is still positive. In addition, for very small thresholds the switchings are not induced much earlier than they would be with zero thresholds due to the force fluctuations. Thus, there is a minimum located at thresholds of order $1/\sqrt{N}$, the magnitude of the force fluctuations. For larger threshold this secondary effect of the thresholds is overcompensated by the main effect of avoiding the undesired trapping of the dynamics. This main effect allows to have similar average displacements of the particles in a shorter on-off cycle time. Therefore, larger thresholds increase the average center-of-mass velocity.

Figs. 5.2 and 5.3 compare analytic and numerical results for the current as a function of the number of particles for fixed nonzero thresholds: Fig. 5.2 for $u_{\rm on} = -u_{\rm off} = 0.1k_BT/L$ and Fig. 5.3 for $u_{\rm on} = 0.6k_BT/L$ and $u_{\rm off} = -0.4k_BT/L$ (which are the optimal values for an infinite number of particles). In Fig. 5.2 we see that the quasideterministic approximation gives a good estimation for large number of particles. In Fig. 5.3 the estimate is more rough due to the fact that the thresholds do not strictly verify the validity condition of the quasideterministic approximation ($|u_\nu| + \Sigma \ll |C_\nu|$). Another interesting result we have found is that for fixed nonzero thresholds the average velocity as a function of N tends to a constant asymptotic value for large number of particles, as Eq. (5.13) predicts. For an infinite number of particles the force fluctuations vanishes, thus, this asymptotic value is given by Eq. (5.13) evaluated at $\Sigma = 0$. See Figs. 5.2 and 5.3.

The optimal threshold protocol gives the same current or better than the

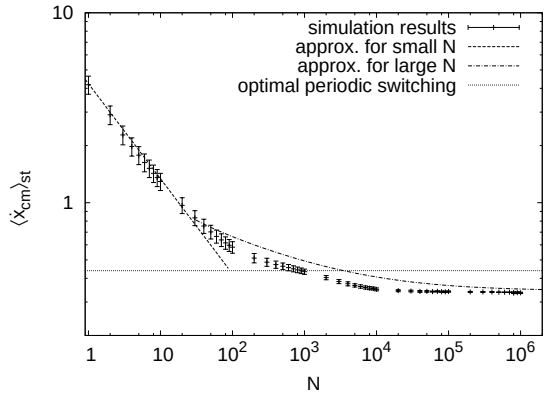

Figure 5.2: Average of the center-of-mass velocity $\langle \dot{x}_{\rm cm} \rangle_{\rm st}$ as a function of the number of particles N for the potential (5.8) with $V_0 = 5k_BT$ and for thresholds $u_{\rm on} = 0.1$ and $u_{\rm off} = -0.1$. The simulations results obtained solving numerically the Langevin equations (5.1) (points with error bars) are compared with the quasideterministic approximation for large N [Eq. (5.13)] and the pure stochastic approximation for small N [Eq. (5.19)]. The dotted horizontal straight line corresponds to the periodic switching protocol with optimal periods. (Units: $L = 1$, $D = 1$, $k_BT = 1$.)

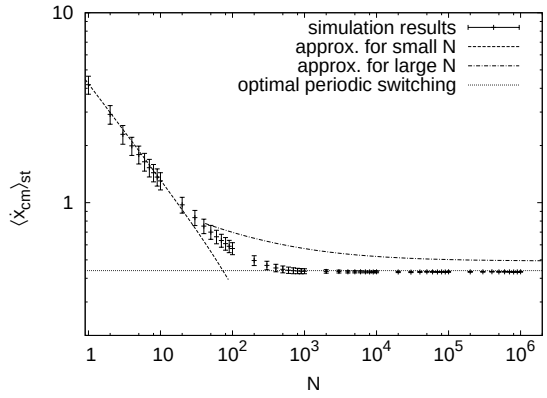

Figure 5.3: Average of the center-of-mass velocity $\langle \dot{x}_{\rm cm} \rangle_{\rm st}$ as a function of the number of particles N for the potential (5.8) with $V_0 = 5k_BT$ and for thresholds $u_{\rm on} = 0.6$ and $u_{\rm off} = -0.4$ (optimal values for $N \to \infty$). The simulations results obtained solving numerically the Langevin equations (5.1) (points with error bars) are compared with the quasideterministic approximation for large N [Eq. (5.13)] and the pure stochastic approximation for small N [Eq. (5.19)]. The dotted horizontal straight line corresponds to the periodic switching protocol with optimal periods. (Units: $L = 1$, $D = 1$, $k_BT = 1$.)

optimal periodic control [8] (Fig. 5.3). In particular, for an infinite number of particles the force fluctuations become negligible and the threshold control becomes equivalent to a periodic switching. The relation between the thresholds and the periods [8]

$$u_\nu = f_\nu^\infty(\mathcal{T}_\nu) \tag{5.14}$$

is obtained here as the limit $N \to \infty$, i.e. $\Sigma = 0$, of Eq. (5.9). This relation permits to get the optimal thresholds for an infinite number of particles from the optimal periods just using the functions $f_{\rm on}^\infty(t)$ and $f_{\rm off}^\infty(t)$ obtained numerically from the Fokker-Planck equation. This avoids the need of integrating numerically N coupled Langevin equations for large values of N. We have numerically checked that the expression (5.14) gives the optimal thresholds (see Sec. 5.3.2 and Fig. 5.7).

Few particles: pure stochastic approximation

When we have few particles the situation is the opposite to that considered in the previous section and the net force has nearly a pure stochastic behavior. A binomial distribution is found for the net force probability distribution, $p(f)$, in Ref. [7] under the approximations that the position of the particles are statistically independent and that the probability of finding a particle in the interval $[0, aL]$ is a. For simplicity this binomial distribution for the net force can be approximated by a Gaussian distribution

$$p(f) \simeq \frac{1}{\sqrt{2\pi\Sigma^2}}\, e^{-\frac{f^2}{2\Sigma^2}}, \tag{5.15}$$

with Σ the amplitude of the fluctuations of the net force, that is given by Eq. (5.7). Neglecting the time correlations in the net force, the average center-of-mass velocity for the threshold protocol [Eq. (5.4)] is given by

$$\langle \dot{x}_{\rm cm}\rangle_{\rm st} = \frac{1}{\gamma}\int_{u_{\rm on}}^{\infty} f p(f)\, df + \frac{1}{\gamma}\int_{u_{\rm off}}^{u_{\rm on}} f p_+(f)\, df\ , \tag{5.16}$$

with $p_+(f)$ the probability of having a net force f and a non-negative value of $\dot{f}_{\rm exp}$ [$p_+(f) \sim p(f)/2$]. This implies that, in the validity range of this small N approximation [$\Sigma \gtrsim \max_t |f^\infty(t)|$], the current is a decreasing function of the threshold $u_{\rm on}$, as can be easily proven comparing the results for $u'_{\rm on}$ and $u_{\rm on}$ with $0 \le u'_{\rm on} < u_{\rm on}$. Eq. (5.16) gives

$$\langle \dot{x}_{\rm cm}\rangle_{\rm st}(u'_{\rm on}) - \langle \dot{x}_{\rm cm}\rangle_{\rm st}(u_{\rm on}) = \frac{1}{\gamma}\int_{u'_{\rm on}}^{u_{\rm on}} f p_-(f)\, df, \tag{5.17}$$

with $p_-(f) \equiv p(f) - p_+(f) \ge 0$. Thus, the last term in the previous expression is non-negative implying

$$\langle \dot{x}_{\rm cm}\rangle_{\rm st}(u'_{\rm on}) - \langle \dot{x}_{\rm cm}\rangle_{\rm st}(u_{\rm on}) \ge 0. \tag{5.18}$$

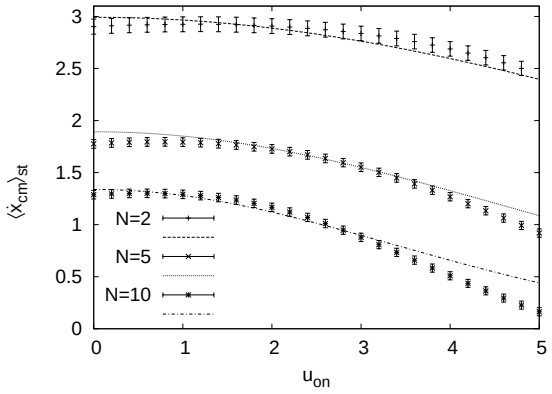

Figure 5.4: Average of the center-of-mass velocity $\langle \dot{x}_{\rm cm} \rangle_{\rm st}$ as a function of the threshold $u_{\rm on}$ for $N = 2, 5,$ and 10 particles for the potential (5.8) with $V_0 = 5k_BT$. Analytical pure stochastic approximation (5.19) (lines) and numerical results from Langevin equations (5.1) (points with error bars) are compared. We have taken $u_{\rm off} = -u_{\rm on}$. (Units: $L = 1$, $D = 1$, $k_BT = 1$.)

Analogously, it can be shown that for $0 \geq u'_{\rm off} > u_{\rm off}$ we have $\langle \dot{x}_{\rm cm} \rangle_{\rm st}(u'_{\rm off}) - \langle \dot{x}_{\rm cm} \rangle_{\rm st}(u_{\rm off}) = (1/\gamma) \int_{u_{\rm off}}^{u'_{\rm off}} (-f) p_+(f) df \geq 0$. This shows that the average center-of-mass velocity is a decreasing function for increasing modulus of the thresholds. Therefore, for small N we get the maximum current for zero thresholds.

For small thresholds we have found an approximate explicit analytical expression for the current. If $u_{\rm off} \simeq -u_{\rm on}$ the contribution of the second integral in Eq. (5.16) is generally small, because it is the integration of a nearly odd function in a nearly symmetric interval around zero. On the other hand, the contribution of the first integral is greater provided the thresholds are small ($u_{\rm on} \lesssim \Sigma$). Then, neglecting the second integral we obtain

$$\langle \dot{x}_{\rm cm} \rangle_{\rm st} \simeq \frac{\Sigma}{\gamma \sqrt{2\pi}} \, e^{-\frac{u_{\rm on}^2}{2\Sigma^2}}. \tag{5.19}$$

(Note that for $u_{\rm on} = 0$ we recover the zero threshold result found in Ref. [7].) This expression, Eq. (5.19), gives good predictions when we have few particles and small thresholds. In particular, we show in Figs. 5.2-5.4 that it correctly predicts the threshold and particle number dependence of the current, even for $u_{\rm on} \sim \Sigma \simeq 3.4$ when $N = 10$ (Fig. 5.4).

5.3.2 General thresholds

In the previous subsection we have studied the threshold protocol when the moduli of the thresholds are small, obtaining approximate analytical expres-

sions for the current. In contrast, in this subsection we study the threshold protocol for general thresholds (that are in general beyond the applicability range of the previous analytical expressions). This study is done performing numerical simulations of the Langevin equation of the threshold protocol for general values of the thresholds.

$u_{\mathbf{off}} = -u_{\mathbf{on}}$

Let us discuss first the results for thresholds that are related by $u_{\rm off} = -u_{\rm on}$.

In the few particle case, when the thresholds are small the current decreases exponentially with the square of the threshold as we have already seen [see Eq. (5.19)]. However, as the rate of the exponential is small, we nearly have a plateau near the maximum at zero thresholds, as shown in Figs. 5.4 and 5.5. On the other hand, for very large thresholds Eq. (5.19) is no longer valid and the current decreases faster than the exponential. Note that the current continues to be a decreasing function, as predicted by Eq. (5.18) (valid for any threshold values in the few particle case). See Figs. 5.4 and 5.5.

In contrast, in the many particle case the maximum of the current is no longer at zero thresholds, but at a finite value. As we have explained before, the introduction of thresholds has the advantage of inducing earlier switchings. This avoids the undesired trapping that otherwise is present for large N implying low current values. The presence of thresholds allows to have similar average displacements of the particles in a shorter on-off cycle time, and therefore increases the average center-of-mass velocity. However, if the thresholds are too large the losses in the displacement become more important than the gains of shortening the on-off cycle time. Therefore, the current has a maximum located at a finite value of the thresholds in the many particle case (Fig. 5.5). (The tiny minimum in the small threshold region is related to another effect: the disadvantages of choosing a not instantly optimal protocol. For a more detailed explanation see Subsec. 5.3.1.)
Another important result in the many particle case is that the maximum obtained for the current as a function of the threshold magnitude is quite flat and nearly independent of the number of particles. See Fig. 5.5.

In summary, in the many particle case the current has a maximum for nonzero thresholds whose position is nearly independent of the number of particles. On the other hand, for few particles the current is maximum for zero thresholds. However, in the few particle case the current is nearly the same up to thresholds of the order of the thresholds that give the maximum for the many particle case (see Figs. 5.4 and 5.5). This has an important implication: the optimal thresholds values for the many particle case give currents close to the maximum for *any* number of particles.

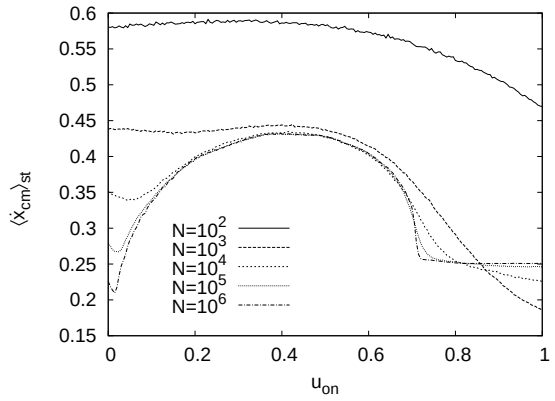

Figure 5.5: Average of the center-of-mass velocity $\langle \dot{x}_{\rm cm} \rangle_{\rm st}$ as a function of the threshold $u_{\rm on}$ with $u_{\rm off} = -u_{\rm on}$ for various N. The lines correspond to the numerical solution of the Langevin equations (5.1) for the potential (5.8) with $V_0 = 5k_BT$. (Units: $L = 1$, $D = 1$, $k_BT = 1$.)

$u_{\rm off} \neq -u_{\rm on}$

The study of the current for completely general thresholds $u_{\rm on}$ and $u_{\rm off}$ (without restrictions) reveals that the behavior is analogous to that described previously. In fact, the optimal thresholds for large number of particles are located not far from the line $u_{\rm on} = -u_{\rm off}$, and these thresholds give currents close to the maximum for any number of particles. (See Figs. 5.6 and 5.7.)

As we have already commented in the previous section, for an infinite number of particles the force fluctuations becomes negligible and the threshold protocol becomes equivalent to a periodic switching. This implies the relation (5.14) between the optimal periods $\mathcal{T}_{\rm on}$ and $\mathcal{T}_{\rm off}$, and the optimal thresholds $u_{\rm on}$ and $u_{\rm off}$, that we have numerically checked (see Fig. 5.7). Therefore, these relations permit to obtain the optimal thresholds for an infinite number of particles from the optimal periods, just using the functions $f^{\infty}_{\rm on}(t)$ and $f^{\infty}_{\rm off}(t)$ obtained numerically from the Fokker-Planck equation. These thresholds give good results for large number of particles. Moreover, it is important to note that these thresholds values also give currents close to the maximum in the few particles case due to the smooth dependence for small thresholds (see Figs. 5.5-5.7).

In particular, we have seen that for the potential (5.8) with $V_0 = 5k_BT$ the optimal switching periods are approximately $\mathcal{T}_{\rm on} = 0.06L^2/D$ and $\mathcal{T}_{\rm off} = 0.05L^2/D$. Therefore, with just a Fokker-Planck simulation for the potential we have found that a good estimation of the optimal thresholds is given by $u_{\rm on} = f^{\infty}_{\rm on}(\mathcal{T}_{\rm on}) = 0.6k_BT/L$ and $u_{\rm off} = f^{\infty}_{\rm off}(\mathcal{T}_{\rm off}) = -0.4k_BT/L$, in good agreement with Fig. 5.7.

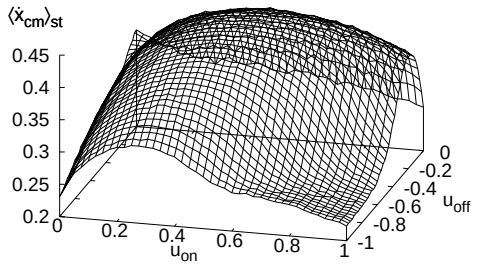

Figure 5.6: Thresholds dependence of the average of the center-of-mass velocity $\langle \dot{x}_{\rm cm} \rangle_{\rm st}$ for $N = 10^4$ particles in the potential (5.8) with $V_0 = 5k_BT$. The grid has been obtained integrating numerically Langevin equations (5.1) for different thresholds $u_{\rm on}$ and $u_{\rm off}$ (Units: $L = 1$, $D = 1$, $k_BT = 1$.)

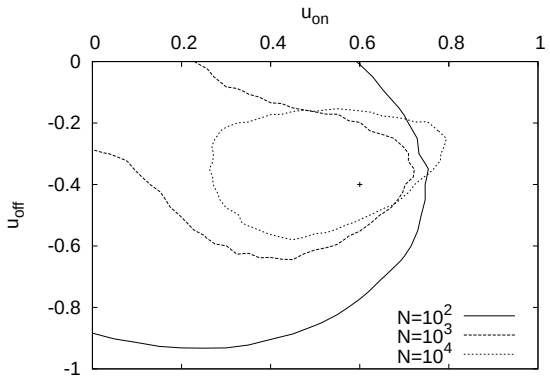

Figure 5.7: Thresholds contour lines corresponding to the value of the average of the center-of-mass velocity $\langle \dot{x}_{\rm cm} \rangle_{\rm st}$ 5% below its maximum for $N = 10^2$, $N = 10^3$ and $N = 10^4$ particles in the potential (5.8) with $V_0 = 5k_BT$. The contour line for $N = 10^5$ is already very similar to that for $N = 10^4$. The point corresponds to the optimal thresholds for $N \to \infty$ obtained from the optimal periods using Eq. (5.14). (Units: $L = 1$, $D = 1$, $k_BT = 1$.)

5.4 Conclusions

In this paper we have analyzed the *threshold control* protocol for a collective flashing ratchet. We have studied the threshold dependence of the current in this closed-loop control protocol. The quasideterministic (for many particles) approximation [7] has been improved through the introduction of an additional characteristic time giving better results for not-so-many particles. Both the quasideterministic and the stochastic (for few particles) approximations [7] have been applied to the threshold control protocol. This has led to analytical expressions for large and small number of particles. We have computed numerically the current dependence on the thresholds and on the number of particles obtaining a good agreement between analytical and numerical results in the validity range of our assumptions. We have also compared these results with the *optimal periodic switching* protocol.

We have seen that for many particles the current has a maximum for nonzero thresholds whose position is nearly independent of the number of particles. On the other hand, for few particles we have demonstrated that the current increases as thresholds moduli decrease, so the maximum current is reached at zero thresholds. However, the current is nearly the same up to thresholds of the order of the optimal thresholds for the many particle case. This implies that the optimal thresholds values for the many particle case give currents close to the maximum for any number of particles. The optimal thresholds for an infinite number of particles can be obtained from the optimal periods of the periodic protocol just solving the Fokker-Planck equation in two particular cases (potential 'on' and 'off', see Section 5.3.1). Therefore, we can get a good estimation of the optimal thresholds for many particles, that also gives currents close to the optimal for any number of particles as we have shown.

The closed-loop threshold control gives the same current as the optimal protocols for the one particle case and for an infinite number of particles, and it gives high currents in between. However, obtaining the best protocol for the maximization of the current is still an open question.

In this work, and in previous ones [7, 8], we have seen that thanks to the information about the fluctuations obtained through the feedback, the performance of the system can be increased. This increase of the performance has thermodynamical limitations that have been studied in a general context for the efficiency [10]. We are now working in order to get a deeper understanding of this interplay between the information and the increase of the performance [11].

Acknowledgments

We acknowledge financial support from the Ministerio de Ciencia y Tecnología (Spain) through the Research Projects BFM2003-02547/FISI and FIS2006-05895. In addition, MF thanks the Universidad Complutense de Madrid (Spain) and FJC thanks ESF Programme STOCHDYN for their financial support.

Bibliography

[1] P. Reimann, Phys. Rep. **361**, 57 (2002).

[2] H. Linke, Appl. Phys. A **75**, 167 (2002).

[3] A. Adjari and J. Prost, C. R. Acad. Sci. Paris II **315**, 1635 (1992).

[4] R.D. Astumian and M. Bier, Phys. Rev. Lett. **72**, 1766 (1994).

[5] M. B. Tarlie, and R. D. Astumian, Proc. Natl. Acad. Sci. **95**, 2039 (1998).

[6] J. M. R. Parrondo, J. M. Blanco, F. J. Cao, and R. Brito, Europhys. Lett. **43**, 248 (1998).

H. Kamegawa, T. Hondou, F. Takagi, Phys. Rev. Lett. **80**, 5251 (1998).

I. Sokolov, Phys. Rev. E **63**, 021107 (2001).

[7] F. J. Cao, L. Dinis and J. M. R. Parrondo, Phys. Rev. Lett. **93**, 040603 (2004).

[8] L. Dinis, J. M. R. Parrondo and F. J. Cao, Europhys. Lett. **71**, 536 (2005).

[9] J. Rousselet, L. Salome, A. Ajdari, and J. Prost, Nature **370**, 040603 (2004).

C. Marquet, A. Buguin, L. Talini, and P. Silberzan, Phys. Rev. Lett. **88**, 168301 (2002).

[10] H. Touchette, and S. Lloyd, Phys. Rev. Lett. **84**, 1156 (2000); Physica (Amsterdam) **331A**, 140 (2004).

[11] Work in progress.

[12] L. Dinis, PhD Thesis, Universidad Complutense de Madrid (2005).

Chapter 6

Time-delayed feedback control of a flashing ratchet

PHYSICAL REVIEW E **76**, 061113 (2007)

Time-Delayed Feedback control of a flashing ratchet

M. Feito[1] and F. J. Cao[1,2]

[1] *Departamento de Física Atómica, Molecular y Nuclear, Universidad Complutense de Madrid, Avenida Complutense s/n, 28040 Madrid, Spain.*
[2] *LERMA, Observatoire de Paris, Laboratoire Associé au CNRS UMR 8112, 61, Avenue de l'Observatoire, 75014 Paris, France.*

Closed-loop or feedback control ratchets use information about the state of the system to operate with the aim of maximizing the performance of the system. In this paper we investigate the effects of a *time delay* in the feedback for a protocol that performs an instantaneous maximization of the center-of-mass velocity. For the *one* and the *few particle* cases the flux decreases with increasing delay, as an effect of the decorrelation of the present state of the system with the information that the controller uses, but the delayed closed-loop protocol succeeds to perform better than its open-loop counterpart provided the delays are smaller than the characteristic times of the Brownian ratchet. For the *many particle* case, we also show that for small delays the center-of-mass velocity decreases for increasing delays. However, for large delays we find the surprising result that the presence of the delay can improve the performance of the nondelayed feedback ratchet and the flux can attain the maximum value obtained with the optimal periodic protocol. This phenomenon is the result of the emergence of a dynamical regime where the presence of the delayed feedback stabilizes one quasiperiodic solution or several (multistability), which resemble the solutions obtained in the so-called threshold protocol. Our analytical and numerical results point towards the feasibility of an *experimental implementation* of a feedback controlled ratchet that performs equal or better than its optimal open-loop version.

PACS numbers: 05.40.-a, 02.30.Yy

6.1 Introduction

The ratchet effect consists of the emergence of a directed transport in a spatially periodic system out of equilibrium through the introduction of an external perturbation. The celebrated ideas of rectifying thermal noise, originally introduced by Smoluchowski [1] and later resumed by Feynman [2], were explicitly used in the context of directed transport in the 1990s [3–5]. Since then, these systems have been studied due to its importance from a

theoretical point of view in nonequilibrium physics [6] and its applications to many other fields such as condensed matter or biology [6, 7].

One of the main ratchet types are the flashing ratchets that operate switching on and off a spatially periodic asymmetric potential. A simple periodic or random switching is able to achieve a rectification of thermal fluctuations and produce a net current of particles. Recently, a new class of control protocols that use instant information about the state of the system to take the decision of switching on or off have been introduced [8]. These so-called closed-loop or feedback control protocols have been proven to be an effective way to increase the net current in collective Brownian ratchets [8–10]. Feedback control can be implemented in systems where particles are monitored [11, 12]. This monitoring gives information about the position of the particles that can be used to switch on or off the potential in real time according to a given protocol. For instance, in Ref. [11] the motion of colloidal particles induced by a sawtooth dielectric potential, which is turned on and off periodically, is experimentally studied monitoring the particles. This suggest that a feedback controlled version of the ratchet in [11] can be constructed gathering information about the state of the system with a charge coupled device (CCD) camera and using this information to decide whether to turn on and off the potential in real time. In addition, feedback ratchets have been recently suggested as a mechanism to explain the stepping motion of the two-headed kinesin [13].

All Brownian feedback ratchets considered until now use instant information to operate, that is, they all measure the state of the system and act *instantaneously* according to that measurement. However, in realistic devices there is always a time delay between the input measurements and the output control action due to physical limitations to the velocity of transmission and processing of the information [14, 15]. For example, in the construction of the feedback controlled version of the ratchet in [11] time delays in the feedback will be present due to the finite time needed to take a picture with a CCD camera, transmit it, process it, and implement the resulting decision of switching on or off the potential. Therefore it is important to compute the effects of time delays in the feedback, because it clarifies in which real ratchet systems it is experimentally feasible to obtain the increase of velocity predicted in [8]. The study of time-delayed feedback is also relevant because it appears naturally in many stochastic processes, such as complex systems with self-regulating mechanisms [16, 17]. For another type of ratchets, deterministic feedback ratchets, some of the effects of time delay in the feedback have been studied [18, 19].

In the current paper we investigate how a time delay in the control of a feedback flashing ratchet affects the net flux. In the next section we describe the ratchet model with the time-delayed feedback control policy. In Sec. 6.3 we study in detail the case of one particle, getting an effective potential description for the flux in the relevant case of small time delays. We also

present an alternative approach to understanding the dependence of the flux with time delay in terms of the covariance, and we describe the behavior for large delays. In Sec. 6.4 we treat the collective ratchet with few particles and relate its center-of-mass velocity with the one particle flux previously studied. In Sec. 6.5 we study the many particle ratchet, which exhibits a somehow counterintuitive behavior; first we briefly review the results for zero delays that will be useful, and thereafter we expose the results in the two dynamical regimes of small delays and large delays. Finally, all the results are summarized and discussed in Sec. 6.6.

6.2 Model

We consider N overdamped Brownian particles at temperature T in a ratchet potential $V(x)$. The force acting on the ith particle at position $x_i(t)$ is $\alpha(t)F(x_i(t))$, where $F(x) = -V'(x)$ and $\alpha(t)$ implements the action of the controller. Therefore the system dynamics is defined by the Langevin equations

$$\gamma \dot{x}_i(t) = \alpha(t)F(x_i(t)) + \xi_i(t); \quad i = 1, \ldots, N, \tag{6.1}$$

where γ is the friction coefficient (related to the diffusion coefficient D through Einstein's relation $D = k_B T/\gamma$) and $\xi_i(t)$ are Gaussian white noises of zero mean and variance $\langle \xi_i(t)\xi_j(t')\rangle = 2\gamma k_B T \delta_{ij}\delta(t-t')$.

In order to study the effects of time-delayed feedback controls let us include a time delay of value τ in the control of the paradigmatic *maximization of the center-of-mass instant velocity* protocol [8]. The controller measures the sign of the net force per particle

$$f(t) = \frac{1}{N}\sum_{i=1}^{N} F(x_i(t)), \tag{6.2}$$

and, after a time τ, it switches on the potential ($\alpha = 1$) if the net force was positive or it switches off ($\alpha = 0$) if it was negative. Thus the control protocol reads

$$\alpha(t) = \begin{cases} \Theta(f(t-\tau)) & \text{if } t \geq \tau, \\ 0 & \text{otherwise,} \end{cases} \tag{6.3}$$

with Θ the Heaviside function [$\Theta(x) = 1$ if $x > 0$, else $\Theta(x) = 0$].

Finally, to completely fix the model we choose a piecewise linear sawtooth potential $V(x) = V(x+L)$ of height V_0 and asymmetry parameter $a < 1/2$,

$$V(x) = \begin{cases} \frac{V_0}{a}\frac{x}{L} & \text{if } 0 \leq \frac{x}{L} \leq a, \\ V_0 - \frac{V_0}{1-a}\left(\frac{x}{L} - a\right) & \text{if } a < \frac{x}{L} \leq 1. \end{cases} \tag{6.4}$$

We have verified that the results found in this paper are valid for other potentials provided they have the same height of the potential V_0 and the

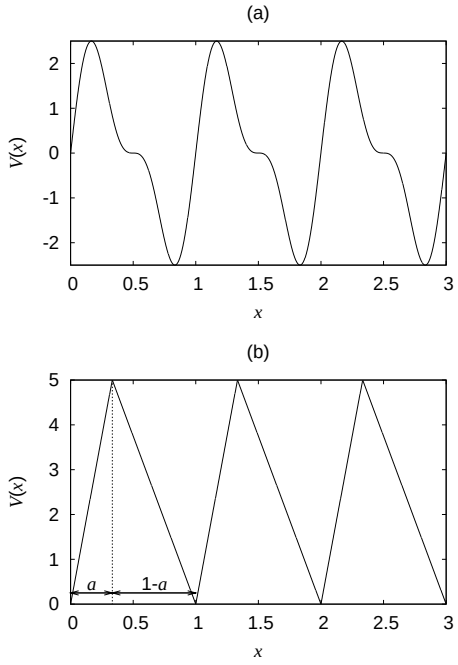

Figure 6.1: Panel (a): 'Smooth' potential (6.5) for $V_0 = 5k_BT$. Panel (b): 'Sawtooth' potential (6.4) for $V_0 = 5k_BT$ and $a = 1/3$. Units: $L = 1$, $k_BT = 1$.

same asymmetry parameter a, with V_0 defined as the difference between the maximum and the minimum values of the potential and aL as the distance between the minimum and the maximum positions. For this verification we have considered the 'smooth' potential

$$V(x) = \frac{2V_0}{3\sqrt{3}} \left[\sin\left(\frac{2\pi x}{L}\right) + \frac{1}{2}\sin\left(\frac{4\pi x}{L}\right) \right], \tag{6.5}$$

which has potential height V_0, period L, and asymmetry $a = 1/3$. See Fig. 6.1.

In the study of these feedback ratchets it proves to be useful to distinguish three cases: one particle, few particles, and many particles. This classification is based on the results of the zero delay studies [8–10], which revealed different characteristics and analytical approximations for each case. The many particle case is formed by those feedback collective ratchets that for zero delay have net force fluctuations smaller than the maximum absolute value of the net force; see Refs. [8–10].

Throughout the rest of this paper, we will use units where $L = 1$, $k_BT = 1$, and $D = 1$.

6.3 One particle

In this section we discuss the simpler case of a ratchet consisting of one particle, so that the position $x(t)$ is governed by Eq. (6.1) with $N = 1$ and $\alpha(t)$ given by Eq. (6.3), which is a nonlinear stochastic delay differential equation. In general, there is no analytical treatment for these time-delayed stochastic equations. Here, we shall write the corresponding delay Fokker-Planck equation [20], and use a perturbative technique [17, 21] to obtain an effective potential description for small delays that leads to approximate analytical expressions for the flux. Finally, in this section we shall get insight in the regime of large delays by studying the covariance of the sign of the net force.

The force that the particle feels with the inclusion of the time delay τ in the control [Eq. (6.3)] depends both on the actual position $x := x(t)$ and on the delayed position $x_\tau := x(t-\tau)$. This force $F_\tau(x, x_\tau)$ is periodic in both arguments, $F_\tau(x, x_\tau) = F_\tau(x+1, x_\tau) = F_\tau(x, x_\tau + 1)$, and reads

$$F_\tau(x, x_\tau) = \begin{cases} 0 & \text{if } 0 \le x_\tau \le a, \\ \frac{-V_0}{a} & \text{if } a < x_\tau \le 1 \text{ and } 0 \le x \le a, \\ \frac{V_0}{1-a} & \text{if } a < x_\tau \le 1 \text{ and } a < x \le 1. \end{cases} \tag{6.6}$$

In particular, $F_\tau(x, x) =: F_0(x)$ corresponds to the effective force of the instant maximization control protocol without delay [8], i.e.,

$$F_0(x) = \begin{cases} 0 & \text{if } 0 \le x \le a, \\ \frac{V_0}{1-a} & \text{if } a < x \le 1. \end{cases} \tag{6.7}$$

In terms of the force (6.6), the evolution of the position of the particle obeys the stochastic delay differential equation

$$\dot{x}(t) = F_\tau(x(t), x(t-\tau)) + \xi(t). \tag{6.8}$$

The probability density $\rho(x, t)$ of this stochastic process satisfies a delay Fokker-Planck equation [17,20–22], which involves the two-point probability density as follows:

$$\begin{aligned} \frac{\partial}{\partial x}\rho(x,t) = -\frac{\partial}{\partial x}\int F_\tau(x, x_\tau)\rho(x, t; x_\tau, t-\tau)\, dx_\tau \\ + \frac{\partial^2}{\partial x^2}\rho(x,t). \end{aligned} \tag{6.9}$$

For small delays, this equation can be treated perturbatively; then, following Refs. [17, 21], the explicit effective force for small delays can be achieved by computing

$$F_{\text{eff}}(x) = \int F_\tau(x, x_\tau) P(x_\tau, t+\tau | x, t)\, dx_\tau, \tag{6.10}$$

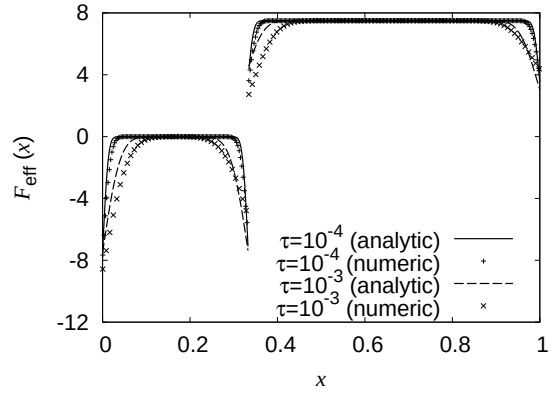

Figure 6.2: Effective force for small delays for potential height $V_0 = 5k_BT$ and asymmetry $a = 1/3$ in the one particle case [Eq. (6.12)]. Units: $L = 1$, $D = 1$, $k_BT = 1$.

where the short time propagator $P(x, t+\tau|x, t)$ (see §4.4.1 in Ref. [23]) is

$$P(x_\tau, t+\tau|x, t) = \frac{1}{\sqrt{2\pi\tau}} \exp\left(-\frac{[x_\tau - x - F_0(x)\tau]^2}{2\tau}\right). \tag{6.11}$$

Due to the Gaussian form of the propagator in this small delay approximation, we can neglect the long tails of the Gaussian propagator and restrict the integration in Eq. (6.10) to the intervals $(a-1, 1)$ and $(0, 1+a)$ for $0 \le x \le a$ and $a < x \le 1$, respectively. We get

$$F_{\text{eff}}(x) = F_{\text{eff}}(x+1) = \begin{cases} -\frac{V_0}{2a}\left[\text{erfc}\left(\frac{x}{\sqrt{2\tau}}\right) + \text{erfc}\left(\frac{a-x}{\sqrt{2\tau}}\right)\right] & \text{if } 0 \le x \le a, \\ \frac{V_0}{2(1-a)}\left[2 - \text{erfc}\left(\frac{1-x-\frac{V_0\tau}{1-a}}{\sqrt{2\tau}}\right) - \text{erfc}\left(\frac{x-a+\frac{V_0\tau}{1-a}}{\sqrt{2\tau}}\right)\right] & \text{if } a < x \le 1, \end{cases} \tag{6.12}$$

where $\text{erfc}(x)$ is the complementary error function. On the other hand, the value of the effective force can be computed numerically by splitting in bins the position of the particle and evaluating the probability of being in those bins. For small delays, Eq. (6.12) gives a good estimation as shown in Fig. 6.2.

The main effect of the inclusion of a small delay in the control is a slant of the effective force near the points of discontinuity. This effect lies on the idea that the closer the particle is to the discontinuities, the more probable is that the controller makes a mistake. For instance, when the particle is to the left of $x = a$ and close to it, there are two possibilities: (i) if the retarded position was to the left too then the controller sets the potential

off, and (ii) if the retarded position was to the right then the controller sets the potential on and the particle feels a negative force $-V_0/a$. Therefore in the points to the left of $x = a$ and close to it the force takes an effective value between 0 and $-V_0/a$, resulting in a negative effective force.

In this effective description the position of the particle evolves with a Langevin equation $\dot{x}(t) = F_{\rm eff}(x) + \xi(t)$, with the associated (nondelayed) effective Fokker-Planck equation

$$\frac{\partial}{\partial t}\rho(x,t) = -\frac{\partial}{\partial x}\left[\rho(x,t)F_{\rm eff}(x)\right] + \frac{\partial^2}{\partial x^2}\rho(x,t), \tag{6.13}$$

with periodic boundary conditions. The average velocity is obtained computing the expectation value of the velocity in the stationary distribution of the effective Fokker-Planck equation [6]:

$$\langle \dot{x} \rangle = \frac{1 - e^{V_{\rm eff}(1) - V_{\rm eff}(0)}}{\int_0^1 dx \int_x^{x+1} dy\; e^{V_{\rm eff}(y) - V_{\rm eff}(x)}}, \tag{6.14}$$

where $V_{\rm eff}(x) = -\int_0^x F_{\rm eff}(s)\, ds$. Integrating $F_{\rm eff}(x)$ we get the expression of the approximate effective potential for small delays $V_{\rm eff}(x)$,

$$V_{\rm eff}(x) = \begin{cases} \frac{V_0\sqrt{2\tau}}{2a}\left[\text{ierfc}\left(\frac{a}{\sqrt{2\tau}}\right) + \text{ierfc}\left(\frac{x}{\sqrt{2\tau}}\right) - \text{ierfc}\left(\frac{a-x}{\sqrt{2\tau}}\right) - \frac{1}{\sqrt{\pi}}\right] \\ \qquad\qquad \text{if } 0 \le x \le a, \\ \frac{V_0\sqrt{2\tau}}{2(1-a)}\left[\frac{2(a-x)}{\sqrt{2\tau}} + \text{ierfc}\left(\frac{1-x-\frac{V_0\tau}{1-a}}{\sqrt{2\tau}}\right) - \text{ierfc}\left(\frac{1-a-\frac{V_0\tau}{1-a}}{\sqrt{2\tau}}\right) + \text{ierfc}\left(\frac{\frac{V_0\tau}{1-a}}{\sqrt{2\tau}}\right)\right. \\ \qquad \left. -\text{ierfc}\left(\frac{x-a+\frac{V_0\tau}{1-a}}{\sqrt{2\tau}}\right) + \frac{2(1-a)}{a}\text{ierfc}\left(\frac{a}{\sqrt{2\tau}}\right) - \frac{2(1-a)}{a\sqrt{\pi}}\right] \\ \qquad\qquad \text{if } a < x \le 1, \end{cases} \tag{6.15}$$

in the interval $[0,1]$, and outside $V_{\rm eff}(x) = V_{\rm eff}(y) + (x-y)V_{\rm eff}(1)$, with $y \equiv x \mod 1$, $y \in [0,1]$. The function ierfc is the first iterated integral of the complementary error function [24],

$$\text{ierfc}(x) = \int_x^\infty \text{erfc}(s)\, ds = -x\,\text{erfc}(x) + \frac{e^{-x^2}}{\sqrt{\pi}}. \tag{6.16}$$

This effective potential is depicted in Fig. 6.3, where we see that an increase of the delay implies a decrease of the average tilt of the potential. Eventually, the stationary flux is calculated inserting Eq. (6.15) in Eq. (6.14). The resulting approximate expression gives good results for very small delays and a good estimate of the decrease rate for small delays. See Fig. 6.4. [This can be understood noting that although for some positions the corrections to the effective force are appreciable already for quite small delays (see Fig. 6.2) this only happens in small space intervals and therefore the results for the flux

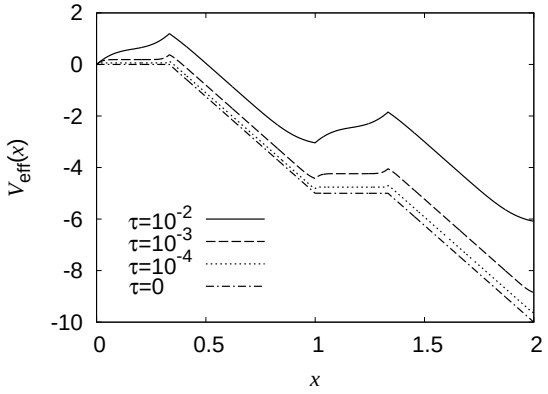

Figure 6.3: Effective potential [Eq. (6.15)] for potential height $V_0 = 5k_BT$ and asymmetry $a = 1/3$ for time delays $\tau = 0$, 10^{-4}, 10^{-3}, and 10^{-2}. Units: $L = 1$, $D = 1$, $k_BT = 1$.

are better than expected.] The approximate analytical expression obtained gives the average velocity in terms of the main magnitudes of the system, namely, the height of the potential V_0, its asymmetry a, and the time delay in the feedback τ. We have checked that this result is in good agreement also for other potentials.

Another approach can be taken to understand the observed decrease in the flux for increasing delay. The instant maximization protocol does not use detailed information about the position of the particles, it simply deals with the sign of the net force, namely, $\mathrm{sgn}f$, [with $\mathrm{sgn}(x) = 1$ for $x > 0$, $\mathrm{sgn}(x) = 0$ for $x = 0$, and $\mathrm{sgn}(x) = -1$ for $x < 0$]. The flux performance of the protocol would be optimal if it would have received the present sign of the net force, $\mathrm{sgn}f(t)$, but it does receive its value a time τ earlier, $\mathrm{sgn}f(t-\tau)$. This earlier value contains information about the present value because both values are correlated, as can be shown computing the covariance

$$\begin{aligned}\widetilde{C}(\tau) :=& \Big\langle [\mathrm{sgn}f(t) - \mu][\mathrm{sgn}f(t-\tau) - \mu] \Big\rangle \\ =& C(\tau) - \mu^2,\end{aligned} \tag{6.17}$$

where

$$\begin{aligned}C(\tau) :=& \langle \mathrm{sgn}f(t)\mathrm{sgn}f(t-\tau)\rangle, \\ \mu :=& \langle \mathrm{sgn}f(t)\rangle = \langle \mathrm{sgn}f(t-\tau)\rangle.\end{aligned} \tag{6.18}$$

The decrease of the function $\widetilde{C}(\tau)$ for increasing τ (Fig. 6.5) explains the decrease of the center-of-mass velocity as a consequence of the loss of information about the present sign of the net force. In addition, we can obtain an estimation of the flux decrease with the following heuristic argument.

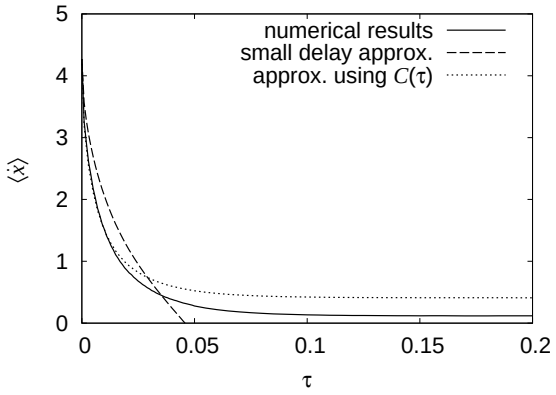

Figure 6.4: One particle flux vs delay. The numerical result (solid line) is compared with the estimations using the effective potential (6.15) (dashed line) and using $C(\tau)$ (dotted line). $V_0 = 5k_BT$ and $a = 1/3$. Units: $L = 1$, $D = 1$, $k_BT = 1$.

Let us calculate the covariance using

$$\begin{aligned} C &= P_{++} + P_{--} - P_{+-} - P_{-+}, \\ \mu &= P_{++} - P_{--} + P_{+-} - P_{-+}, \end{aligned} \tag{6.19}$$

where P_{ij} is the joint probability of having a positive ($i = +$) or negative ($i = -$) net force at time t and a positive ($j = +$) or negative ($j = -$) net force at time $t-\tau$. These probabilities can be computed if we assume that the system performance can be explained with the simplified description that $\mathrm{sgn} f(t-\tau)$ is different from $\mathrm{sgn} f(t)$ with probability p. This description allows us to use the results found in [25] for the instantaneous maximization protocol with a controller receiving $\mathrm{sgn} f(t)$ through a noisy channel with noise level p. In fact, notice that the plot of the effective potential (Fig. 6.3) resembles the form of the effective potential found in Ref. [25] for the noisy channel. This elementary description gives the values $P_{-+} = bp$, $P_{--} = b(1-p)$, $P_{+-} = (1-b)p$ and $P_{++} = (1-b)(1-p)$ for the joint probabilities, with b the probability of $\mathrm{sgn} f(t)$ being negative. Thus Eqs. (6.19) can be rewritten in terms of the probability of error $p = P_{+-} + P_{-+}$ and the probability $b = P_{-+} + P_{--}$ as

$$\begin{aligned} C &\approx 1 - 2p, \\ \mu &\approx 1 - 2b. \end{aligned} \tag{6.20}$$

In [25] it is shown that for small potential heights (small V_0) $b \approx a$ and

$$\langle \dot{x} \rangle \approx V_0(1-2p). \tag{6.21}$$

Therefore this simplified description suggests

$$\langle \dot{x} \rangle \sim V_0 C. \tag{6.22}$$

For larger potential heights, a better estimation is obtained evaluating the general expression $\langle \dot{x} \rangle(p)$ of Ref. [25] at $p(\tau) = [1-C(\tau)]/2$. This estimation is plotted in Fig. 6.4, where it is compared with numerical results and the analytical small delay approximation [Eqs. (6.14) and (6.15)].

The average velocity of the particle for large delays is not zero, but reaches a constant value independent of the delay (see Fig. 6.4). We have seen that the function $C(\tau)$ also tends to a constant nonzero value in the same characteristic time that the velocity does, in qualitative agreement with the estimation described after Eq. (6.22), although this estimation does not give the correct value of the flux. Therefore this estimation gives good quantitative results for small delays and the qualitative behavior for large delays. The large τ behavior observed for the flux implies an effective force independent of the time delay τ for large enough values of τ, as we show in Fig. 6.6. The average over x of the numerical large τ effective force is positive, in agreement with the positive net flux obtained. For example, for asymmetry parameter $a = 1/3$ and potential heights $V_0 = 1$, 5, and 10, the net flux is $\langle \dot{x} \rangle_{\tau\to\infty} \approx 0.01$, 0.12, and 0.18, respectively. The convergence to this constant value can be understood realizing that the covariance $\widetilde{C}$ becomes negligible for large delays, i.e., the fluctuations of $\mathrm{sgn} f$ around its mean value at t and at $t-\tau$ are independent. This indicates that the system dynamics is effectively the same as that for an open-loop control protocol, as the correlation between the switches and the state of the system are negligible.

Comparing the results for the delayed instant maximization protocol with the optimal periodic open-loop protocol, we see that the former performs better than the latter even for nonzero delay, provided the delay is smaller than the characteristic times of the dynamics of the Brownian ratchet. Therefore the instant maximization protocol gives a larger flux than the optimal open-loop control protocol for time delays τ such that $\tau \ll \mathcal{T}_{\mathrm{on}}$, $\tau \ll \mathcal{T}_{\mathrm{off}}$, where $\mathcal{T}_{\mathrm{on}} \sim (1-a)^2/V_0$ and $\mathcal{T}_{\mathrm{off}} \sim a^2/2$ are the on-potential and off-potential times in the optimal periodic protocol [5]. See, for example, Fig. 6.4 and compare with $\langle \dot{x} \rangle_{\mathrm{open}} \approx 0.3$ that is the value for the optimal periodic protocol for $V_0 = 5$ and $a = 1/3$, which has $\mathcal{T}_{\mathrm{on}} \approx 0.06$ and $\mathcal{T}_{\mathrm{off}} \approx 0.05$.

6.4 Few particles

In this section we deal with a collective ratchet compounded of a few particles. We will show that the center-of-mass velocity for the few particle case

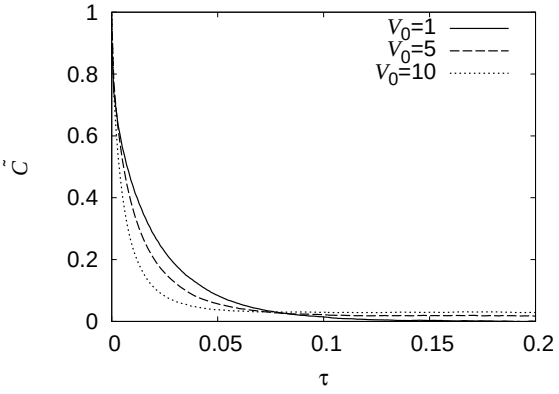

Figure 6.5: Covariance $\widetilde{C}$ [Eq. (6.17)] as a function of the time delay for potential heights $V_0 = k_BT$, $5k_BT$, and $10k_BT$. Asymmetry parameter $a = 1/3$. Units: $L = 1$, $D = 1$, $k_BT = 1$.

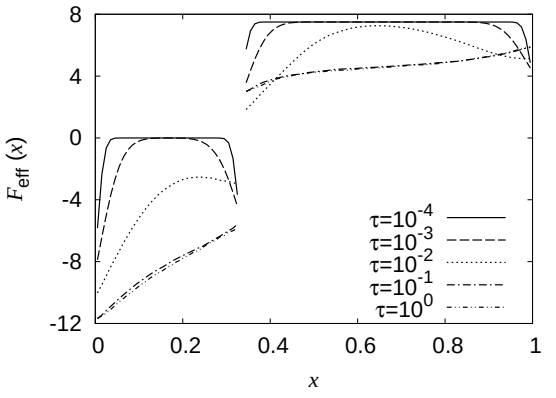

Figure 6.6: Effective force (from numerical simulations) ($N = 1$) for several time delays. $V_0 = 5k_BT$ and $a = 1/3$. Units: $L = 1$, $D = 1$, $k_BT = 1$.

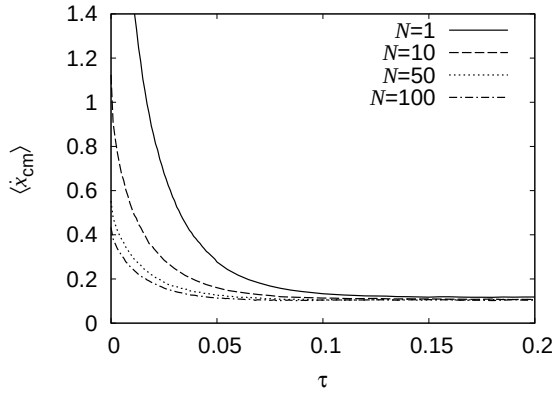

Figure 6.7: Center-of-mass velocity as a function of the time delay for number of particles $N = 1$, 10, 50, and 100. Parameters of the potential: $V_0 = 5k_BT$ and $a = 1/3$. Units: $L = 1$, $D = 1$, $k_BT = 1$.

can be related with the velocity obtained for the one particle ratchet studied in the section before.

As in the one particle case, the effect of the inclusion of a delay is a decrease in the covariance and in the center-of-mass velocity (Fig. 6.7). Therefore we can also interpret the decrease in the center-of-mass velocity as a consequence of the loss of information of the present sign of the net force, and then assume that the system performance can be explained with the simplified description that $\mathrm{sgn} f(t-\tau)$ is different from $\mathrm{sgn} f(t)$ with probability p. This simplified description leads for small potential heights [25, 26] to

$$\begin{aligned} C_N(\tau) &\sim 1 - 2p_N, \\ \mu_N &\sim 1 - 2b_N, \\ \langle \dot{x}_{\mathrm{cm}} \rangle_N &\approx \frac{V_0(1-2p_N)}{\sqrt{2\pi a(1-a)N}} \sim \frac{V_0 C_N}{\sqrt{2\pi a(1-a)N}}, \end{aligned} \tag{6.23}$$

where the subscript N denotes that the quantities are the values in the case of N particles. We have numerically found that the function $C_N(\tau)$ is approximately the same for any number of particles in this regime of a few particles, and $C_N \sim C$. Thus we have the relation

$$\langle \dot{x}_{\mathrm{cm}} \rangle_N(\tau) \approx \frac{\langle \dot{x} \rangle(\tau)}{\sqrt{2\pi a(1-a)N}} \tag{6.24}$$

between the velocities for one and for N particles for a given delay τ. This Eq. (6.24) gives good results for small values of the delay. In particular, inserting Eq. (6.14) in Eq. (6.24) we obtain an analytical approximate expression for the case of few particles in the regime of small delays.

We stress that, analogously to the zero delay case [8], the main effect of having a collective ratchet is a decrease in the magnitude of the force fluctuations. This fact gives a center-of-mass velocity inversely proportional to the square-root of the number of particles, as Eq. (6.24) states. Thereby, if the number N of particles increases, there will be a decrease of the values of the delay that give better performances for the delayed instant maximization protocol than for the optimal periodic protocol.

On the other hand, for large time delays the analogy between the delayed protocol and the noisy channel protocol no longer gives a good estimate. In this regime of large delays the covariance $\widetilde{C}(\tau) = C(\tau) - \mu^2$ becomes negligible indicating that $\mathrm{sgn}f(t-\tau)$ and $\mathrm{sgn}f(t)$ are nearly uncorrelated and that the system effectively behaves as if it were driven by an effective open-loop control protocol. In addition, we observe that the value of the center-of-mass velocity becomes independent of the number of particles (see Fig. 6.7). This is a hallmark of collective open-loop control ratchets, in which the absence of feedback decouples the Langevin equations provided the particles do not explicitly interact with each other.

6.5 Many particles

We study here the effects of time delays in the feedback controlled Brownian ratchet described in Sec. 6.2 for the many particle case, considering both the 'smooth' potential and the 'sawtooth' potential for various potential heights and different initial conditions.

We find that the system presents two regimes separated by a delay $\tau_{\min}$ for which the center-of-mass velocity has a minimum; see Fig. 6.8. In the small delay regime ($\tau < \tau_{\min}$) the flux decreases with increasing delays as one could expect. On the contrary, in the large delay regime ($\tau > \tau_{\min}$) we have observed and explained a surprising effect, namely, the center-of-mass velocity increases for increasing delays and the system presents several stable solutions. We have found that this critical time delay $\tau_{\min}$ is inversely proportional to the potential height $\tau_{\min} \propto 1/V_0$ with a proportionality constant that mildly depends on the number of particles.

6.5.1 Zero delay

The many particle ratchet in absence of delay (i.e., $\tau = 0$ in the model of Sec. 6.2) has been studied in Ref. [8]. It has been shown that the net force per particle exhibits a quasideterministic behavior that alternates large periods of time t_{on} with $f(t) > 0$ (on dynamics) and large periods of time t_{off} with $f(t) < 0$ (off dynamics). The center-of-mass velocity can be computed as

$$\langle \dot{x}_{\mathrm{cm}} \rangle = \frac{\Delta x(t_{\mathrm{on}})}{t_{\mathrm{on}} + t_{\mathrm{off}}}, \tag{6.25}$$

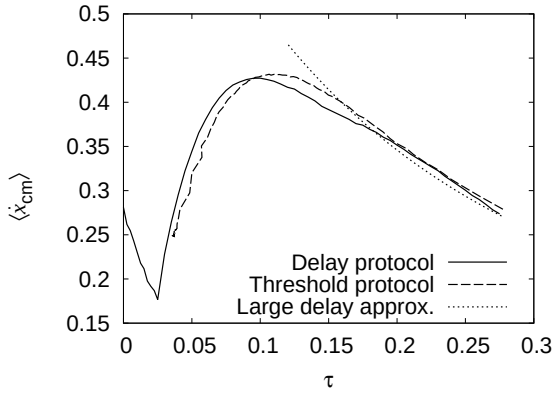

Figure 6.8: Many particle case: Center-of-mass velocity as a function of the delay (for large delays only the first branch is represented here), and comparison with the results obtained with the threshold protocol and with the large delay approximation Eq. (6.33). For the 'smooth' potential (6.5) with $V_0 = 5k_BT$ and $N = 10^5$ particles. Units: $L = 1$, $D = 1$, $k_BT = 1$.

with

$$\Delta x(t_{\rm on}) = \Delta x_{\rm on}[1 - e^{-t_{\rm on}/(2\Delta t_{\rm on})}], \tag{6.26}$$

where $\Delta x_{\rm on}$ and $\Delta t_{\rm on}$ are obtained fitting the displacement during the 'on' evolution for an infinite number of particles (see Ref. [10] for details).

On the other hand, for many particles the fluctuations of the net force are smaller than the maximum value of the net force (see Fig. 6.9). This allows the decomposition of the dynamics as the dynamics for an infinite number of particles plus the effects of the fluctuations due to the finite value of N. The late time behavior of the net force $f(t)$ for an infinite number of particles is given for the on and off dynamics by [8]

$$f_\nu^\infty(t) = C_\nu e^{-\lambda_\nu(t-\tau_\nu)} \text{ with } \nu = \text{on, off.} \tag{6.27}$$

The coefficients C_ν, λ_ν, and τ_ν can be obtained fitting this expression with the results obtained integrating a mean field Fokker-Planck equation obtained in the limit $N \to \infty$ and without delay; see Refs. [8, 10] for details. For a finite number of particles the fluctuations in the force induce switches of the potential and the times on and off are computed equating f_ν^∞ to the amplitude of the force fluctuations, resulting in [8]

$$t_{\rm on} + t_{\rm off} = b + d \ln N, \tag{6.28}$$

with $b = C_{\rm on} + C_{\rm off}$ and $d = (\lambda_{\rm on} + \lambda_{\rm off})/(2\lambda_{\rm on}\lambda_{\rm off})$.

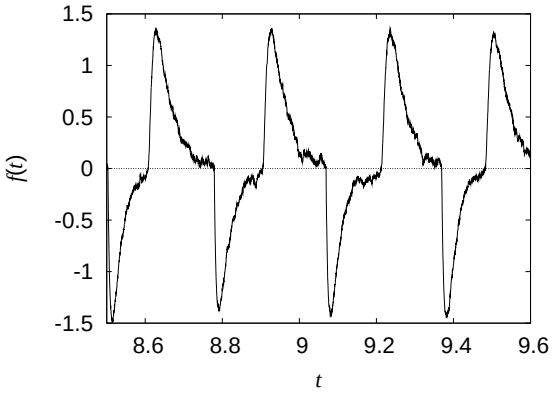

Figure 6.9: Many particle case: Evolution of the net force with zero delay ($\tau = 0$) for the 'smooth' potential Eq. (6.5) with $V_0 = 5k_BT$ and $N = 10^5$ particles. Units: $L = 1$, $D = 1$, $k_BT = 1$.

6.5.2 Small delays

For small delays, $\tau < \tau_{\min}$, we observe that the flux decreases with the delay. See Fig. 6.8. We have seen that this decrease is slower than that found for the few particle case (Sec. 6.4), and that the expressions derived to describe this decrease in the few particle case does not hold here. However, the decrease observed here can be understood noting that a change in the sign of $f(t)$ is perceived by the controller a time τ after, what delays the reaction of the system and makes the tails of $f(t)$ longer and implies an increase of the time interval between switches. In addition, the form of $f(t)$ is less smooth than for no delay because the delayed reaction of the controller allows to have several sign flips in the $f(t)$ tails before the system reacts. This sign flips give short epochs of fast switches of the potential (between long on and off epochs), which lead to large fluctuations in $f(t)$. These large fluctuations eventually destabilize these long period solutions for $\tau \sim \tau_{\min}$. See Fig. 6.10.

As the main effect of the delay is to stretch the 'on' and 'off' times of the dynamics, using the many particle approximation [8] we can write

$$\langle \dot{x}_{\rm cm} \rangle = \frac{\Delta x_{\rm on}}{t_{\rm on} + t_{\rm off} + \Delta\tau} = \frac{\Delta x_{\rm on}}{b + d \ln N + \Delta\tau}, \tag{6.29}$$

where we have found that the increase of the length of the on-off cycle $\Delta\tau$ is proportional to the delay $\Delta\tau \propto \tau$.

6.5.3 Large delays

After the minimum flux is reached for $\tau = \tau_{\min}$, the flux begins to increase with the time delay (see Fig. 6.8). This increase is due to a change in the

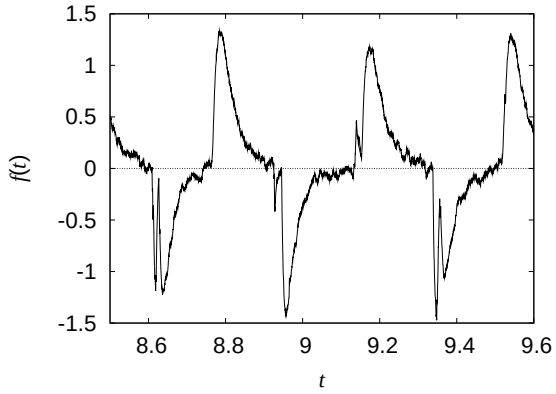

Figure 6.10: Many particle case: Evolution of the net force with a small delay ($\tau = 0.02$) for the 'smooth' potential Eq. (6.5) with $V_0 = 5k_BT$ and $N = 10^5$ particles. Units: $L = 1$, $D = 1$, $k_BT = 1$.

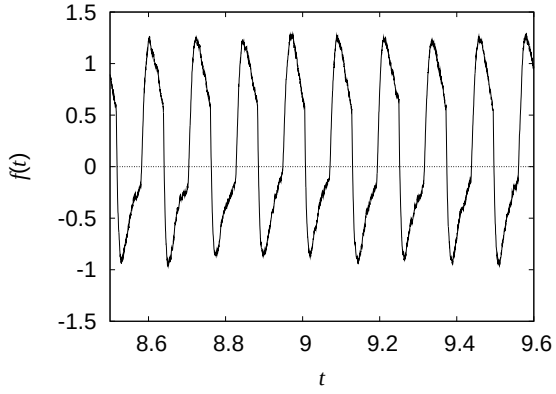

Figure 6.11: Many particle case: Evolution of the net force with a large delay ($\tau = 0.12$) for the 'smooth' potential Eq. (6.5) with $V_0 = 5k_BT$ and $N = 10^5$ particles. Units: $L = 1$, $D = 1$, $k_BT = 1$.

dynamical regime: for $\tau > \tau_{\min}$ the present net force starts to be nearly synchronized with the net force a time τ ago. This *self-synchronization* gives rise to a quasiperiodic solution of period $\mathcal{T} = \tau$. Note that there is not a strict periodicity due to stochastic fluctuations in the 'on' and 'off' times. Looking at the $f(t)$ dependence, Fig. 6.11, we see that the solutions stabilized by the self-synchronization are similar to those obtained with the threshold protocol [9, 10]. In Fig. 6.8 we show that the threshold protocol that has the same period gives similar center-of-mass velocity values, confirming the picture. (Differences are due to the fact that we have considered for the threshold protocol simulations with on and off thresholds of the same magnitude, while Fig. 6.11 shows that the effective thresholds are different.)

This picture allows one to understand the increase of velocity for increasing delay, and the presence of a maximum. This maximum is related with the optimal values of the thresholds that have been shown in [10] to give a quasiperiodic solution of period $\mathcal{T} = \mathcal{T}_{\rm on} + \mathcal{T}_{\rm off}$, with $\mathcal{T}_{\rm on}$ and $\mathcal{T}_{\rm off}$ the optimal 'on' and 'off' times of the periodic protocol. Therefore if we know the values of $\mathcal{T}_{\rm on}$ and $\mathcal{T}_{\rm off}$ for the optimal periodic protocol [$\mathcal{T}_{\rm on} \sim (1-a)^2/V_0$ and $\mathcal{T}_{\rm off} \sim a^2/2$] we can predict that the maximum of the center-of-mass velocity is reached for a delay

$$\tau_{\max} = \mathcal{T}_{\rm on} + \mathcal{T}_{\rm off}, \tag{6.30}$$

and has a value

$$\langle \dot{x}_{\rm cm} \rangle_{\rm closed}(\tau_{\max}) = \langle \dot{x}_{\rm cm} \rangle_{\rm open}^{\max}, \tag{6.31}$$

with $\langle \dot{x}_{\rm cm} \rangle_{\rm open}^{\max}$ the center-of-mass velocity for the optimal open-loop protocol. Thus this expression gives the position and height of the maximum of the delayed feedback control protocol in terms of the characteristic values of the optimal open-loop control. In particular, it implies that the position and height of the maximum for the flux is independent of the number of particles.

As an example we can apply these expressions to the 'smooth' potential with $V_0 = 5$ that for the optimal periodic protocol gives $\langle \dot{x}_{\rm cm} \rangle = 0.44$ for $\mathcal{T}_{\rm on} = 0.06$ and $\mathcal{T}_{\rm off} = 0.05$, so we obtain $\tau_{\max} = 0.06 + 0.05 = 0.11$ in agreement with Fig. 6.8.

For values of the delay of the order of or larger than $\tau_{\max}$ quasiperiodic solutions of other periods start to be stable; see Fig. 6.12. The periods for the net force $f(t)$ that are found are those that fit an integer number of periods inside a time interval τ, verifying that the present net force is synchronized with the net force a time τ ago, that is, the quasiperiodic solutions have periods $\mathcal{T} = \tau/2$, $\mathcal{T} = \tau/3$, ... In addition, it can be seen that the center-of-mass velocity of the n branch $\langle \dot{x}_{\rm cm} \rangle_{\tau/n}$ whose $f(t)$ has period $\mathcal{T} = \tau/n$ is related with that of the $\mathcal{T} = \tau$ branch through

$$\langle \dot{x}_{\rm cm} \rangle_{\tau/n}(\tau) = \langle \dot{x}_{\rm cm} \rangle_{\tau}(\tau/n). \tag{6.32}$$

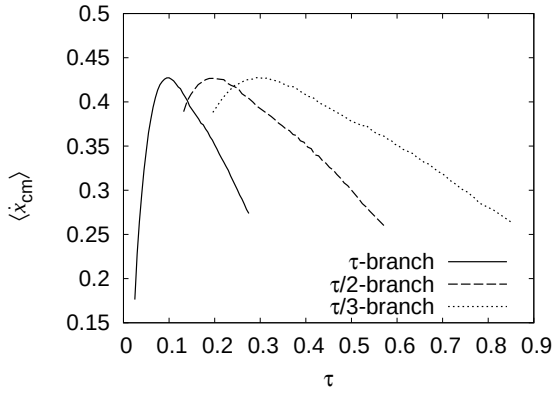

Figure 6.12: Many particle case: First three branches of stable solutions for the 'smooth' potential (6.5) with $V_0 = 5k_BT$ and $N = 10^5$ particles. Units: $L = 1$, $D = 1$, $k_BT = 1$.

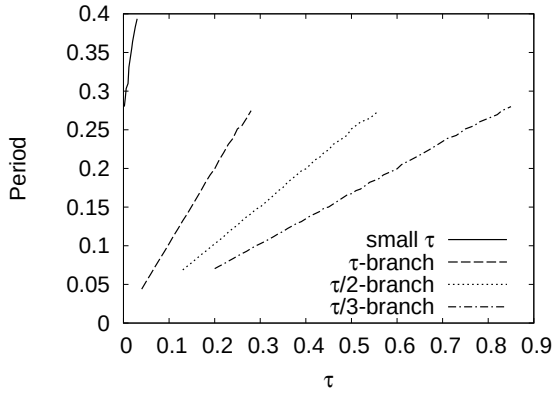

Figure 6.13: Many particle case: Period $\mathcal{T}$ of the quasiperiodic solutions for small delays and for large delays. For large delays only the first three branches of stable solutions are shown. 'Smooth' potential (6.5) with $V_0 = 5k_BT$ and $N = 10^5$ particles. Units: $L = 1$, $D = 1$, $k_BT = 1$.

We highlight that several branches can be stable for the same time delay τ. Whether the system finally goes to one or another stable solution depends on the initial conditions and on the particular realization of the noise. See Figs. 6.12 and 6.13. For these branches we have found initial conditions that go to these solutions and that remain in them during several thousands of periods, indicating that they are stable solutions or at least metastable solutions with a large lifetime.

The analogy with the threshold protocol allows one to use the analytic results of [10] to get further insight in the numerical results. The behavior for large delays for the $\mathcal{T} = \tau$ branch can be obtained using the relation

$$\langle \dot{x}_{\rm cm} \rangle = \frac{\Delta x(\tau)}{\tau}, \tag{6.33}$$

with $\Delta x(\tau)$ given by Eq. (6.26). This equation gives a good prediction for the largest delays of the first branch (see Fig. 6.8).

On the other hand, for very large values of the delays of the first branch the solutions in a given branch start to become unstable, which can be understood noting that this happens when the fluctuations of the net force become of the order of the absolute value of the net force. Thus the maximum delay that gives a stable solution in the first branch is

$$\tau_{\rm inst} = t_{\rm on} + t_{\rm off} = b + d \ln N, \tag{6.34}$$

where b and d are determined as in Eq. (6.28). For example, for the 'smooth' potential with $V_0 = 5$, which has $b = -0.070$ and $d = 0.031$, we obtain for $N = 10^5$ particles the value $\tau_{\rm inst} = 0.29$ in accordance with the numerical results shown in Figs. 6.8 and 6.12.

The previous results for the first branch, Eqs. (6.33) and (6.34), can be extended to other branches by direct application of the relation (6.32).

6.6 Conclusions

In this paper we have faced a fundamental question intrinsically related with feedback Brownian ratchets, namely, the effects of a time delay in such a feedback controlled stochastic system. We have focused on the task of studying the dependence of the flux with the time delay for both the case of one particle and for the collective version of the ratchet with few particles.

For *one particle* ratchets and small delays we have obtained an effective potential which contains the basic ingredients that come into play, and gives an approximate analytical expression for the flux. The effects of the delay in the shape and the average slant of the effective potential allows one to easily understand the decrease of the flux with increasing delays. The approximate analytical expression obtained [Eqs. (6.14) and (6.15)] gives the average velocity in terms of the main magnitudes of the system: the height of the

potential V_0, its asymmetry a, and the time delay in the feedback τ. In particular, it allows one to obtain predictions of the characteristic time scale of the decrease due to the delay. This relation is also useful in the *few particle* case thanks to the relation (6.24) found between the flux for the one and the few particle cases.

The decrease of the covariance of the sign of the net force for increasing delays provides an alternative approach to understand the dependence of the flux with the delay. This approach has given the relation between the covariance and the flux, and has allowed us to relate the flux obtained in the few particle case with the results of the one particle case [Eq. (6.24)]. In addition, the fact that the covariance becomes negligible for large delays indicates that the delayed control protocol effectively behaves as if it were an open-loop control protocol. This results in a constant value of the flux for large delays that is independent on the number of particles.

We want to stress as an important result of this paper that the feedback controlled system for one or few particles is able to perform better than its open-loop counterpart even for nonzero time delays (provided the delays are smaller than the characteristic times of the dynamics of the Brownian ratchet). Furthermore, even for arbitrarily large delays the net flux does not vanish but it reaches a positive value, albeit it performs worse than the optimal open-loop protocol. We also highlight the importance of this study for realistic *experimental* situations that necessarily have to face with time delays. For the ratchet considered in [11] the colloidal particles have diameter 0.25, 0.4, and 1 μm, and the sawtooth dielectric potential has period $L = 50$ μm and asymmetry $a \sim 1/3$. The maximum velocities obtained with a periodic switching were reported [11] to be of 0.2 μm/s with $\mathcal{T}_{\text{on}} \sim 30$ s and $\mathcal{T}_{\text{off}} \sim 50$ s. As the trapping energy is significantly greater than kT and $a \sim 1/3$ the introduction of feedback can increase the velocity up to a factor $(1/2 - a)^{-1} \sim 6$ approximately [8, 13], attained when the time delay in the feedback is negligible. The results obtained in this paper indicate that for delays in the feedback smaller than the characteristic times of the system (of order 10 s, *i.e.*, of order 10^{-3} in the adimensional units used throughout our paper) it is possible to obtain velocities greater than the maximum of open-loop protocols. The use of a conventional CCD camera (30 fps) and conventional electronics is enough to achieve a feedback control performance with a time delay of the order of 0.1 s (10^{-4} in adimensional units), for this time delay an increase of the velocity of a factor of 4 is expected. This points towards the feasibility of implementing experimentally a feedback controlled ratchet that performs better than its optimal open-loop version.

We have also studied the effects of time delays in the *many particle* case, where surprising and interesting results arise. Although in the many particle case without delay the instantaneous maximization protocol performs worse than the optimal open-loop protocol, the introduction of a delay can

increase the center-of-mass velocity up to the values given by the optimal open-loop control protocol. For small delays the asymptotic average velocity decreases for increasing delays, until it reaches a minimum. After this minimum, a change of regime happens and the system enters a selfsynchronized dynamics with the net force at present highly correlated with the delayed value of the net force used by the controller. This self-synchronization stabilizes several of the quasiperiodic solutions that can fit an integer number of periods in a time interval of the length of the time delay. The stable quasiperiodic solutions have a structure similar to those solutions appearing in the threshold protocol. This analogy has allowed us to make numerical and analytical predictions using the previous results for the threshold protocol [10]. In particular, we have established the location and value of the maximum, and also the value of the time delay beyond which a quasiperiodic solution becomes unstable. The results obtained show that for most time delays several solutions are stable and therefore the systems present multistability; which stable solution is reached depends on the past history of the system. The possibility to choose the quasiperiod of the solution we want to stabilize just tuning the time delay can have potential applications to easily control the particle flux. Note that we can even leave some branch just going to time delays where the branch is already unstable, and force the system to change to another branch of solutions.

In summary, we have studied the effects of time delays in the feedback control of a flashing ratchet. The results for one and few particles point towards the feasibility of an experimental implementation of a feedback controlled ratchet that performs better than its optimal open-loop version. On the other hand, the many particle case presents an unexpected improvement of the flux due to the stabilization of one or more quasiperiodic solutions for large enough delays.

Acknowledgments

We acknowledge financial support from the MEC (Spain) through Research Projects FIS2005-24376-E and FIS2006-05895, and from the ESF Programme STOCHDYN. In addition, M.F. thanks the Universidad Complutense de Madrid (Spain) for support through grant “Beca Complutense”.

Bibliography

[1] M. V. Smoluchowski, Phys. Z. 13, 1069 (1912).

[2] R. P. Feynman, R. B. Leighton, and M. Sands, The Feynman Lectures on Physics (Addison-Wesley, Reading, MA, 1963).

[3] A. Ajdari and J. Prost, C. R. Acad. Sci. Paris II **315**, 1635 (1993).

[4] M. O. Magnasco, Phys. Rev. Lett. **71**, 1477 (1993).

[5] R. D. Astumian and M. Bier, Phys. Rev. Lett. **72**, 1766 (1994).

[6] P. Reimann, Phys. Rep. **361**, 57 (2002).

[7] H. Linke, Appl. Phys. A **75**, 167 (2002).

[8] F. J. Cao, L. Dinis and J. M. R. Parrondo, Phys. Rev. Lett. **93**, 040603 (2004).

[9] L. Dinis, J. M. R. Parrondo, and F. J. Cao, Europhys. Lett. **71**, 536 (2005).

[10] M. Feito and F. J. Cao, Phys. Rev. E **74**, 041109 (2006).

[11] J. Rousselet, L. Salome, A. Ajdari, and J. Prost, Nature **370**, 446 (1994).

[12] C. Marquet, A. Buguin, L. Talini, and P. Silberzan, Phys. Rev. Lett. **88**, 168301 (2002).

[13] M. Bier, Biosystems **88**, 301 (2007).

[14] R. F. Stengel, *Optimal Control and Estimation* (Dover, New York, 1994).

[15] J. Bechhoefer, Rev. Mod. Phys. **77**, 783 (2005).

[16] G. A. Bochanov and F. A. Rihan, J. Comput. Appl. Math. **125**, 183 (2000).

[17] T. D. Frank, Phys. Rev. E **71**, 031106 (2005).

[18] M. Kostur, P. Hänggi, P. Talkner, and J. L. Mateos, Phys. Rev. E **72**, 036210 (2005).

[19] W. S. Son, J. W. Ryu, D. U. Hwang, S. Y. Lee, Y. J. Park, C. M. Kim, nlin.CD/0612039 preprint (2006).

[20] S. Guillouzic, I. L'Heureux and A. Longtin, Phys. Rev. E **59**, 3970 (1999).

[21] T. D. Frank, Phys. Rev. E **72**, 011112 (2005).

[22] T. D. Frank, Phys. Rev. E **66**, 011914 (2002).

[23] H. Risken, *The Fokker-Planck equation, Methods of Solution and Applications* (Springer-Verlag, Berlin, 1989).

[24] M. Abramowitz and I. A. Stegun, *Handbook of Mathematical Functions* (Dover, New York, 1972).

[25] F. J. Cao, M. Feito and H. Touchette, *Information and flux in a feedback controlled Brownian ratchet*, arXiv:cond-mat/0703492 (2007).

[26] M. Feito and F. J. Cao, Eur. Phys. J. B **59**, 63 (2007).

Chapter 7

Transport reversal in a delayed feedback ratchet

PHYSICA A **387**, 4553 (2008)
Transport reversal in a delayed feedback ratchet

M. Feito[1] and F. J. Cao[1,2]

[1] *Departamento de Física Atómica, Molecular y Nuclear, Universidad Complutense de Madrid, Avenida Complutense s/n, 28040 Madrid, Spain.*
[2] *LERMA, Observatoire de Paris, Laboratoire Associé au CNRS UMR 8112, 61, Avenue de l'Observatoire, 75014 Paris, France.*

Feedback flashing ratchets are thermal rectifiers that use information on the state of the system to operate the switching on and off of a periodic potential. They can induce directed transport even with symmetric potentials thanks to the asymmetry of the feedback protocol. We investigate here the dynamics of a feedback flashing ratchet when the asymmetry of the ratchet potential and of the feedback protocol favor transport in opposite directions. The introduction of a time delay in the control strategy allows one to non-trivially tune the relative relevance of the competing asymmetries leading to an interesting dynamics. We show that the competition between the asymmetries leads to a current reversal for large delays. For small ensembles of particles current reversal appears as the consequence of the emergence of an open-loop like dynamical regime, while for large ensembles of particles it can be understood as a consequence of the stabilization of quasiperiodic solutions. We also comment on the experimental feasibility of these feedback ratchets and their potential applications.

PACS numbers: 05.40.-a, 02.30.Yy

7.1 Introduction

Brownian motors or ratchets are spatially periodic systems that are able to induce direct transport rectifying thermal fluctuations. Two conditions are generally sufficient for the emergence of direct transport in these systems: breaking of thermal equilibrium and breaking of spatial inversion symmetry [1]. These systems permit one to get an insight into non-equilibrium processes and are receiving increasing interest also due to their applications in nanotechnology and biology [1–3].

Flashing ratchets are devices that rectify the motion of Brownian particles by subjecting them to a spatially periodic potential that is alternatively switched on and off. Open-loop flashing ratchets operate without regard to the state of the system (open-loop control) implementing a periodic or random switching to rectify thermal fluctuations by taking advantage of the asymmetry of the potential [4–6]. On the contrary, feedback ratchets (or

closed-loop ratchets) use information on the particle distribution of the system to operate [7–13], and the asymmetry of the feedback control protocol is able to induce a directed transport even for symmetric ratchet potentials. For instance, in the so-called maximization of the center-of-mass velocity protocol [7] the controller switches on the potential only if switching on would imply a positive displacement for the center-of-mass position (i.e., if the net force with the potential on would be positive). Feedback flashing ratchets have been recently suggested as a mechanism to explain the stepping motion of the two-headed kinesin [14]. In another context, a feedback scheme has been used to perform control of chaotic trajectories in inertia ratchets [15].

Feedback flashing ratchets could be experimentally implemented monitoring the positions of a set of Brownian particles [16–18] and subsequently using the information gathered to decide whether to switch on or off a ratchet potential according to a giving protocol. This experimental design will have to deal with a finite time lag between the collection of the information about the state of the system and the action because of the time interval needed for the measurement, transmission and processing of the information [19, 20]. Time delays in the feedback also appear naturally in complex systems with self regulating mechanisms (see [21, 22] and references therein). It is also remarkable for the ability of controlling chaos and improving coherence in excitable systems under delayed feedback [23, 24]. The feasibility of nanotechnological feedback flashing ratchet devices and their performance under the presence of a time delay has been analyzed very recently in Refs. [12,13]. In those works, and also in previous ones [7–11], the two sources of spatial asymmetry involved, namely the feedback control and the shape of the potential, *cooperate* with the aim of maximizing the performance of the system. On the contrary, in this paper we investigate the effects of the *competition* between the potential asymmetry and the control asymmetry in a delayed feedback ratchet.

We have observed a rich dynamics that includes transport reversal. The inversion of the current direction upon the variation of the system parameters is a well-known phenomenon in Brownian motors that can be produced by varying the characteristics of the non-equilibrium fluctuations [25, 26] or the parameters of the time-dependent perturbation that drives the system out of equilibrium [27–31]. It also appears in other ratchet-like systems, such as deterministic inertial ratchets [32, 33]. The phenomenon of current reversal has great importance in particle separation devices [34], and in biology systems [35]. In our present study current reversal is achieved just by varying the time delay of the system.

We start below with the description of the collective flashing ratchet and the delayed feedback protocol that we consider. In the next section, Sec. 7.3, the evolution equations of the system are solved by Langevin dynamics simulations and the rich dynamics encountered (transport reversal,

quasi-periodic modes of oscillation, multistability) is analyzed. We finally review and further discuss in Sec. 7.4 the implications of the results.

7.2 Model

The feedback ratchet that we consider consists of N Brownian particles at temperature T in a periodic potential $V(x)$. The force acting on the particles is $F(x) = -V'(x)$, where the prime denotes the spatial derivative. The state of this system is described by the positions $x_i(t)$ of the particles satisfying the overdamped Langevin equations

$$\gamma \dot{x}_i(t) = \alpha(t) F(x_i(t)) + \xi_i(t); \quad i = 1, \ldots, N, \tag{7.1}$$

where γ is the friction coefficient (related to the diffusion coefficient D through Einstein's relation $D = k_B T/\gamma$), $\xi_i(t)$ are Gaussian white noises of zero mean and variance $\langle \xi_i(t)\xi_j(t')\rangle = 2\gamma k_B T \delta_{ij}\delta(t-t')$, and $\alpha(t)$ stands for the action of the controller. The feedback policy uses the sign of the net force per particle,

$$f(t) = \frac{1}{N}\sum_{i=1}^{N} F(x_i(t)), \tag{7.2}$$

as follows: The controller measures the sign of the net force and, after a time τ, switches the potential on ($\alpha = 1$) if the net force was positive or switches the potential off ($\alpha = 0$) if the net force was negative. Therefore, the delayed control protocol considered is

$$\alpha(t) = \begin{cases} \Theta(f(t-\tau)) & \text{if } t \geq \tau, \\ 0 & \text{otherwise,} \end{cases} \tag{7.3}$$

with Θ the Heaviside function [$\Theta(x) = 1$ if $x > 0$, else $\Theta(x) = 0$]. We have used a sawtooth potential of period L, i.e. $V(x) = V(x+L)$, height V_0, and asymmetry parameter a:

$$V(x) = \begin{cases} \frac{V_0}{a}\frac{x}{L} & \text{if } 0 \leq \frac{x}{L} \leq a, \\ V_0 - \frac{V_0}{1-a}\left(\frac{x}{L} - a\right) & \text{if } a < \frac{x}{L} \leq 1. \end{cases} \tag{7.4}$$

The height V_0 of the potential is the difference between the value of the potential at the minimum and at the maximum, while aL is the distance between the minimum and the maximum consecutive positions (Fig. 7.1). Thus when $a < 1/2$ both the asymmetry of the potential and the feedback protocol favor transport in the same direction, whereas when $a > 1/2$ there is a competition between them. We consider here the latter case.

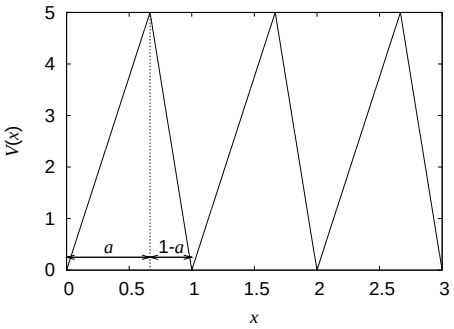

Figure 7.1: Sawtooth potential [Eq. (7.4)] of height $V_0 = 5k_BT$ and asymmetry parameter $a = 2/3$. Units: $L = 1$ and $k_BT = 1$.

7.3 Results

We have performed numerical simulations of the Langevin equations (7.1) by using an Euler-Maruyama scheme [36], which reveals different dynamics of the collective ratchet for different ensemble sizes when the delayed feedback is present. We distinguish between few particles (including $N = 1$ as a particular case) and many particles. Following previous works [7], we refer to the few particle case when the average long-time limit velocity of the center-of-mass, $\langle \dot{x}_{\rm cm} \rangle$, is greater for the non-delayed feedback maximization protocol than for the optimal open-loop protocol, and many particle case otherwise. Typically the frontier between these regimes corresponds to $N = 10^2 - 10^3$ particles for potential heights of the order of $5k_BT$ or greater.

Let us begin our analysis with the non-delayed ($\tau = 0$) feedback ratchet.

7.3.1 Non-delayed feedback ratchet

For *one particle* ($N = 1$) the exact expression for the average velocity can be obtained by solving a Fokker-Planck equation with the proper effective potential that includes the action of the controller. This expression has been derived in [7], and is indeed valid for any asymmetry parameter $0 < a < 1$. It gives a positive flux that grows as $DV_0/(k_BTL)$ for small potential heights ($V_0 \lesssim k_BT$), and tends to the finite value $2D/(a^2L)$ for large potential heights ($V_0 \gg k_BT$). The fact that the flux goes to a constant value for large potential heights is a direct consequence of the overdamped nature of the ratchet. We remark that enlarging the value of the ratio $V_0/(k_BT)$ corresponds to effectively diminish the intensity of the white noise that accounts for thermal fluctuations.

For the collective ratchet compounded of a *few particles* an approximation for the center-of-mass velocity can be obtained assuming a purely stochastic behavior (see Ref. [7] for details). As the magnitude of the fluctua-

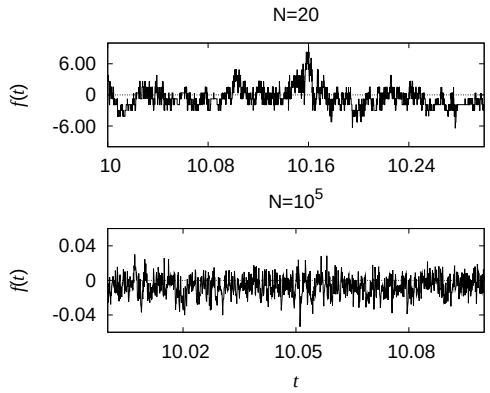

Figure 7.2: Evolution of the net force per particle for the non delayed feedback ratchet for $N = 20$ (few particles) and $N = 10^5$ (many particles). The potential is "on" only in the time intervals such that $f(t)$ is positive. Parameters of the potential: $V_0 = 5k_BT$ and $a = 2/3$. Units: $L = 1$, $D = 1$, and $k_BT = 1$.

tions of the force are of the order of the inverse of the square-root of the number of particles the stochastic approximation predicts the $\langle \dot{x}_{\rm cm} \rangle \sim 1/\sqrt{N}$ decay observed in our simulations for any asymmetries. In fact this qualitative behavior remains valid for any number of particles (including *many particles*) provided the asymmetry is $a > 1/2$. In this latter case the potential asymmetry acts against the feedback protocol, which tries to favor positive currents, and then the potential is turned on in very small intervals of time as the controller rapidly switches it off. See Fig. 7.2. Thus the systems dynamics is effectively stochastic, contrary to the many particle case with cooperating asymmetries, where switches are slower and allow the system to have enough time to evolve in a quasideterministic way [7]. Therefore when the potential asymmetry competes against the feedback the flux decays with the number of particles as $1/\sqrt{N}$ even for many particles, contrary to the much slower $1/\ln N$ dependence observed when both asymmetries cooperate [7].

In any case the non-delayed protocol always gives a positive flux because it only switches on when it implies a positive displacement of the center-of-mass position.

7.3.2 Delayed feedback ratchet

The presence of a lag time in the control can cause negative currents and complicated dynamics that depends on the number of particles. Let us first study the few particle case (including one particle).

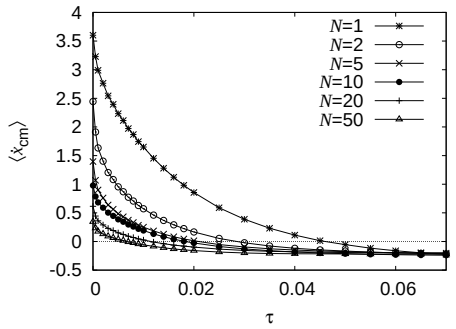

Figure 7.3: Center-of-mass velocity $\langle \dot{x}_{\rm cm} \rangle$ as a function of the time delay τ for different numbers N of particles under the few particle regime. Parameters of the potential: $V_0 = 10 k_B T$ and $a = 2/3$. Units: $L = 1$, $D = 1$, and $k_B T = 1$.

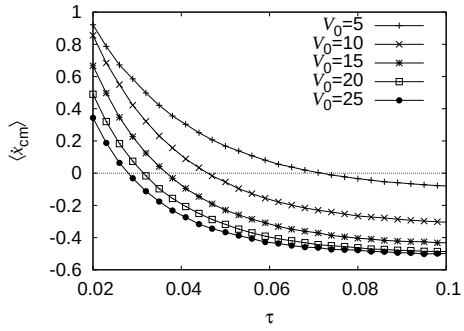

Figure 7.4: One particle velocity versus the time delay for different heights V_0 of the potential and asymmetry parameter $a = 2/3$. Units: $L = 1$, $D = 1$, and $k_B T = 1$.

Few particles

When the control protocol presents a time delay the system performs worse because the delayed action of the controller implies some wrong actions. Moreover, for large time delays the controller is unable to surmount the potential shape asymmetry and eventually the net current becomes negative. See Figs. 7.3 and 7.4.

For increasing time delays the correlation between the present sign of the net force and the measured sign that the controller actually uses decreases. Thus the controller action begins to be uncorrelated to the present state of the system and it effectively begins to act as an open-loop ratchet [12]. In fact, for large delays the correlation between the state of the system and the measured retarded state is negligible and the negative flux becomes inde-

pendent of the delay, because the ratchet is effectively open-loop controlled; see Fig. 7.3. Therefore transport reversal appears here as a consequence of the competition between the asymmetry of the ratchet potential and the inherent asymmetry of the protocol. We stress that the influence of the asymmetry of the feedback protocol itself is not tuned here trivially, but changing the delay τ in the control. Other ways of tuning the influence of the feedback protocol could not lead to current reversal. For example, it can be shown that a feedback protocol that switches on/off following the maximization protocol but with a probability of error $0 < p < 1/2$ does not enable negative fluxes even for asymmetries $a > 1/2$ (see Ref. [9]).

For the delayed protocol considered the critical value of the delay that gives zero current (thus the current is positive for smaller delays and negative for larger delays) is related with the characteristic time in which the information about the state of the system is effectively lost, so the delayed maximization protocol is not able to achieve its goal of producing a positive current for delays larger than the critical one. Increasing the height V_0 of the potential implies a faster dynamics. Therefore the critical delay is expected to decrease with the height of the potential, in agreement with our simulations; see Fig. 7.4. It is important to note that this critical delay tends to a constant *nonzero* value as $V_0 \to \infty$. The reason is the same that makes the absolute value of the flux in both closed-loop and open-loop ratchets does not grow indefinitely as the potential goes up. These fluxes tend to a finite value because the time spent by the particles in diffusing during the off potential state goes to a constant in the absence of inertia. Note also that the critical delay decreases with the number of particles (see Fig. 7.3.)

Let us now study the many particle case, which exhibits a completely different dynamics.

Many particles

For large ensembles of particles ($N > 10^2 - 10^3$) the flux is nearly zero in the non-delayed protocol (see Sec. 7.3.1), but the introduction of a time delay stabilizes quasiperiodic solutions that give noticeable negative currents. We have found that, after a transient time, the delayed control allows the system to synchronize into a stable mode of oscillation such that the net force per particle evolves quasi-periodically. The evolution is not strictly periodic due to the stochastic nature of the dynamics. See Fig. 7.5.

For small delays the on and off times of the non-delayed dynamics (Sec. 7.3.1) are enlarged owing to the delay, and the net force per particle evolves with a more regular pattern (Fig. 7.5, left). When the potential is switched on the net force per particle begins to diminish (because the potential asymmetry acts against the feedback protocol) and rapidly gets negative, but the potential still remains 'on' during a time τ after the force changed its sign. On the other hand, when the potential is switched off

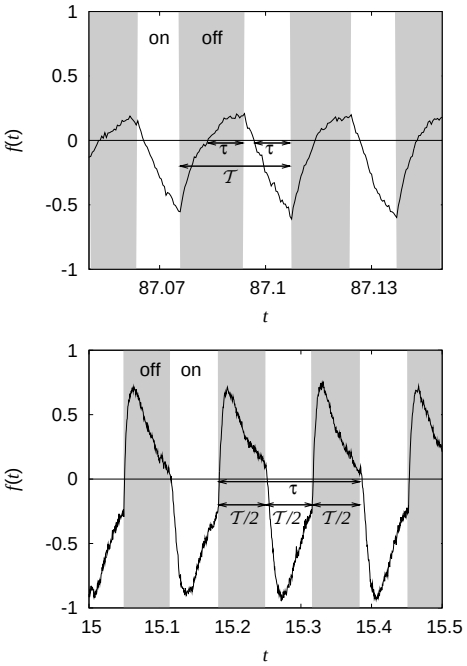

Figure 7.5: Evolution of the net force per particle for time delays $\tau = 0.01$ (left) and $\tau = 0.20$ (right) in the many particle case ($N = 10^5$). White background regions stand for "on" potential and gray background regions for "off" potential. Parameters of the potential: $V_0 = 5k_BT$ and $a = 2/3$. Units: $L = 1$, $D = 1$, and $k_BT = 1$.

the net force grows, becomes positive, and induces an 'on' switching a time τ later. The result is a quasiperiodic dynamics with an small quasiperiod $\mathcal{T} > 2\tau$; see Fig. 7.5 (left). We highlight that these types of solution are only observed for asymmetries $a > 1/2$, as they are consequences of the competing asymmetry of the potential; they do not appear for asymmetries $a < 1/2$ that support positive transport and exhibit a different behavior related with the enlargement of the tails of the net force per particle [12,13].

For larger delays there are stable solutions of quasiperiods $\mathcal{T} = 2\tau/(2n+1),\ n = 0, 1, \ldots$, i.e., solutions that contain an odd number of semiperiods $\mathcal{T}/2$ in the time delay τ. See Fig. 7.5 (right) for instance. The competing asymmetry of the potential causes the stabilization of those solutions where, due to the delay, the controller switches on when the present net force is negative and switches off when it would be positive, that is, the controller acts contrary to its intentions and gives a negative flux. These branches are the counterparts of the solutions of quasiperiods $\mathcal{T} = \tau/n,\ n = 1, 2, \ldots$ (τ containing an even number of semi-quasiperiods) observed for asymmetries $a < 1/2$ [12]. The difference of one semiperiod is due to the effectively reversed operation of the controller caused by the combined effect of the competing asymmetry of the potential and the delay. Some of these branches are plotted in Fig 7.6 for both the cases of cooperation (positive currents) and competition (negative currents) of asymmetries.

It is important to note that the average velocity for all these branches can be reexpressed in terms of one of them. Let us define $g(\tau) := \langle \dot{x}_{\rm cm} \rangle_\tau(\tau)$ as the average velocity for the branch of period $\mathcal{T} = \tau$, which is present for cooperative potential asymmetry. For these asymmetries, $a < 1/2$, we showed in Ref. [12] that the average velocities of the branches of periods $\mathcal{T} = \tau/n$ are given by

$$\langle \dot{x}_{\rm cm} \rangle_{\frac{\tau}{n}}(\tau) = g\left(\tfrac{\tau}{n}\right) \qquad \text{for } a < 1/2. \tag{7.5}$$

On the contrary, for competing asymmetries, $a > 1/2$, we have found here that the solutions have quasiperiods $\mathcal{T} = 2\tau/(2n+1)$, and furthermore, the average velocities of these branches are given by

$$\langle \dot{x}_{\rm cm} \rangle_{\frac{2\tau}{2n+1}}(\tau) = -g\left(\tfrac{2\tau}{2n+1}\right) \qquad \text{for } a > 1/2. \tag{7.6}$$

Consequently, given one of the branches all the others can be predicted; see Fig. 7.6. This also implies that the analytical results obtained in Ref. [12] for cooperative potential asymmetry ($a < 1/2$) are directly extended to the competing potential asymmetry case ($a > 1/2$), just using the relation in Eq. (7.6).

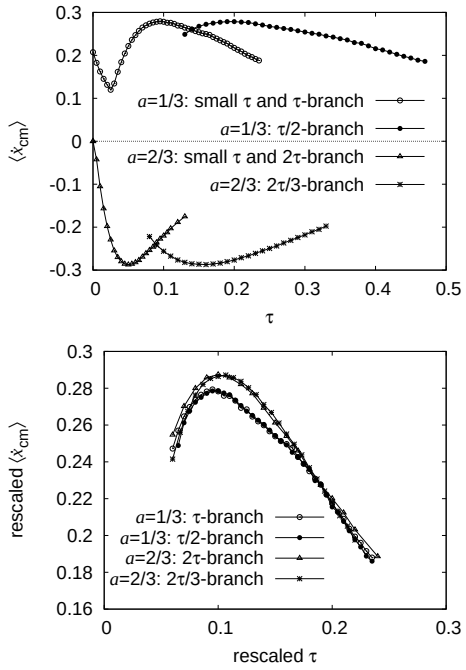

Figure 7.6: Left panel: Center-of-mass velocity $\langle \dot{x}_{\rm cm} \rangle$ versus the delay τ in the many particle case ($N = 10^5$). The region of small delays and the first two branches for asymmetries parameters $a = 1/3$ (positive flux) and $a = 2/3$ (negative flux) are plotted for height of the potential $V_0 = 5k_BT$. Units: $L = 1$ and $k_BT = 1$. Right panel: First two branches for asymmetries $a = 1/3$ and $a = 2/3$ for potential height $V_0 = 5k_BT$ and $N = 10^5$ particles, rescaled according to scaling laws (7.5) and (7.6).

7.4 Conclusions

We have studied the performance of feedback flashing ratchets when there is competition between the asymmetry in the potential and the asymmetry in the control protocol, and we have also studied the effects of tuning their relative influences in the dynamics by the introduction of a time delay. An experimental realization of a flashing ratchet has been performed in [16] by using polystyrene latex spheres of diameters $d \simeq 0.25 - 1\ \mu m$ in an aqueous solution [viscosity $\eta \simeq 10^{-3}\ Pa \cdot s$; $D = k_B T/(3\pi\eta d)$] exposed to a sawtooth dielectric potential of period $L \simeq 50\ \mu m$. This experimental setup can be modified to become an experimental realization of a feedback flashing ratchet by monitoring the particles with a conventional charge-coupled device (CCD) of about 30 fps and processing the images to switch on or off the ratchet potential in accordance with the particle positions. The time delays considered here are introduced by delaying the action of the controller a time between $\tau = 0.01L^2/D \sim 10s$ and $\tau = 0.5L^2/D \sim 500s$. (For a more detailed discussion see Ref. [12].) Indeed a sophisticated feedback control has been recently implemented in Ref. [18], where images of a Brownian particle are acquired on a high-sensitivity CCD of up to 300 fps and thereafter a software processes the information to extract the position of the particle and apply a feedback voltage. On the other hand, we highlight that the viscous friction coefficient γ depends on the shape and the size of the Brownian particle. Thus, as the adimensional delay must be multiplied by the factor $L^2/D = \gamma L^2/k_B T$ in order to recover physical units, Brownian particles of different shape and size respond differently to a given time delay. This effect could be useful for separating different kinds of macromolecules.

We have seen that the performance of the system with competing asymmetries differs significatively from its counterpart ratchet with cooperating asymmetries. In the absence of delay the competition of asymmetries implies a decay of the current with the size of the ensemble much stronger than in the cooperative case ($1/\sqrt{N}$ vs $1/\ln N$). In the presence of delay the dynamics becomes richer with a current reversal for large delays. In the few particle regime the change from positive to negative current can be understood as a change from a purely closed-loop control to an effective open-loop control. On the other hand, in the many particle case the negative current regime appears for large enough delays as the consequence of the stabilization of several branches of quasiperiodic solutions. These stable branches have the opposite sign and are one semiperiod displaced with respect to those obtained for cooperating asymmetries, they also have a direct relation with them that allows the extension for the competing asymmetries case of the analytical results found in Ref. [12] for cooperative asymmetries.

Acknowledgments

We acknowledge financial support from the Ministerio de Ciencia y Tecnología (Spain) through the Research Project FIS2006-05895. In addition, M.F. thanks the Universidad Complutense de Madrid (Spain) and F.J.C. thanks ESF Programme STOCHDYN for their financial support.

Bibliography

[1] P. Reimann, Phys. Rep. **361**, 57 (2002).

[2] H. Linke, Appl. Phys. A **75**, 167 (2002).

[3] E. R. Kay, D. Leigh, and F. Zerbetto, Angew. Chem. Int. Ed. **46**, 72 (2007).

[4] A. L. R. Bug and B. J. Berne, Phys. Rev. Lett. **59**, 948 (1987)

[5] A. Ajdari and J. Prost, C. R. Acad. Sci. Paris II **315**, 1635 (1992).

[6] R. D. Astumian and M. Bier, Phys. Rev. Lett. **72**, 1766 (1994).

[7] F. J. Cao, L. Dinis and J. M. R. Parrondo, Phys. Rev. Lett. **93**, 040603 (2004).

[8] M. Feito and F. J. Cao, Eur. Phys. J. B **59**, 63 (2007).

[9] F. J. Cao, M. Feito, and H. Touchette, *Information and flux in a feedback controlled Brownian ratchet*, arXiv:cond-mat/0703492 (2007).

[10] L. Dinis, J. M. R. Parrondo, and F. J. Cao, Europhys. Lett. **71**, 536 (2005).

[11] M. Feito and F. J. Cao, Phys. Rev. E **74**, 041109 (2006).

[12] M. Feito and F. J. Cao, Phys. Rev. E. **76**, 061113 (2007).

[13] E. M. Craig, B. R. Long, J. M. R. Parrondo, and H. Linke, Europhys. Lett. **81**, 10002 (2008).

[14] M. Bier, Biosystems **88**, 301 (2007).

[15] U. E. Vincent, A. N. Njah, and J. A. Laoye, Physica D **231**, 130 (2007).

[16] J. Rousselet, L. Salome, A. Ajdari, and J. Prost, Nature **370**, 446 (1994).

[17] C. Marquet, A. Buguin, L. Talini, and P. Silberzan, Phys. Rev. Lett. **88**, 168301 (2002).

[18] A. E. Cohen and W. E. Moerner, Proc. Natl. Acad. Sci. **103**, 4362 (2006).

[19] R. F. Stengel, *Optimal Control and Estimation* (Dover, New York, 1994).

[20] J. Bechhoefer, Rev. Mod. Phys. **77**, 783 (2005).

[21] G. A. Bochanov and F. A. Rihan, J. Comput. Appl. Math. **125**, 183 (2000).

[22] T. D. Frank, Phys. Rev. E **71**, 031106 (2005).

[23] E. Schöll and H. G. Schuster (ed), *Handbook of Chaos Control, second completely revised and enlarged edition* (Wiley, 2007).

[24] T. Prager, H-P Lerch, L. Schimansky-Geier, and E. Schöll, J. Phys. A **40**, 11045 (2007).

[25] C. R. Doering, W. Horsthemke, and J. Riordan. Phys. Rev. Lett. **72**, 2984 (1994).

[26] M. M. Millonas and M. I. Dykman, Phys. Lett. A **185**, 65 (1994).

[27] R. Bartussek, P. Hänggi and J. G. Kissner, Europhys. Lett. **28**, 459 (1994).

[28] D. Dan, M.C. Mahato, and A. Jayannavar, Phys. Rev. E **63**, 056307 (2001).

[29] B. Ai, L. Wang, and L. Liu, Phys. Rev. E **72**, 031101 (2005).

[30] M. Bier and R. D. Astumian, Phys. Rev. Lett. **76**, 4277 (1996).

[31] J. F. Chauwin, A. Ajdari, and J. Prost, Europhys. Lett. **32**, 373 (1995).

[32] J. L. Mateos, Phys. Rev. Lett. **84**, 258 (2000).

[33] M. Barbi and M. Salerno, Phys. Rev. E **62**, 1988 (2000).

[34] C. Kettner, P. Reimann, P. Hänggi and F. Müller, Phys. Rev. E **61** 312 (2000).

[35] U. Henningsen and M. Schliwa, Nature **389**, 93 (1997).

[36] P. E. Kloeden and E. Platen, *Numerical Solution of Stochastic Differential Equations* (Springer, 1992).

Chapter 8

Rocking feedback controlled ratchets

arXiv:0902.3941 (SUBMITTED)

Rocking feedback controlled ratchets

M. Feito[1], J. P. Baltanás[2], and F. J. Cao[1,3]

[1] *Departamento de Física Atómica, Molecular y Nuclear, Universidad Complutense de Madrid, Avenida Complutense s/n, 28040 Madrid, Spain.*
[2] *Departamento de Física Aplicada II, Universidad de Sevilla, Av. Reina Mercedes 2, 41012 Sevilla, Spain.*
[3] *LERMA, Observatoire de Paris, Laboratoire Associé au CNRS UMR 8112, 61, Avenue de l'Observatoire, 75014 Paris, France.*

We investigate the different regimes that emerge when a periodic driving force, the rocking force, acts on a collective feedback flashing ratchet. The interplay of the rocking and the feedback control gives a rich dynamics with different regimes presenting several unexpected features. In particular, we show that for both the one-particle ratchet and the collective version of the ratchet an appropriate rocking increases the flux. This mechanism gives the maximum flux that has been achieved in a ratchet device without an a priori bias.

PACS numbers: 05.40.-a, 05.60.Cd

8.1 Introduction

Ratchets can be viewed as controllers that act on stochastic systems with the aim of inducing directed motion by breaking of thermal equilibrium and certain time-space symmetries [1, 2]. As usual in control theory [3], these systems are divided into *open-loop* ratchets [1], when the actuation does not use any knowledge of the state of the system; and *closed-loop* ratchets [4,5], when information on the state of the system is used to decide how to operate on the system. These closed-loop ratchets —also called feedback or information ratchets— have recently attracted attention as Maxwell's demon devices that are capable of maximizing the performance of ratchets [6,7]. They may also be relevant to get insight into the motion of linear, two headed, processive molecular motors [8]. In addition, experimental realizations of feedback ratchets have been recently proposed [4, 9, 10] and implemented [11] due to their potential relevance as nanotechnological devices.

A relevant class of ratchets are *flashing* ratchets, which operate switching on and off a spatially periodic potential. Flashing ratchets have been studied in both open-loop (e.g. [1, 12–14]) and closed-loop (e.g. [4, 5, 15, 16]) schemes. A generalization of these ratchets are pulsated ratchets [1], in which the amplitude of the ratchet potential is modulated in time, but not

necessarily flashed on and off. On the other hand, *rocking* ratchets operate thanks to a periodic driving force, and thus they perform an open-loop control. Rocking ratchets reveals a rich dynamics, which includes current reversals [17, 18], distinct stable trajectories [17], and quantization of the deterministic current [17, 19, 20]. The combination of open-loop pulsated ratchets and rocking ratchets has been studied in Refs. [21–24], giving the possibility of a reverse of the sign of the flux with respect to the simple rocked ratchet.

In the present paper we study the effects of adding a periodic driving force that rocks a feedback controlled flashing ratchet. We analyze the new intriguing dynamics that emerge due to the interplay between the feedback control and the rocking. In particular, we show that the rocking of a feedback ratchet allows the system to improve the flux performance. The optimization of the flux performance of ratchets is potentially relevant for their nanotechnological applications, and the enhancement of the flux performance in flashing ratchets due to feedback [7] has been recently verified experimentally [11]. We show here how this flux performance can be further improved thanks to the effects produced by an additional rocking force. In the next section we describe the rocked feedback controlled ratchet, and after, in Sec. 8.3, we study the one-particle ratchet. The collective version of the ratchet compounded of more than one particle is analyzed in Sec. 8.4 in the regimes of few and many particles. We finally summarize and comment our main results in Sec. 8.5.

8.2 The rocked feedback controlled ratchet

Let us consider N Brownian particles at temperature T in a periodic potential $V(x)$, the ratchet potential. The state of the system is described by the positions $x_i(t)$ of the particles ($i = 1, \ldots, N$) satisfying the overdamped Langevin equations with a fluctuating (rocking) force of amplitude A and frequency Ω,

$$\gamma \dot{x}_i(t) = \alpha(x_1(t), \ldots, x_N(t), t) F(x_i(t)) + A\cos(\Omega t) + \xi_i(t). \tag{8.1}$$

Here, $F(x) = -V'(x)$, γ is the friction coefficient (related to the diffusion coefficient D through Einstein's relation $D = k_B T/\gamma$), and $\xi_i(t)$ are Gaussian white noises of zero mean and variance $\langle \xi_i(t)\xi_j(t')\rangle = 2\gamma k_B T \delta_{ij}\delta(t-t')$. Note that the control parameter α depends explicitely on the state of the system. Therefore, this ratchet is feedback controlled, what implies an effective coupling between the particles.

We shall consider the relevant control policy that maximizes the instant center-of-mass velocity introduced in [5]. In this feedback protocol, the controller computes the force per particle due to the ratchet potential if it

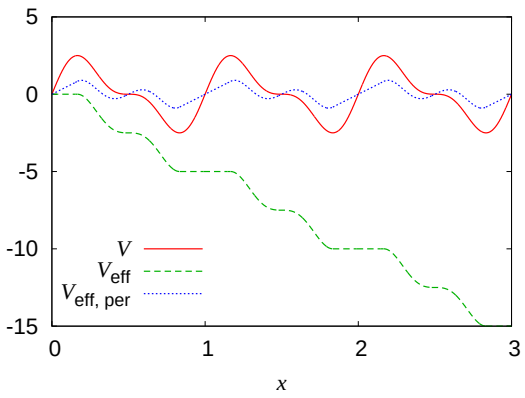

Figure 8.1: (Color online) Ratchet potential V (solid red line) [Eq. (8.4) with $V_0 = 5$], one-particle effective potential $V_{\rm eff}$ (dashed green line), and one-particle periodic effective potential $V_{\rm eff}^{\rm per}$ (dotted blue line). Units: $k_B T = 1$, $L = 1$.

were on,

$$f(x_1(t), \ldots, x_N(t)) = \frac{1}{N} \sum_{i=1}^{N} F(x_i(t)), \tag{8.2}$$

and switches the potential on ($\alpha = 1$) if $f(t)$ is positive or switches the potential off ($\alpha = 0$) otherwise. Therefore, the feedback control protocol considered is

$$\alpha(x_1(t), \ldots, x_N(t)) = \Theta(f(x_1(t), \ldots, x_N(t))), \tag{8.3}$$

with Θ the Heaviside function [$\Theta(x) = 1$ if $x > 0$, else $\Theta(x) = 0$].

In this study we have performed numerical computations of the Langevin equations (8.1), with the control parameter α given by Eq. (8.3), by using the Euler-Maruyama algorithm [25]. We have verified that these numerical results were not affected by systematic errors due to time discretization, initial transitories or finite number of realizations. The graphs that illustrate the results of this paper have been obtained considering the periodic asymmetric potential

$$V(x) = \frac{2V_0}{3\sqrt{3}} \left[\sin\left(\frac{2\pi x}{L}\right) + \frac{1}{2} \sin\left(\frac{4\pi x}{L}\right) \right], \tag{8.4}$$

which has potential height V_0 and period L; see Fig. 8.1. We can introduce an asymmetry parameter a for the potential such that aL is defined as the distance between a minimum of the potential and the first maximum at the righthand-side. The potential in Eq. (8.4) has an asymmetry parameter of $a = 1/3$. We have also performed computations with other potentials and found analogous results.

8.3 One-particle ratchet

For the one-particle ratchet ($N = 1$), the maximization of the instant velocity control policy, Eq. (8.3), only depends of the position $x(t)$ of the particle. Hence, we can define an effective force $F_{\text{eff}}(x) = \alpha(x)F(x)$ that allows us to rewrite the Langevin equation (8.1) as

$$\gamma\dot{x}(t) = F_{\text{eff}}(x(t)) + A\cos(\Omega t) + \xi(t). \tag{8.5}$$

The effective force F_{eff} derives from an effective potential $V_{\text{eff}}(x)$ that is no longer periodic, but tilted downhill. This V_{eff} can be recasted as a periodic potential $V_{\text{eff}}^{\text{per}}(x)$ of height aV_0 and asymmetry a, plus a linear term V_0x/L accounting for the bias, where V_0 is the height of the ratchet potential, a its asymmetry parameter, and L its period. Therefore, we can write $V_{\text{eff}}(x) = V_{\text{eff}}^{\text{per}}(x) - V_0x/L$, as we illustrate in Fig. 8.1 for the potential (8.4). In view of these considerations, the feedback rocking ratchet can be reinterpreted as an open-loop rocking ratchet with a biased asymmetric potential. Thus Eq. (8.5) stands for the celebrated SQUID ratchet [26],

$$\gamma\dot{x}(t) = -\frac{d}{dx}V_{\text{eff}}^{\text{per}}(x(t)) + V_0/L + A\cos(\Omega t) + \xi(t). \tag{8.6}$$

This equation of motion describes the dynamics of a tilted rocking ratchet, i.e. of a periodically driven single Brownian particle in a tilted washboard potential, and it has been extensively studied analytically and numerically [19,26–30] (even when inertial terms are also present [31]). For instance, for the adiabatic regime, i.e. the regime of slow driving [20], the flux can be approximated by

$$\langle\dot{x}\rangle = \frac{1}{\mathcal{T}}\int_0^{\mathcal{T}} \langle\dot{x}\rangle_{G(t)}\, dt, \tag{8.7}$$

where $\mathcal{T} = 2\pi/\Omega$ is the period of the driving force and $\langle\dot{x}\rangle_{G(t)}$ is the asymptotic flux that would be obtained if the driving force were fixed at the instant t to its value $G(t) = A\cos(\Omega t)$. This flux can be obtained by solving a Fokker-Plank equation for the resulting constant external force [6]. Other analytical results have been reported for the high-frequency regime [32,33], or the deterministic (zero temperature) regime [34,35]. Thanks to the equivalence found between the one particle rocked feedback ratchet [Eqs. (8.1) and (8.3)] and the SQUID ratchet [Eq. (8.6)], all the effects found for the rocked feedback ratchet have their counterparts in the extensively studied SQUID ratchet. However, it is important to emphasize that the tilt appears in our results not as an a priori bias, but as part of an effective description of the effects of the feedback.

Here, we discuss the results for the different regimes obtained by performing numerical simulations of the Langevin equation. We shall first discuss the case of zero temperature and later the case of nonzero temperature.

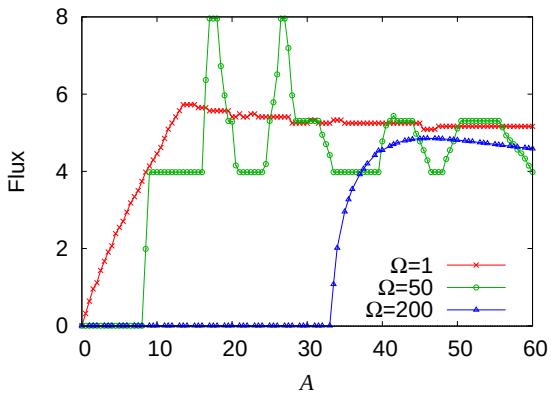

Figure 8.2: (Color online) One-particle case. Flux for the deterministic (zero temperature) rocked feedback ratchet as a function of the amplitude A of the rocking and frequencies $\Omega = 1, 50, 200$ for the ratchet potential of Fig. 8.1. Units: $V_0 = 5$, $L = 1$, $\gamma = 1$.

In the deterministic case of zero temperature there is no diffusion and only the rocking force can help the particle to cross the flat regions of the effective potential V_{eff} (see Fig. 8.1). This makes the flux strictly zero for small amplitudes such that the particle cannot overcome the flat part of the effective tilted potential; see Fig. 8.2. For higher amplitudes the flux exhibits remarkable characteristic effects. Our simulations show that the deterministic flux is quantized and it presents a step-like structure, a well-known effect for open-loop rocking ratchets [26–28]. This structure is specially clear for the frequency $\Omega = 50$ in Fig. 8.2. The flux quantization is owing to the synchronization with the phase of the periodic driving (see [26–28] for details). Its step-like structure presents a self-similar structure when successive zoom-in views are performed, which is known as Devil's staircase [19, 28].

Let us now discuss the case of nonzero temperature. A finite thermal noise leads to particle diffusion, which provides another mechanism to overcome the flat regions. This diffusion makes that the quantized step-like structure for the flux is smeared and finally wiped out. On the other hand, a surprising effect is found for this case, namely a flux increase when the feedback policy and the rocking forcing are both present. Unexpectedly, the resulting flux is greater than the sum of the flux values due to each separated effect, as we show in Fig. 8.3. In fact, the synchronization of the driving force with the feedback mechanism gives positive large fluxes even for the case of negative fluxes for the pure rocking, i.e. with the ratchet potential always on (compare, for instance, curves for $A = 40$ in top and bottom panels of Fig. 8.3, or curves for $\Omega = 100$ in panels of Fig. 8.4). Therefore, adding an external fluctuating force to the maximization of the

instant velocity feedback protocol allows us to improve the performance of the system in a nontrivial way which to our knowledge has not been previously reported. This fact is not only relevant from a theoretical point of view, but also for experimental ratchet devices designed to maximize the flux [4, 11].

Further insight on the behavior observed in the top panels of Figs. 8.3 and 8.4 can be obtained studying the fast driving regime. In this regime, it is useful to introduce a slow variable $y(t)$ such that the position $x(t)$ can be written as $x(t) = y(t) + \psi(t)$, where $\psi(t) = r\sin(\Omega t)$ is the fast contribution due to the fast driving, and $r := A/(\gamma\Omega)$. When the driving is fast enough, a large number of oscillations in $\psi(t)$ take place before a significant change in $y(t)$ occurs; thus we can proceed to the adiabatic elimination of the fast variable $\psi(t)$ by averaging it over time. This procedure leads to an effective equation for the slow variable

$$\gamma\dot{y}(t) = \bar{F}_{\rm eff}(y(t)) + \xi(t), \tag{8.8}$$

where $\bar{F}_{\rm eff}(y) = -\bar{V}'_{\rm eff}(y)$, with

$$\bar{V}_{\rm eff}(y(t)) := \frac{1}{\mathcal{T}}\int_0^{\mathcal{T}} V_{\rm eff}(y(t)+\psi(s))\, ds. \tag{8.9}$$

This effective potential allows us to give a closed-form expression for the flux [1],

$$\langle\dot{x}\rangle = \frac{Lk_BT\left[1 - e^{(\bar{V}_{\rm eff}(L)-\bar{V}_{\rm eff}(0))/k_BT}\right]}{\gamma\int_0^L dx\int_x^{x+L} dy\; e^{(\bar{V}_{\rm eff}(y)-\bar{V}_{\rm eff}(x))/k_BT}}. \tag{8.10}$$

Note that the potential $\bar{V}_{\rm eff}(y(t))$ only depends on the characteristics of the driving force through the quotient $r = A/(\gamma\Omega)$, and hence the same is true for the flux obtained within this fast driving regime. This approach is known as the *vibrational mechanics* scheme [36]. It has been successfully applied to the characterization of the so called vibrational resonance in bistable systems, both in the absence [37–39] and presence [40] of noise, as well as to the study of harmful effects (supression of the firing activity) of strong, high-frequency fields on the response of excitable systems [41]. In the context of ratchets, it has been used in the study of the effects of high frequency modulation on the output of Brownian particles moving in periodic one-dimensional substrates under the action of low frequency input signals [42, 43]. The results obtained with this vibrational mechanics procedure are valid when the rocking force has frequencies much larger than the rest of characteristic frequencies of the system [36]. The average in Eq. (8.9) makes the original potential barriers appear effectively lowered and flattened, eventually dissappearing as the ratio r increases. In particular, in our system, the periodic part of the one-particle effective potential $V_{\rm eff}(x) = V_{\rm eff}^{\rm per}(x) - V_0 x/L$ becomes smoother and smoother as an effect of

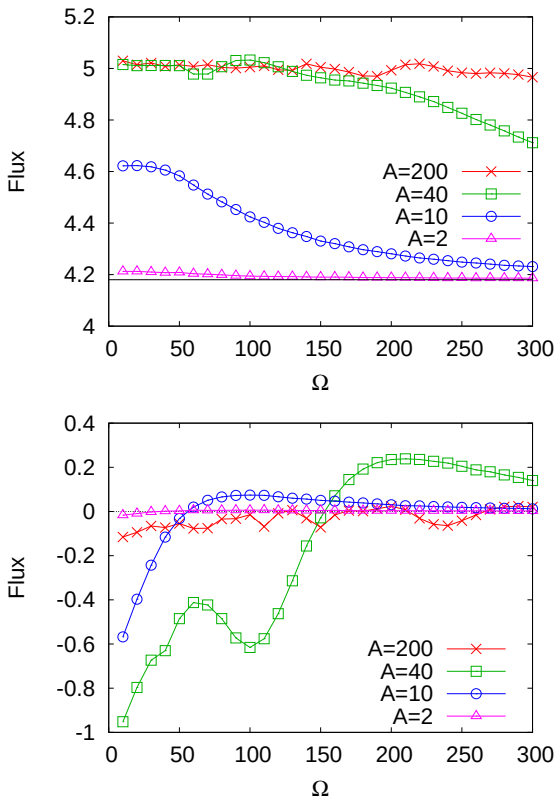

Figure 8.3: (Color online) One-particle case. *Top panel:* Flux $\langle \dot{x} \rangle$ versus frequency Ω for the rocked feedback ratchet. The horizontal solid line stands for the pure feedback ratchet —without rocking, i.e. $A = 0$.— *Bottom panel:* Flux $\langle \dot{x} \rangle$ versus frequency Ω for the pure rocking ratchet —without feedback flashing, i.e. $\alpha(t) = 1$.— We have used the ratchet potential of Fig. 8.1. Units: $k_B T = 1$, $L = 1$, $\gamma = 1$.

the averaging process as r growths, and for large r only the linear term survives in the effective potential, giving a flux value of $V_0/(L\gamma)$. Top panels of Figs. 8.3 and 8.4, and Fig. 8.5 show how this value is reached for large amplitudes. Indeed, this is the largest value of the flux that has been obtained in a ratchet device without an a priori bias; see Fig. 8.6.

The previous analysis also provides predictions on the dependency of the flux with the amplitude and frequency of the driving force. Within the vibrational regime, if the frequency is increased for a fixed amplitude, i.e. r is decreased, then the flux will decrease until the value of the pure feedback ratchet (see top panel of Fig. 8.3 and Fig. 8.5). Note that the values of the flux corresponding to low frequencies can be explained with the adiabatic description in Eq. (8.7). On the other hand, if the amplitude is increased

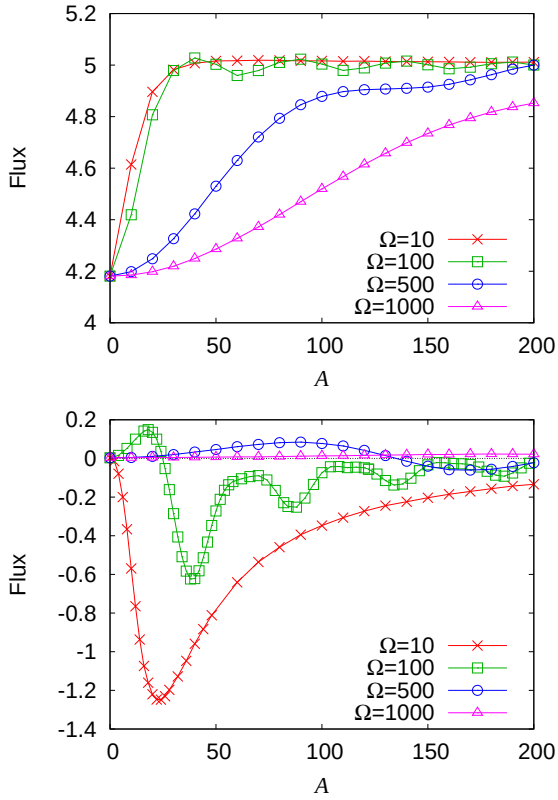

Figure 8.4: (Color online) One-particle case. *Top panel:* Flux $\langle \dot{x} \rangle$ versus amplitude A for the rocked feedback ratchet. The pure feedback ratchet —without rocking— corresponds to the point $A = 0$. *Bottom panel:* Flux $\langle \dot{x} \rangle$ versus amplitude A for the pure rocking ratchet —without feedback flashing, i.e. $\alpha = 1$.— We have used the ratchet potential of Fig. 8.1. Units: $k_B T = 1$, $L = 1$, $\gamma = 1$.

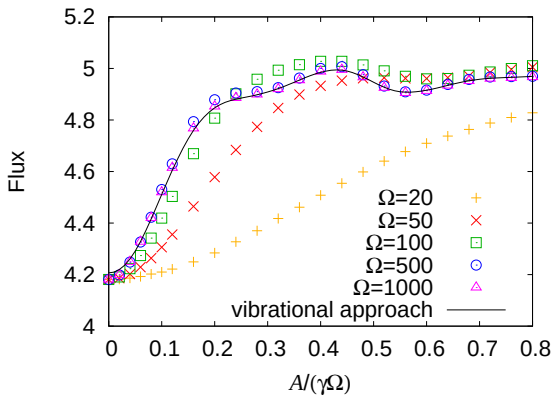

Figure 8.5: Flux $\langle \dot{x} \rangle$ versus $r = \frac{A}{\gamma\Omega}$ for the one-particle rocked feedback ratchet. For increasing frequencies the values of the flux tend to the curve of the vibrational approximation. We have used the ratchet potential (8.4) with $V_0 = 5$. Units: $k_B T = 1$, $L = 1$, $\gamma = 1$.

for a fixed frequency, i.e. r is increased, then the flux will increase from the value of the pure feedback ratchet up to the maximum value $V_0/(L\gamma)$ (see top panel of Fig. 8.4 and Fig. 8.5).

The effective potential $\bar{V}_{\rm eff}$ has allowed us to describe the dynamics in the vibrational regime. We have compared the results obtained directly from Eqs. (8.9) and (8.10) with numerical simulations of the Langevin equation (8.1), with a good agreement for the fast driving regime (Fig. 8.5). This stress again the significance of the vibrational approach that has been revealed as a useful approach for both qualitative and quantitative predictions. On the other hand, we have found that fluxes greater than $V_0/(L\gamma)$ can be attained outside the vibrational regime in the quasideterministic regime, i.e. for large values of the potential height and the driving force amplitude. [For example, the ratchet potential (8.4) with $V_0 = 40$, and a rocking force with $A = 160$ and $\Omega = 290$ gives $\langle \dot{x} \rangle \simeq 43$ in units $k_B T = 1$, $L = 1$, and $\gamma = 1$]. This result is in accordance with the results found in Ref. [29] for a tilted rocking ratchet in the quasideterministic regime.

8.4 Collective ratchet

The dynamics of the collective ratchet compounded of more than one particle differs significatively from that of the one-particle ratchet discussed before. For collective closed-loop ratchets the feedback effectively couples the particles with each other and no simplifying description in terms of an effective potential has been found.

The behavior of the deterministic (zero temperature) collective ratchet

is similar to that of the one-particle ratchet, including the quantization of the flux and the step-like structure commented in Sec. 8.3. We shall now focus in the nonzero temperature case for few- and many-particle collective ratchets where important differences emerge.

In the few particle case the maximum averaged center-of-mass flux is achieved for finite amplitudes and frequencies of the rocking force. Contrary to the one-particle case, the flux diminishes as the amplitude increases over its optimal value. On the other hand, we point out that for collective ratchets the maximum flux diminishes with the number of particles N. For a critical number of particles the dependence of the flux with N practically disappears, indicating the transition to the many-particle case; see Fig. 8.6. The value for this N-independent maximum flux that is obtained in the many-particle case coincides with the maximum flux obtained in the corresponding rocked flashing ratchet (open-loop). This coincidence is analogous to the coincidence between the maximum flux for the threshold protocol in the many-particle case and the maximum flux obtained from the corresponding flashing ratchet [16] (see also Fig. 8.6). Both of these coincidences can be interpreted as a consequence of the fact that these feedback protocols only use one bit of information about the system. This fact together with the increase of degrees of freedom of the system as N increases, makes that for systems with a large number of particles those feedback protocols cannot significantly beat their open-loop counterparts. In the following we discuss the interesting cooperative effects appearing in the many-particle case.

In the many-particle case, the force per particle due to the ratchet potential, $f(t)$ (defined in Sec. 8.2), has a quasideterministic evolution, as fluctuations in $f(t)$ are subdominant. The analysis of $f(t)$ has revealed to be very helpful to understand the dynamics. For the pure feedback ratchet (without rocking) with many particles the system dynamics gets trapped with the potential 'on' or 'off' because the force fluctuations responsible of the switchings are negligible [5]. Consequently, the system dynamics is near equilibrium most of the time and the net force is nearly zero. This implies an average asymptotic center-of-mass velocity $\langle \dot{x}_{CM} \rangle$ tending to zero as N increases [5]. However, the introduction of the driving force allows the system to avoid this trapping and can result in an increase of the flux.

Let us first discuss the cases of frequencies Ω of lower or similar order to $2\pi/\mathcal{T}_f$, with $\mathcal{T}_f$ the quasiperiod of $f(t)$ for the pure feedback ratchet [5]. The maximum values of the flux in the many-particle case are obtained in this low frequency regime. When the driving force is added, a complex synchronization appears between the quasideterministic dynamics of $f(t)$ and the driving force $A\cos(\Omega t)$. We show in Fig. 8.7 (top panel) a typical time evolution of the forces for this case. The value of the flux depends on the details of this synchronization and it shows local maxima and minima when the system's parameters are tuned; see bottom panel of Fig. 8.7. For the ratchet of this Figure the maximum flux $\langle \dot{x}_{CM} \rangle \simeq 2.1$ is achieved for

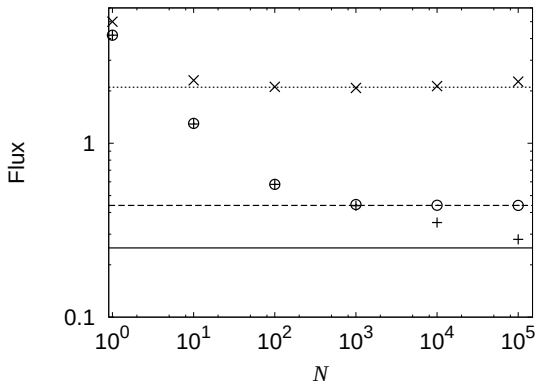

Figure 8.6: Maximum center-of-mass flux versus number of particles N for the optimal rocked feedback ratchet ($\times$), the optimal threshold protocol ($\circ$), the instant maximization protocol —pure feedback— ($+$), the optimal rocked flashing ratchet (dotted line), the optimal periodic protocol (dashed line), and the optimal rocking ratchet —pure rocking— (solid line). We have used the ratchet potential (8.4) with $V_0 = 5$. Units: $k_BT = 1$, $L = 1$, $\gamma = 1$.

a driving force of amplitude $A \simeq 20$ and frequency $\Omega \simeq 55$, expressed in units $k_BT = 1$, $L = 1$, $\gamma = 1$. We want to call the attention to the fact that this frequency coincides with the characteristic frequency of the optimal threshold protocol [16] and of the optimal flashing ratchet $\Omega = 2\pi/0.11 \simeq 57$. The maximum flux for the many-particle rocked feedback ratchet is reached when the rocking force has this characteristic frequency and pushes forward during the off period and backwards during the on period. This makes that the ratchet potential only hinders the backward pushes of the rocking force. Contrary to the one-particle case, the flux diminishes as the amplitude increases over its optimal value; compare Fig. 8.4, top panel, and Fig. 8.7, bottom panel.

On the other hand, in the regime of large frequencies ($\Omega \gg 2\pi/\mathcal{T}_f$) the pattern of $f(t)$ resembles the pattern for the pure feedback ratchet [5], but modulated by the high frequency signal (Fig. 8.8). For moderate values of the amplitude of the rocking, the system behaves more or less as if the fluctuations were increased. Therefore, an enlargement of the flux is possible for appropriate amplitude of the driving force that succeeds in preventing the trapping similarly to the so-called threshold protocol [15, 16]. We show in Fig. 8.8 this resonantlike effect for this regime. We note that for small amplitudes A the system is not able to avoid trapping, while for too large amplitudes the characteristic quasideterministic $f(t)$ pattern is erased and the flux goes to zero.

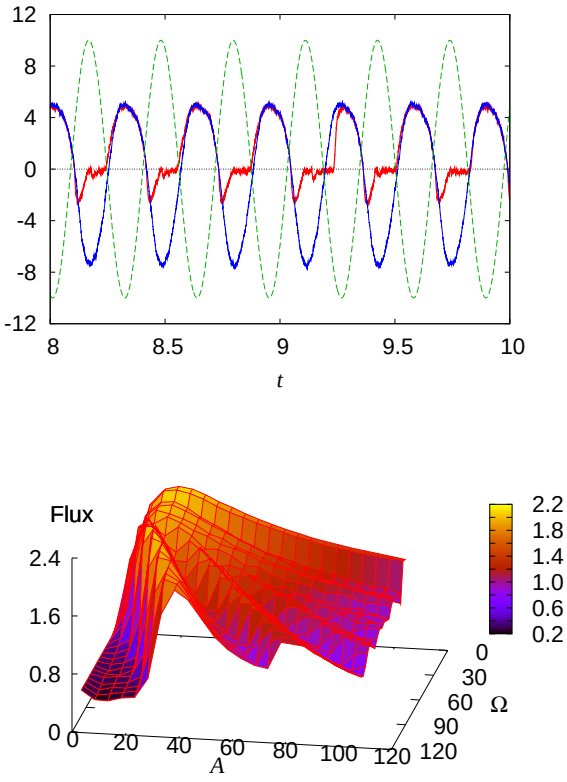

Figure 8.7: (Color online) Low and medium frequency rocking in the many-particle case ($N = 10^4$). *Top panel:* Time evolution of the force f [Eq. (8.2)] for the rocked feedback ratchet (thick red line) and for the pure rocking ratchet (thin blue line), both with a rocking force (dashed line) of amplitude $A = 10$ and frequency $\Omega = 20$. *Bottom panel:* Flux $\langle \dot{x}_{CM} \rangle$ versus amplitude and frequency for the rocked feedback ratchet. We have used the ratchet potential (8.4) with $V_0 = 5$. Units: $k_B T = 1$, $L = 1$, $\gamma = 1$.

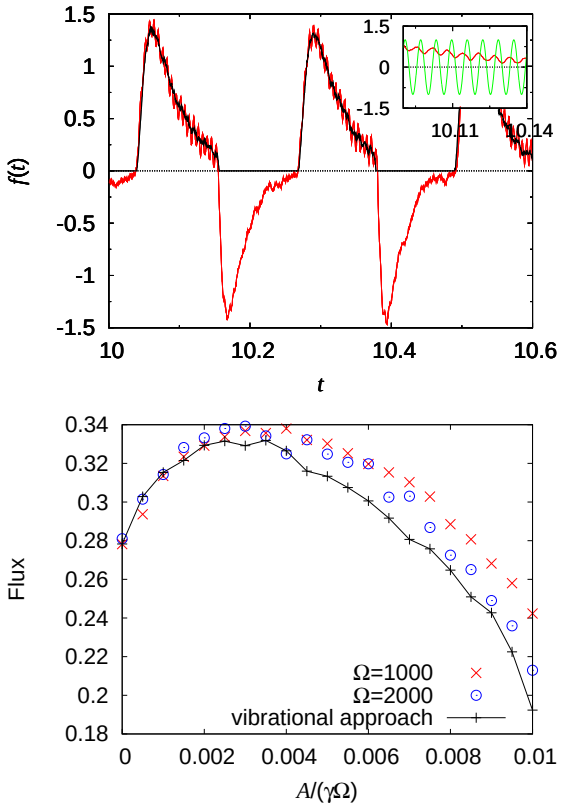

Figure 8.8: (Color online) Many-particle case ($N = 10^5$) high-frequency rocking ($\Omega = 1000$) for the ratchet potential (8.4) with $V_0 = 5$. *Top panel:* Evolution of the force f [Eq. (8.2)] for the feedback ratchet rocked with a high-frequency rocking force of amplitude $A = 1$ compared with the average force $\sum_{i=1}^{N} \bar{F}_i/N$ with $\bar{F}_i$ given by Eq. (8.12). We illustrate in the inset the modulation of $f(t)$ (thick red line) due to the high-frequency rocking (thin green line). *Bottom panel:* Flux $\langle \dot{x}_{CM} \rangle$ versus $A/(\gamma\Omega)$ for two high-frequency rockings compared with the prediction of the vibrational approximation [Eqs. (8.11), (8.12)]. Units: $k_B T = 1$, $L = 1$, $\gamma = 1$.

As in the one-particle ratchet, a vibrational regime appears when the displacements induced by the driving force are faster than the effects of the other terms. This is shown in the bottom panel of Fig. 8.8. In this panel, the dependence of the flux on the ratio $r = A/(\gamma\Omega)$ for two different high-frequency rocking forces is compared with the flux obtained by assuming an effective dynamics defined as follows. As for the case $N = 1$, we introduce the slow variables $y_i(t) = x_i(t) - \psi(t)$, with $\psi(t) = r\sin(\Omega t)$ the displacements induced by the fast driving. Numerical simulations confirm that the dynamics in this regime is governed by the slow variables verifying the following averaged evolution equations:

$$\gamma\dot{y}_i(t) = \bar{F}_i(y_1(t), \ldots, y_N(t)) + \xi_i(t), \tag{8.11}$$

where

$$\begin{aligned}\bar{F}_i(y_1, \ldots, y_N) = \frac{1}{\mathcal{T}}\int_0^{\mathcal{T}} ds\, \alpha(y_1 + \psi(s), \ldots, y_N + \psi(s)) \\ \times F_i(y_1 + \psi(s), \ldots, y_N + \psi(s)),\end{aligned} \tag{8.12}$$

with α given by Eq. (8.3). This implies as before that within this regime the flux only depends on the characteristics of the driving force through the quotient $r = A/(\gamma\Omega)$. We have numerically checked this for the few and the many-particle cases with high frequency driving forces, finding a better agreement in the few-particle case. However, we have also found a good agreement in the many-particle case for small values of the rocking amplitude (see Fig. 8.8 bottom) when $\sum_{i=1}^{N} \bar{F}_i/N$ is a good average description of the force $f(t)$ (see Fig. 8.8 top). In addition to computations with the ratchet potential (8.4), we have also performed computations with other potentials and found analogous results.

8.5 Concluding remarks

In this paper we have studied the effects of rocking a feedback ratchet. The interplay between the rocking and the feedback policy gives an intriguing rich dynamics that we have analyzed and discussed.

For the one-particle rocked feedback ratchet we have found an effective description in terms of a tilted rocking ratchet. Our simulations for rocked feedback ratchets show a relevant effect, namely, the magnification of the flux with respect to both the pure rocking and the pure feedback. That is, the rocked feedback ratchet is able to give fluxes even larger than the sum of the two fluxes separately. At this point, we remark that one of the main advantages of feedback ratchets over their open-loop counterparts is their ability to enlarge the particle flux, as it has been proved theoretically [5] and experimentally [11]. In that sense, the introduction of the fluctuating force

in feedback ratchets provide a way to further enhance the flux performance. In fact, the one-particle rocked feedback ratchet studied here gives the maximum flux that has been achieved in a ratchet device without an a priori bias (see Fig. 8.6). This improvement in the flux performance is relevant for nanotechnological applications of the ratchets. In addition, the observed dependence of the flux on the frequency and amplitude of the rocking signal has been explained for the whole range of parameters of interest.

The rocking term also helps to enlarge the flux in the few- and many-particle case, as we have shown in Fig. 8.6. We have numerically shown the dependence of the flux with the amplitude and frequency of the driving force for these collective ratchets. The details of this dependence follow from the synchronization between the driving force and the feedback. In addition, we have found a new resonantlike effect when the amplitude of the rocking is tuned in the regime of high-frequency signals. This later effect can be viewed as similar to an effective enlargement of the fluctuations in the net force, which prevents the trapping of the dynamics near equilibrium and results in an increase of the flux.

To sum up, we have proposed and discussed a new closed-loop ratchet that is able to perform better than other known ratchets as a consequence of the nontrivial interplay of the feedback scheme and the rocking force.

Acknowledgments

MF and FJC acknowledge financial support from MCYT (Spain) through the Research Project FIS2006-05895, from the ESF Programme STOCHDYN, and from UCM and CM (Spain) through CCG07-UCM/ESP-2925 and CCG08-UCM/ESP-4062. JPB acknowledges support from the Universidad de Huelva (project FQM-276) and from the Ministerio de Ciencia e Innovación (Spain) under the research project FIS2008-02873.

Bibliography

[1] P. Reimann, Phys. Rep. **361**, 57 (2002).

[2] H. Linke, Appl. Phys. A **75**, 167 (2002).

[3] J. Bechhoefer, Rev. Mod. Phys. **77**, 783 (2005).

[4] E. M. Craig, N. J. Kuwada, B. J. Lopez, H. Linke, Ann. Phys. **17**, 115 (2008).

[5] F. J. Cao, L. Dinis and J. M. R. Parrondo, Phys. Rev. Lett. **93**, 040603 (2004).

[6] M. Feito and F. J. Cao, Eur. Phys. J. B **59**, 63 (2007).

[7] F. J. Cao, M. Feito, and H. Touchette, Physica A **388**, 113 (2009).

[8] M. Bier, Biosystems **88**, 301 (2007).

[9] M. Feito and F. J. Cao, Phys. Rev. E **76**, 061113 (2007).

[10] E. M. Craig, B. R. Long, J. M. R. Parrondo, and H. Linke, Europhys. Lett. **81**, 10002 (2008).

[11] B. J. Lopez, N. J. Kuwada, E. M. Craig, B. R. Long, and H. Linke, Phys. Rev. Lett **101**, 220601 (2008).

[12] A. L. R. Bug and B. J. Berne, Phys. Rev. Lett. **59**, 948 (1987)

[13] R. D. Astumian and M. Bier, Phys. Rev. Lett. **72**, 1766 (1994).

[14] A. Ajdari and J. Prost, C. R. Acad. Sci. Paris II 315, 1638 (1993).

[15] L. Dinis, J. M. R. Parrondo, and F. J. Cao, Europhys. Lett. **71**, 536 (2005).

[16] M. Feito and F. J. Cao, Phys. Rev. E **74**, 041109 (2006).

[17] R. Bartussek, P. Hänggi, and J. G. Kissner, Europhys. Lett. **28**, 459 (1994).

[18] M. Schreiner, P. Reimann, P. Hänggi, and E. Pollak, Europhys. Lett. **44** 416 (1998).

[19] A. Ajdari, D. Mukamel, L. Peliti, and J. Prost, J. Phys. I **4** 1551 (1994).

[20] M. O. Magnasco, Phys. Rev. Lett. **71**, 10 (1993).

[21] S. Savel'ev, F. Marchesoni, P. Hänggi, and F. Nori, Eur. Phys. J. B. **40**, 403 (2004).

[22] S. Savel'ev, F. Marchesoni, P. Hänggi, and F. Nori, Europhys. Lett. **67**, 179 (2004).

[23] S. Savel'ev, F. Marchesoni, P. Hänggi, and F. Nori, Phys. Rev. E **70**, 066109 (2004).

[24] M. Borromeo and F. Marchesoni, Chaos **15**, 026110 (2005).

[25] P. E. Kloeden and E. Platen, *Numerical Solution of Stochastic Differential Equations* (Springer, 1992).

[26] I. Zapata, R. Bartussek, F. Sols, and P. Hänggi, Phys. Rev. Lett. **77**, 2292 (1996).

[27] P. Jung and P. Hänggi, Ber. Bunsen-Ges. Phys. Chem. **95**, 311 (1991) [Reports des Instituts für Physik der Universität Augsburg **9**].

[28] F. R. Alatriste and J. L. Mateos, Physica A **372**, 263 (2006).

[29] D. Reguera, P. Reimann, P. Hänggi, and J. M. Rubí, Europhys. Lett. **57**, 644 (2002).

[30] W. T. Coffey, J. L. Déjardin, and Yu. P. Kalmykov, Phys. Rev. E **61**, 4599 (2000).

[31] J. L. Mateos and F. R. Alatriste, Chaos **18**, 043125 (2008).

[32] J. Plata, Phys. Rev. E **57**, 5154 (1998).

[33] P. Reimann, Lect. Notes Phys. **557**, 50 (2000).

[34] I. Bena, C. Van den Broeck, R. Kawai, and K. Lindenberg, Phys. Rev. E **68**, 041111 (2003).

[35] I. Bena, C. Van den Broeck, R. Kawai, and K. Lindenberg, Phys. Rev. E **66**, 045603(R) (2002).

[36] I. I. Blechman, *Vibrational Mechanics* (World Scientific, Singapore, 2000).

[37] P. S. Landa and P. V. E. McClintock, J. Phys. A **33**, L433 (2000).

[38] A. A. Zaikin, L. López, J. P. Baltanás, J. Kurths, and M. A. F. Sanjuán, Phys. Rev. E **66** 011106 (2002)

[39] J. P. Baltanás, L. López, I. I. Blechman, P. S. Landa, A. Zaikin, J. Kurths, and M. A. F. Sanjuán, Phys. Rev. E **67** 066119 (2003).

[40] J. Casado-Pascual and J. P. Baltanás, Phys. Rev. E **69** 046108 (2004).

[41] D. Cubero, J. P. Baltanás and J. Casado-Pascual, Phys. Rev. E **73** 061102 (2006).

[42] M. Borromeo and F. Marchesoni, Europhys. Lett. **72** 362 (2005).

[43] M. Borromeo and F. Marchesoni, Phys. Rev. E **73** 016142 (2006).

Chapter 9

Information and flux in a feedback controlled Brownian ratchet

PHYSICA A **388**, 113 (2009)

Information and flux in a feedback controlled Brownian ratchet

F. J. Cao[1,2], M. Feito[1], and H. Touchette[3]

[1] *Departamento de Física Atómica, Molecular y Nuclear, Universidad Complutense de Madrid, Avenida Complutense s/n, 28040 Madrid, Spain.*
[2] *LERMA, Observatoire de Paris, Laboratoire Associé au CNRS UMR 8112, 61, Avenue de l'Observatoire, 75014 Paris, France.*
[3] *School of Mathematical Sciences, Queen Mary, University of London, London E1 4NS, UK*

We study a feedback control version of the flashing Brownian ratchet, in which the application of the flashing potential depends on the state of the particles to be controlled. Taking the view that the ratchet acts as a Maxwell's demon, we study the relationship that exists between the performance of the demon as a rectifier of random motion and the amount of information gathered by the demon through measurements. In the context of a simple measurement model, we derive analytic expressions for the flux induced by the feedback ratchet when acting on one particle and a few particles, and compare these results with those obtained with its open-loop version, which operates without information. Our main finding is that the flux in the feedback case has an upper bound proportional to the square-root of the information. Our results provide a quantitative analysis of the value of information in feedback ratchets, as well as an effective description of imperfect or noisy feedback ratchets that are relevant for experimental applications.

PACS numbers: 05.40.-a, 89.70.+c, 02.30.Yy

9.1 Introduction

Thermal ratchets or Brownian motors can be viewed as controllers that act on stochastic systems with the aim of inducing directed motion through the rectification of fluctuations [1–7]. In most cases, the system to be controlled is modelled as a collection of Brownian particles undergoing Langevin dynamics, and the control action—that is, the rectification mechanism—is implemented by applying random or deterministic time-dependent perturbations to the particles. In this context, one can distinguish, as is common in control theory [8], two types of ratchets: (i) *open-loop* ratchets, which are ratchets that apply a rectifying potential independently of the state of the system to be controlled; (ii) *closed-loop* or *feedback* ratchets, whose rectification action on a system has an explicit dependence on that system's evolution in time.

Examples of open-loop ratchets include the flashing ratchet [2,3] and the rocking ratchet [1,3]. An example of closed-loop ratchet based on the flashing ratchet was proposed in [6] (see also [7]). This feedback flashing ratchet could be implemented experimentally by monitoring colloidal particles suspended in solution and by exposing the particles to a saw-tooth dielectric potential as in [9], but with the potential turned on and off depending on particles' state. The feedback ratchet of [6] has also been proposed as a mechanism to explain the stepping motion of a two-headed motor protein [10]. In a more general context, recent experiments have shown that information about the location of a macrocycle in a rotaxane—an organic molecule with a ring threaded onto an axle—can be used to induce direct transport away from thermal equilibrium [11]. The operation of such a molecular ratchet is information-dependent, as it relies on knowledge of the position of the ring. The use of information is also relevant in other chemical and biological ratchet-like systems [12].

The main motivation for studying closed-loop ratchets is that they have the potential to perform better as rectifiers of motion than open-loop ratchets, thereby opening the possibility of improving the technological applications of ratchets. Our goal in this paper is to establish a quantitative comparison between closed- and open-loop ratchets that explicitly focuses on what distinguishes them, namely the use of information. This is done in three steps using the feedback ratchet of [6] as a case example. First, we show how the information used by this ratchet can be quantified (Sec. 9.2). Then we study how the performance of that ratchet, measured by the magnitude of the flux of particles that it induces, varies as a function of the amount of information used in the ratchet effect (Sec. 9.3). The results obtained are discussed in Sec. 9.4 and compared with those obtained with the open-loop version of the flashing ratchet, which operates without information. In Sec. 9.4, we also discuss the performance of the feedback ratchet as a function of the correlation established between the controlled system and the controller, and briefly discuss other performance measures for feedback ratchets, including the power output and the thermodynamic efficiency. The results that we obtain are in the end specific to the feedback ratchet of [6], but the method that we describe, which is inspired from Maxwell's concept of thermodynamic demons [13], information theory [14] and the work of one of us [15], is general and can be applied to other feedback ratchets and other control systems.

9.2 Feedback ratchet and information

The model of feedback ratchet that we study is constructed as follows [6]. We consider a system of N particles with positions $x_i(t)$, whose evolution is

described by a set of overdamped Langevin equations:

$$\gamma \dot{x}_i(t) = \alpha(t) F\left(x_i(t)\right) + \xi_i(t); \quad i = 1, \ldots, N. \tag{9.1}$$

Here, γ is the friction coefficient related to the diffusion coefficient D through Einstein's relation $D = k_B T/\gamma$, and $\xi_i(t)$ are Gaussian white noises of zero mean satisfying the fluctuation-dissipation relations $\langle \xi_i(t)\xi_j(t')\rangle = 2\gamma k_B T \delta_{ij}$ $\delta(t-t')$. All the particles are subjected to the same potential force $F(x) = -V'(x)$, derived from the following asymmetric, saw-tooth potential:

$$V(x) = \begin{cases} \frac{xV_0}{aL} & \text{if } 0 \le \frac{x}{L} \le a \\ V_0 - \frac{V_0}{1-a}\left(\frac{x}{L} - a\right) & \text{if } a < \frac{x}{L} \le 1, \end{cases} \tag{9.2}$$

which is made periodic by the condition $V(x+L) = V(x)$; see Fig. 9.1(a). Finally, $\alpha(t)$ is a control parameter that switches the potential on ($\alpha = 1$) or off ($\alpha = 0$). In the open-loop flashing ratchet, the value of $\alpha(t)$ is typically changed periodically in time, whereas in the feedback ratchet of [6], $\alpha(t)$ is set to 1 if the net force

$$f(t) = \frac{1}{N} \sum_{i=1}^{N} F\left(x_i(t)\right) \tag{9.3}$$

applied to the particles is positive; otherwise, $\alpha(t) = 0$. Thus $\alpha(t) = \Theta\left(f(t)\right)$, where $\Theta(x)$ is the Heaviside function. This feedback control strategy is the best possible strategy for maximizing the average velocity of one particle, but not the best strategy when it comes to more than one particle. This can be understood by noting that the system's dynamics tends to get trapped as $N \to \infty$, with the consequence that the particle flux decreases to zero in this limit [6]. By contrast, the open-loop ratchet induces a flux of particles which is independent of the number of particles.

For the remaining, it is useful to picture the ratchet as a Maxwell's demon [13] which rectifies the motion of the Brownian particles by repeatedly estimating the sign of $f(t)$, and by subjecting the particles to the on or off potential depending on the value of the sign measured. When selecting the potential at a given time t, the demon uses only the sign of $f(t)$ or, equivalently, $\alpha(t)$ at time t. It does not use past information about $f(t)$, nor does it use any detailed information about the positions of the particles. Accordingly, what should be quantified as the relevant information used by the feedback ratchet is the information content or *variability* of $\alpha(t)$, given by its entropy

$$I = H(b) = -b \log_2 b - (1-b)\log_2(1-b), \tag{9.4}$$

where b represents the probability that $f(t)$ is negative. The information I is measured in bits, and represents the *average* information content of $\alpha(t)$

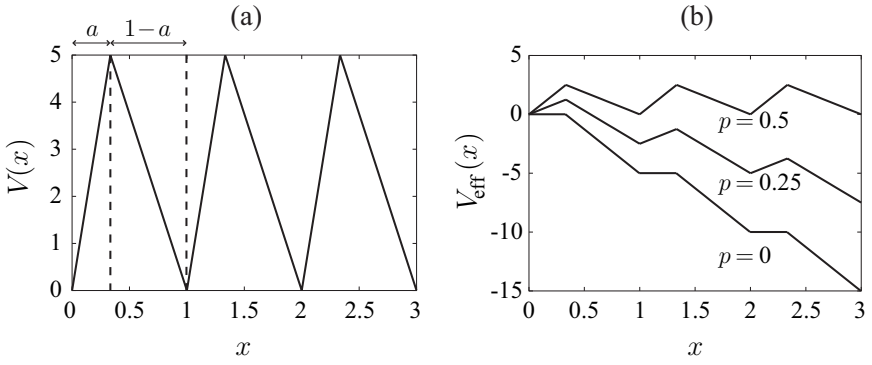

Figure 9.1: (a) Ratchet potential. (b) Corresponding effective potential in the case of one particle for three values of the noise level p. The potentials are plotted for $V_0 = 5$ and $a = 1/3$. Units: $L = 1$, $D = 1$ and $k_BT = 1$.

in that it corresponds to the average number of bits needed to store the random outcomes of $\alpha(t)$ [14].

Since our goal is to study the performance of the demon as a function of I, we need to supplement our measure of information with a way to vary that information. This is accomplished by introducing noise in the estimation of $f(t)$. It should be said that noise is always present in control systems in the measurement step, in the transmission of the measurement information to the controller, or even in the control-actuation step. Moreover, adding noise to a ratchet model can provide an effective way of describing an imperfect feedback controlled ratchet, such as one plagued by time delays [16].

Here we assume that there is a noise in the estimation of $f(t)$, which leads the demon to wrongly estimate the sign of $f(t)$ with a probability $p \in [0, 1/2]$, thereby leading it to apply the wrong potential with probability p. Thus, when $f(t) \geq 0$, the demon inadvertently switches off the potential with probability p, resulting in an effective on potential $V_{\text{eff,on}}(x) = (1 - p)V(x)$. Conversely, when $f(t) < 0$, the demon inadvertently switches on the potential with probability p, resulting in an effective off potential $V_{\text{eff,off}}(x) = pV(x)$. The combination of these two situations leads, in effect, to having the following "noisy" control strategy:

$$\alpha_{\text{eff}}(t) = (1 - p)\Theta(f) + p\Theta(-f). \tag{9.5}$$

From the point of view of information theory, the noisy measurement of the sign of $f(t)$ is equivalent to a noisy transmission channel known as the binary symmetric channel [14]. The average amount of information transmitted through this channel is measured in terms of a quantity known as the mutual information (see [14] for a general definition of this quantity). In our case, the mutual information can be calculated exactly (see Sec. 8.1.4

of [14]), and has for expression

$$I = H(q) - H(p), \tag{9.6}$$

where H is, as in Eq. (9.4), the binary entropy function, p is the noise level, and q is the probability that the corrupted sign of $f(t)$ is negative. In terms of the probability b that the *actual* sign of $f(t)$ is negative, we have $q = (1-p)b + p(1-b)$. Note that b depends in general on the number N of particles, the characteristics of the ratchet potential $V(x)$, as well as p, so that I is a function of all these parameters.

9.3 Results

The noise model that we consider is such that the ratchet operates with maximum information when $p = 0$, in which case $I = H(b) \leq 1$, and with minimum information ($I = 0$) when $p = 1/2$. To study the exact performance of the ratchet in and in between these two regimes, we derive in this section the expression of the flux of rectified particles as a function of p, and rewrite this expression as a function of I using Eq. (9.6). Both the cases of one particle and a few particles are considered.

9.3.1 One-particle case

For a single controlled particle, the net force is simply $f(t) = F(x(t))$, with $x(t)$ the position of the particle. Recalling the form of the saw-tooth potential defined in Eq. (9.2), we have that $f(t) < 0$ for $x \in (0, aL)$, and $f(t) > 0$ for $x \in (aL, L)$. As a result, the effective control parameter $\alpha_{\text{eff}}(t)$ can be rewritten as

$$\alpha_{\text{eff}}(x) = \begin{cases} p & \text{if } 0 < \frac{x}{L} \leq a \\ 1-p & \text{if } a < \frac{x}{L} \leq 1. \end{cases} \tag{9.7}$$

From this expression, we obtain an exact analytical expression for the average flux $\langle \dot{x} \rangle$ of the particle by solving the Fokker-Planck equation associated with the effective force $F_{\text{eff}}(x) = \alpha_{\text{eff}}(x)F(x)$ that derives from the effective control potential depicted in Fig. 9.1(b). The result in the stationary regime is

$$\langle \dot{x} \rangle = \frac{p^2(1-p)^2 V_0^2 A}{AE - B^+ B^-}, \tag{9.8}$$

with

$$\begin{aligned} A &= 1 - e^{(2p-1)V_0} \\ B^{\pm} &= e^{\pm pV_0}[a(1-p) + p(1-a)] - e^{\pm(2p-1)V_0} p(1-a) - a(1-p) \\ E &= a^2(1-p)^2(1 - pV_0 - e^{-pV_0}) \\ &\quad + ap(1-a)(1-p)(1-e^{-pV_0})[1 - e^{(1-p)V_0}] \\ &\quad + p^2(1-a)^2[1 - e^{(1-p)V_0} + (1-p)V_0], \end{aligned} \tag{9.9}$$

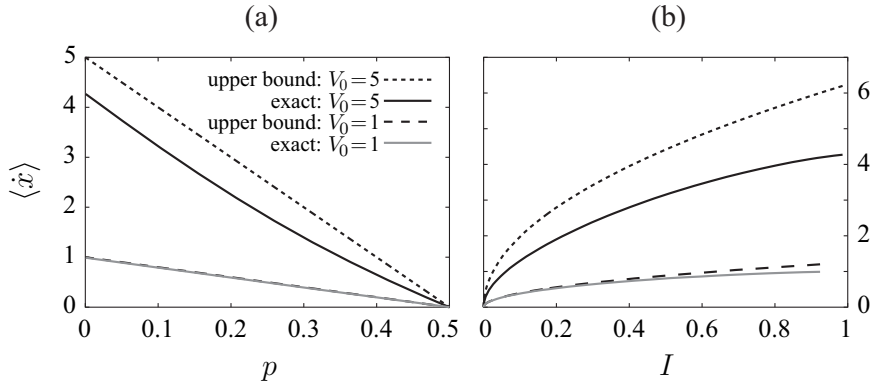

Figure 9.2: (a) Stationary flux as a function of the noise level p for the potential heights $V_0 = 1$ and $V_0 = 5$ in the one particle case. (b) Stationary flux as a function of the information I. Units: $L = 1$, $D = 1$ and $k_BT = 1$.

in units where $L = 1$, $D = 1$, and $k_BT = 1$. We have checked that this result is correct by performing Langevin simulations of the feedback ratchet. As seen in Fig. 9.2(a), the flux is maximum for $p = 0$ and decreases monotonically to zero as p goes to $1/2$.

To transform the expression of $\langle \dot{x} \rangle$ shown above into a function of I, we need to invert the expression of I shown in (9.6) to obtain p as a function of I. This requires the expression of b, which is obtained by integrating over the space interval $[0, aL]$ the stationary distribution of the effective Fokker-Planck equation,

$$b = \langle \dot{x} \rangle \left(\frac{a}{pV_0} \right)^2 \left\{ (1 - e^{-pV_0}) \left[1 + \frac{1 - e^{pV_0} - e^{pV_0}(1 - e^{-V_0(1-p)}) \frac{(1-a)p}{(1-p)a}}{e^{-V_0(1-2p)} - 1} \right] - pV_0 \right\}, \tag{9.10}$$

with $\langle \dot{x} \rangle$ given in (9.8), and units $L = 1$, $D = 1$, and $k_BT = 1$. This inversion gives the exact result for $\langle \dot{x} \rangle$ versus I, which is plotted in Fig. 9.2(b). Unfortunately, we cannot provide a closed-form expression of $\langle \dot{x} \rangle(I)$ because $p(I)$ seems to have no closed-form expression. However, it is possible to derive a useful approximation of the exact numerical result reported in Fig. 9.2(b). Indeed, we can expand $I(p)$ to second order in p around the minimum located at $p = 1/2$ to obtain

$$p(I) \approx \frac{1}{2} - \sqrt{\frac{I \ln 2}{8b(1-b)}}, \tag{9.11}$$

assuming that b does not depend on p. Then, for small potentials, i.e.,

$V_0 \ll k_B T$, we have $b \approx a$ and

$$\langle \dot{x} \rangle \approx \frac{V_0}{L\gamma}(1-2p) \tag{9.12}$$

from Eq. (9.8), so that

$$\langle \dot{x} \rangle \approx \frac{V_0}{L\gamma}\sqrt{\frac{I \ln 2}{2a(1-a)}}. \tag{9.13}$$

This approximation is a priori valid only in the regime where $I \ll 1$ and $V_0 \ll k_B T$, but Fig. 9.2(b) shows that it is accurate over the whole range of I even when $V_0 \approx k_B T$. An additional benefit of Eq. (9.13) is that it is an upper bound on $\langle \dot{x} \rangle$ versus I for any value of I and any potential height V_0. This follows because the right-hand side of (9.12) is an upper bound on the exact result shown in Eq. (9.8) [18]; see Fig. 9.2.

9.3.2 Few-particle case

Approximations similar to those given in (9.12) and (9.13) can also be derived for the case where more than one particle is controlled by the feedback ratchet. In the case of a few particles, the net force has a distribution $\rho(f)$ which can be approximated by a Gaussian distribution,

$$\rho(f) \approx \frac{1}{\sqrt{2\pi\Sigma^2}}\, e^{-\frac{f^2}{2\Sigma^2}}, \tag{9.14}$$

having a zero mean and variance

$$\Sigma = \frac{V_0}{L\sqrt{a(1-a)N}}. \tag{9.15}$$

This Gaussian approximation is derived under two basic assumptions [6]: (i) the positions of the particles are statistically independent; (ii) the probability of finding a particle in a negative force interval (for example $[0, aL]$) is a. It can be shown that these two assumptions are verified for small potential even in the presence of noise (i.e., $p \neq 0$).

Using the approximation shown in (9.14), we can obtain an approximate expression for the average center-of-mass velocity $\langle \dot{x}_{\rm cm} \rangle$ as a function of the transmission error p using the relation

$$\langle \dot{x}_{\rm cm} \rangle \approx \frac{1}{\gamma}\int_{-\infty}^{\infty} \alpha_{\rm eff}(f) f \rho(f) df, \tag{9.16}$$

with $\alpha_{\rm eff}(f)$ given by Eq. (9.5). In our case, we find

$$\langle \dot{x}_{\rm cm} \rangle \approx \frac{V_0}{L\gamma\sqrt{2\pi a(1-a)N}}(1-2p). \tag{9.17}$$

We have compared this results with Langevin simulations and found good fits for small potentials. For $p = 0$, the results of [6] for $\langle \dot{x}_{\rm cm} \rangle$ is recovered. In addition, we have verified numerically that Eq. (9.17) is an upper bound of the exact flux for any given potential height.

To turn the expression in (9.17) into an expression involving the information I, we use the approximation shown in (9.11) again to obtain

$$\langle \dot{x}_{\rm cm} \rangle \approx \frac{V_0}{L\gamma\sqrt{2\pi a(1-a)N}} \sqrt{\frac{I \ln 2}{2b(1-b)}}, \tag{9.18}$$

with b the probability of having a negative force in the few particle case. This probability can be approximated as

$$b \approx \sum_{n>aN}^{N} \binom{N}{n} a^n (1-a)^{N-n} \tag{9.19}$$

using the same assumptions as those involved in the Gaussian approximation for $\rho(f)$. The resulting approximation for $\langle \dot{x}_{\rm cm} \rangle$ is similar to the approximation derived for the one-particle ratchet in that it is a good approximation for small values of the potential height, in addition to being an upper bound on the flux for any given potential height. The latter property was checked numerically. The accuracy of the approximation for the probability b was also checked numerically.

9.4 Discussion

(1) The two approximations shown in (9.13) and (9.18) express the performance of the ratchet demon as a function of the information I that the demon gathers through the noisy measurement of $\alpha(t)$. Overall, we see from these results that the flux induced by the demon is maximum when it has maximum information, i.e., $I = H(b)$, and is zero when it has zero information. This applies both for the one-particle and few-particle ratchets. In both cases, we further have that the flux decreases monotonically as I decreases, and that the flux is approximately proportional to $\sqrt{I}$. The proportionality constant entering in this relation depends on the system's characteristics, and shows, in the case of a few particles, an N dependence that has the effect of reducing the flux as the number of particles is increased. This extra reduction of the flux is related to the fact that the fluctuations of the force have a smaller amplitude as N grows.

The decrease of flux directly associated with the decrease of information can be explained by noting again that the on and off potentials are partially 'mixed' or randomized by the noise. This is particularly evident when $p = 1/2$, i.e., when $I = 0$. In this case, the demon has a completely random estimate of the sign of $f(t)$ which is uncorrelated with its true sign; hence

$I = 0$. With the random value of the sign, the demon then applies a random potential to the particles, thereby injecting the noise of the estimation back into the motion of the particles. Such a feedback of estimation noise is often encountered in real control systems, and can be counteracted in various ways. The most common is to rely on past measurements of the controlled system to better estimate its actual state (filtering) [8]. For our demon, this would mean acting with memory of past measurements of the sign of $f(t)$, and error-correcting those measurements to avoid inferring the wrong value of the sign of $f(t)$.

(2) The expressions for the center-of-mass velocity as a function of the noise level p or of the information I can be rewritten in terms of the correlation

$$C = \langle \mathrm{sgn} f \ \mathrm{sgn} \tilde{f} \rangle, \tag{9.20}$$

where $\mathrm{sgn} f$ is the real sign of the net force that the particles would feel if the potential were on, while $\mathrm{sgn} \tilde{f}$ is the value that the controller receives. This correlation can be computed by using

$$C = P_{++} + P_{--} - P_{+-} - P_{-+}, \tag{9.21}$$

where P_{ij} is the joint probability that the real net force f is positive ($i = +$) or negative ($i = -$) and that the controller receives a positive ($j = +$) or negative ($j = -$) net force $\tilde{f}$. This joint probability is easily computed knowing that $\mathrm{sgn} f$ is different from $\mathrm{sgn} \tilde{f}$ with probability p. Thus we have $P_{-+} = bp$, $P_{--} = b(1-p)$, $P_{+-} = (1-b)p$ and $P_{++} = (1-b)(1-p)$, where b is the probability of $\mathrm{sgn} f$ being negative, so that

$$C = 1 - 2p. \tag{9.22}$$

Using this relation in Eqs. (9.8), (9.12) and (9.17), we obtain the expressions for the center-of-mass velocity as a function of the correlation C. In particular, for small potentials, we obtain

$$\langle \dot{x}_{\mathrm{cm}} \rangle \approx \frac{V_0}{L\gamma} C \tag{9.23}$$

for one particle, and

$$\langle \dot{x}_{\mathrm{cm}} \rangle \approx \frac{V_0}{L\gamma \sqrt{2\pi a(1-a)N}} C \tag{9.24}$$

for few particles.

As for Eqs. (9.12) and (9.17), the expressions shown above are upper bounds for the center-of-mass velocity for all potential heights, which show that the flux performance is reduced when the correlation between the controlled system and the controller decreases. This loss of correlation is always present in physical systems, and can be due to noise in the measurement

of $f(t)$ or in the transmission of this measurement to the controller. In this sense, the expressions shown in (9.23) and (9.24) can be thought of as describing a noisy feedback ratchet for which all the noise sources are effectively described by C. Such an effective description in terms of C can be used, in addition, to model other imperfect feedbacks, such as time-delayed feedbacks [16]. In the latter case, $\tilde{f} = f(t-\tau)$, where τ is a positive time delay, implying a loss of correlation between the actual force $f = f(t)$ and the applied force $\tilde{f}$.

Time delays are expected to be present in the experimental implementation of the feedback ratchet mentioned in the introduction, in which colloidal particles suspended in a solution are monitored and exposed to a saw-tooth dielectric potential. The previous discussion can directly be applied to this situation by computing C from the time series of $f(t)$ and the delayed signal $f(t-\tau)$, allowing the use of Eqs. (9.23) and (9.24) to predict the effects of time delays on the flux. The present noisy feedback model could also be useful as an effective description of the operation of an imperfect feedback loop in other ratchet-like systems [10, 11].

(3) Experimental implementations of feedback ratchets are unavoidably imperfect and noisy due to the aforementioned time delays and other experimental imperfections. These real-world limitations can be modelled, to a first level of approximation, by an effective noise level p acting at the level of estimation. With this in mind, one can use our noisy feedback ratchet model as a valuable effective model for estimating the improvement in flux that can be obtained in experimental implementations, such as those proposed in [6, 16, 17]. The authors of [17], for example, propose a feedback ratchet based on a scanning line optical trap. From the relevant parameters of their experimental set-up they found a probability of 1% of calculating the wrong sign of $f(t)$, and an information content of about $I = 0.9$ bits. Using the results presented here, they obtain that no more than 95% of the maximum gain achieved by the feedback strategy can be observed for that real system. The experimental realization of this system is currently under way [17].

(4) In general, the flux generated by the open-loop ratchet is much smaller than the flux generated by the feedback ratchet [6]. For the saw-tooth potential considered here, the *optimal* open-loop protocol generating the largest flux is the periodic protocol with on-potential time $T_{\rm on}$ and off-potential time $T_{\rm off}$. For $V_0 = 5k_BT$ and $a = 1/3$, the optimal values of these times are $T_{\rm on} \approx 0.06$ and $T_{\rm off} \approx 0.05$, in units where $D = 1$ and $L = 1$, yielding $\langle \dot{x}_{\rm cm} \rangle_{\rm open} \approx 0.3$. For the one-particle case, we have by comparison $\langle \dot{x}_{\rm cm} \rangle_{\rm closed} \approx 4.3$ when I is maximum. For other values of I, the previous results for one and few particles state that the center-of-mass flux $\langle \dot{x}_{\rm cm} \rangle$ is upper-bounded by $M\sqrt{I}$, where M is a constant depending on the system's characteristics; this upper-bound is also greater than the open-loop value for most values of I. Therefore, we can write

$$\langle \dot{x}_{\rm cm} \rangle_{\rm closed} - \langle \dot{x}_{\rm cm} \rangle_{\rm open} \leq M\sqrt{I}. \tag{9.25}$$

The feedback protocol that we have considered, which performs an instantaneous maximization of the center-of-mass velocity [6], is the optimal protocol that maximizes the flux in the one particle case for a noiseless channel ($p = 0$). We expect this protocol to give a flux close to the maximum possible value in the few particles case and in the presence of noise with a memoryless protocol (note that protocols with memory can perform error correction). Therefore, we expect Eqs. (9.13) and (9.18) to be upper bounds of the maximum flux that can be obtained with a memoryless closed-loop control protocol that uses an amount of information I about the system. Similarly, the inequality shown in Eq. (9.25) is expected to set an upper-bound on the maximum improvement that can result from changing an open-loop protocol to a memoryless closed-loop protocol. This, at least, is the case for one particle, as the instant maximization protocol is optimal when applied to one particle. For the few particle case, we expect the inequality to hold, although it could be violated by protocols other than the one considered here, as these could potentially be more efficient.

(5) We have focused here on proving an upper bound for the particle flux because this quantity can readily be measured in experimental realizations of feedback ratchets [17]. In a recent paper [19], written after the present one, an analogous upper bound was derived for the power output of a feedback ratchet, based on the results and techniques presented here. The difference between the particle flux and the power output is that the latter quantity requires that we impose a constant load force against the flux so as to compute the work done against the load; see [19] for more details.

(6) Another important performance measure for ratchets is the efficiency [20]. For the computation of this quantity, it is important to note that feedback ratchets have an extra energy input compared to open-loop ratchets, related to the fact that information has an energy cost [13]. This energy cost, known as Landauer's erasure cost because it is incurred when information is erased, effectively prevents Maxwell's demon-type engines, like feedback ratchets, to have efficiencies greater than one (as required by the second law of thermodynamics) [13]. The calculation of this energy cost requires the computation of the mutual information between the controlled system and the controller, conditioned on the past history of the controller's evolution [15, 21]. The role of the conditioning is to take into account the correlations between the measurements, and to avoid redundancies in the computation of the entropy reduction. The conditioning is also consistent with the fact that the controller's measurement record, seen as blocks of bits, must be compressed before it is erased in order to minimize the erasure cost; see Ref. [22].

(7) We have not addressed the many particle case, i.e., the case where

the fluctuations in the net force are smaller than the typical values of the net force. The reason for this omission is that, in the many particle case, the maximum increase of performance that results from changing the optimal open-loop protocol to a closed-loop protocol is negligible.

9.5 Summary

In summary, we have quantified the information gathered by a feedback control ratchet, and have derived analytical upper bounds, expressed as a function of the information, which establish limits on the difference between the flux of particles created by a closed-loop, flashing ratchet and the flux created by its open-loop version. These bounds provide a direct evaluation of the performance of the feedback ratchet as a function of the information that it uses, and make more precise the idea that feedback ratchets act like Maxwell's demons that use information about the state of particles to rectify the particles' motion. In addition, the analytic results found for the flux are useful in that they provide an effective description of a feedback flashing ratchet affected either by noise in the measurement process or other imperfections in the feedback mechanism. This effective description is useful for predicting the results of experimental realizations of feedback ratchets, as any experimental realization is subjected to noises, delays, and other imperfections in the feedback.

Acknowledgments

This work was supported by MCYT (Spain) (Grants BFM2003-02547/FISI, FIS2005-24376-E, and FIS/2006-05895), and by the ESF program STOCHDYN. M.F. acknowledges support from UCM (Spain) through the grant Beca Complutense. H.T. was supported by NSERC (Canada), the Royal Society, and HEFCE (England).

Bibliography

[1] M. O. Magnasco, Phys. Rev. Lett. **71**, 1477 (1993).

[2] A. Ajdari and J. Prost, C. R. Acad. Sci. Paris II **315**, 1635 (1993).

[3] R. D. Astumian and M. Bier, Phys. Rev. Lett. **72**, 1766 (1994).

[4] P. Reimann, Phys. Rep. **361**, 57 (2002).

[5] H. Linke, Appl. Phys. A **75**, 167 (2002).

[6] F. J. Cao, L. Dinis, and J. M. R. Parrondo, Phys. Rev. Lett. **93**, 040603 (2004).

[7] L. Dinis, J. M. R. Parrondo, and F. J. Cao, Europhys. Lett. **71**, 536 (2005); M. Feito and F. J. Cao, Phys. Rev. E **74**, 041109 (2006).

[8] R. F. Stengel, *Optimal Control and Estimation* (Dover, New York, 1994). See also J. Bechhoefer, Rev. Mod. Phys. **77**, 783 (2005).

[9] J. Rousselet, L. Salome, A. Ajdari, and J. Prost, Nature **370**, 446 (1994).

[10] M. Bier, Biosystems **88**, 301 (2007).

[11] V. Serreli, C.-F. Lee, E. R. Ray, and D. Leigh, Nature (London) **445**, 523 (2007).

[12] E. A. Kay, D. A. Leigh, and F. Zerbetto, Angew. Chem. Int. Ed. **46**, 72 (2007).

[13] H. S. Leff and A. F. Rex, *Maxwell's Demon: Entropy, Classical and Quantum Information, Computing* (Institute of Physics, Bristol, 2003).

[14] T. M. Cover and J. A. Thomas, *Elements of Information Theory* (John Wiley, New York, 1991).

[15] H. Touchette and S. Lloyd, Phys. Rev. Lett. **84**, 1156 (2000); Physica A **331**, 140 (2004).

[16] M. Feito and F. J. Cao, Phys. Rev. E **76**, 061113 (2007).

E. M. Craig, B. R. Long, J. M. R. Parrondo, and H. Linke, Europhys. Lett. **81**, 10002 (2008).

M. Feito and F. J. Cao, Physica A **387**, 4553 (2008).

[17] E. M. Craig, N. J. Kuwada, B. J. López, and H. Linke, Ann. Phys. **17**, 115 (2008).

[18] The upper bound on $\langle \dot{x} \rangle$, taken as a function of p, was verified numerically.

[19] M. Feito and F. J. Cao, Eur. Phys. J. B **59**, 63 (2007).

[20] J. M. R. Parrondo, J.M. Blanco, F. J. Cao, R. Brito, Europhys. Lett. **43**, 248 (1998).

[21] F. J. Cao, M. Feito, *Thermodynamics of feedback controlled systems*, arXiv:0805.4824 (2008).

[22] W. H. Zurek, Phys. Rev. A **40**, 4731 (1989); Nature **341**, 119 (1989).

Chapter 10

Information and maximum power in a feedback controlled Brownian ratchet

THE EUROPEAN PHYSICAL JOURNAL B **59**, 63 (2007)

Information and maximum power in a feedback controlled Brownian ratchet

M. Feito[1] and F. J. Cao[1,2]

[1] *Departamento de Física Atómica, Molecular y Nuclear, Universidad Complutense de Madrid, Avenida Complutense s/n, 28040 Madrid, Spain.*
[2] *LERMA, Observatoire de Paris, Laboratoire Associé au CNRS UMR 8112, 61, Avenue de l'Observatoire, 75014 Paris, France.*

Closed-loop or feedback controlled ratchets are Brownian motors that operate using information about the state of the system. For these ratchets, we compute the power output and we investigate its relation with the information used in the feedback control. We get analytical expressions for one-particle and few-particle flashing ratchets, and we find that the maximum power output has an upper bound proportional to the information. In addition, we show that the increase of the power output that results from changing the optimal open-loop ratchet to a closed-loop ratchet also has an upper bound that is linear in the information.

PACS numbers: 05.40.-a, 89.70.+c, 02.30.Yy

10.1 Introduction

Brownian ratchets have been studied in different contexts due to their theoretical importance in non-equilibrium statistical mechanics and their potential relevance for applications in disciplines like nanotechnology, condensed matter or biology [1–4]. Many studies deal with the performance of these devices (see refs. [1,5] for comprehensive reviews) concentrating on open-loop ratchets, as those obtained fluctuating an uniform external force (rocking ratchets [6,7]), or an external asymmetric potential (flashing ratchets [6,8]), either randomly or periodically. On the other hand, closed-loop or feedback controlled ratchets, as the so-called instant maximization protocol [9] and the threshold protocol [10], use information of the state of the system to operate. The feedback ratchet of [9] has been recently proposed as an effective model to describe the stepping motion of the two-headed kinesin [3]. Other 'information-dependent' rectification mechanism have been recently proposed to model certain chemical and biological systems [4].

The previous works [9–11] about closed-loop ratchets focussed on the study of the flux and its maximization. In particular, it has been shown that the increase of the flux performance when the optimal open-loop control is changed to a closed-loop control has an upper bound proportional to the square root of the information used by the controller [11].

In this paper, we consider another measure of the performance, viz. the power output, with the aim of getting further insight in the relation between information and the increase of performance in a system with thermal fluctuations. We oppose to the flux a constant load force [12] in order to compute the potential energy gain by the particles thanks to the action of the controller. The generalization of the methods developed in [11] allow us to obtain the relations between the maximum power output and the information that the controller uses.

10.2 The model

The collective feedback ratchet that we investigate has two basic ingredients, namely, N Brownian particles and a controller. The controller acts on the particles switching on and off a potential $V(x)$ according to the control policy and to the information received about the state of Brownian particles through a noisy channel.

Specifically, we consider N overdamped Brownian particles at temperature T in a piecewise linear saw-tooth potential

$$V(x) = \begin{cases} \frac{xV_0}{aL} & \text{if } 0 \leq \frac{x}{L} \leq a, \\ V_0 - \frac{V_0}{1-a}\left(\frac{x}{L} - a\right) & \text{if } a < \frac{x}{L} \leq 1, \end{cases} \tag{10.1}$$

of height V_0, asymmetry parameter a, and period L, *i.e.* $V(x) = V(x+L)$. The potential is switched on and off according to the instant maximization of the center-of-mass velocity protocol (see ref. [9]), which switches on the potential only when the net force due to the potential on the particles would be positive. In order to obtain work from the system operation we oppose to the flow of particles an homogeneous static force F_{ext}; thus, the total force acting on the particles when the potential is on is $F_{\text{tot}}(x) = F(x) - F_{\text{ext}}$, with $F(x) = -V'(x)$, and $F_{\text{tot}}(x) = -F_{\text{ext}}$ when the potential is off. The state of the system is described by the positions $x_i(t)$ of the particles that satisfy the Langevin equations

$$\gamma \dot{x}_i(t) = \alpha(t) F(x_i(t)) - F_{\text{ext}} + \xi_i(t); \quad i = 1, \ldots, N, \tag{10.2}$$

where γ is the friction coefficient (related to the diffusion coefficient D through Einstein's relation $D = k_B T/\gamma$) and $\xi_i(t)$ are Gaussian white noises of zero mean and variance $\langle \xi_i(t)\xi_j(t')\rangle = 2\gamma k_B T \delta_{ij}\delta(t-t')$. The dichotomous function $\alpha(t)$ [$\alpha = 0$ (potential off) or $\alpha = 1$ (potential on)] implements the action of the controller. The control policy uses the information received from the system through a noisy channel that we model with a binary symmetric channel [13]. This channel passes the sign of the net force

$$f(t) = \frac{1}{N} \sum_{i=1}^{N} F(x_i(t)) \tag{10.3}$$

to the controller with an error probability p known as the noise level of the channel, so when $f(t) > 0$ (< 0) the controller switches on (off) the potential with probability $1 - p$. Therefore, the feedback protocol and the noisy channel lead to the effective control policy

$$\alpha_{\rm eff}(t) = (1-p)\Theta(f) + p\Theta(-f), \tag{10.4}$$

with Θ the Heaviside function [$\Theta(x) = 1$ if $x > 0$, else $\Theta(x) = 0$]. This effective control policy is equivalent to the protocol of instant maximization through a noisy channel provided many measurement and control actions are performed in the characteristic time of the system evolution, which is the case we consider here.

Our aim is to study the dependence of the maximum power output with the information. On one hand, the average information transmitted through the noisy channel is quantified in terms of the mutual information [13] that the controller gets from the state of the system. Our case —the noisy measurement of the sign of the net force— is equivalent to a noisy channel called the binary symmetric channel in information theory. For this case the mutual information can be computed (see sec. 8.1.4 of [13]), and it is given (in bits) by

$$I = H(q) - H(p), \tag{10.5}$$

with $H(x) = -x\log_2 x - (1-x)\log_2(1-x)$, $q = (1-p)b + p(1-b)$ the probability that the controller receives a negative sign, and b the probability that the actual sign of the net force is negative. Therefore, the information I that the controller gets about the system is greatly determined by the noise level p of the channel; the maximum information is reached for $p = 0$ and it is at most 1 bit, while for $p = 1/2$ the channel becomes completely random and no information of the system is received by the controller. When the probability b does not depend on p, the relation between the noise level p and the information I can be easily expanded around $p = 1/2$ and reads

$$I(p) = \frac{1}{\ln 2}\sum_{k\ \rm even}\frac{2^k}{k(k-1)}\left[1-(1-2b)^k\right]\left(p-\frac{1}{2}\right)^k. \tag{10.6}$$

Inverting this relation to leading order we get for $p < 1/2$ the result [11]

$$p \simeq \frac{1}{2} - \sqrt{\frac{I\ln 2}{8b(1-b)}}. \tag{10.7}$$

On the other hand, a positive power output is obtained when there is a net flux against the load $F_{\rm ext}$ that tilts the potential. In the stationary regime the center-of-mass moves with a mean velocity $\langle \dot{x}_{\rm cm}\rangle$ and then the average power output (work obtained per unit time) is given by

$$P = F_{\rm ext}\langle \dot{x}_{\rm cm}\rangle. \tag{10.8}$$

We first analyze the dependence of the power output with the information for the case of one particle and later for the few-particle ratchet.

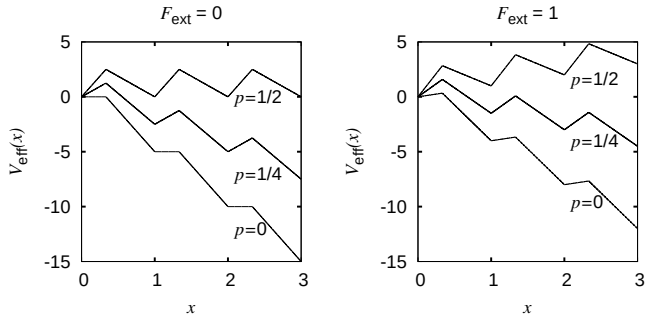

Figure 10.1: Effective potentials for one particle and noise levels $p = 0$, $1/4$, and $1/2$ with $V_0 = 5$ and $a = 1/3$. Left panel without external load, and right panel with external load $F_{\rm ext} = 1$. Units: $L = 1$, $D = 1$, and $k_B T = 1$. Note that for $p = 1/2$ the effective potential is equal to $V(x)/2 + F_{\rm ext} x$.

10.3 One particle

We start with the one particle case ($N = 1$) where an effective potential that includes the effects of the load, the control protocol, and the binary symmetric channel can be constructed. The system dynamics can be viewed as the result of the action of the periodic effective force $F_{\rm eff}(x) = \alpha_{\rm eff}(x)F(x) - F_{\rm ext}$ that derives from an effective potential. Using units $L = 1$ and $k_B T = 1$, this effective potential can be written in terms of $K := pV_0 + F_{\rm ext} a$ and $M := (1-p)V_0 - F_{\rm ext}(1-a)$ as

$$V_{\rm eff}(x) = \begin{cases} \frac{xK}{a} & \text{if } 0 \le x \le a, \\ K - M\frac{x-a}{1-a} & \text{if } a < x \le 1 \end{cases} \tag{10.9}$$

in the interval $[0, 1]$, and outside $V_{\rm eff}(x) = V_{\rm eff}(y) + (x-y)V_{\rm eff}(1)$, with $y \equiv x \mod 1$, $y \in [0, 1]$. eq. (10.9) and fig. 10.1 show that the effect of increasing the noise level p is to diminish in the effective potential the average tilt that induces a positive flux, while the effect of increasing the load $F_{\rm ext}$ is to tilt the effective potential opposing the positive flux.

Solving the stationary Fokker-Planck equation for this effective potential the stationary mean velocity for one particle is obtained (in units $L = 1$ and $k_B T = 1$):

$$\langle \dot{x} \rangle = \frac{DK^2 M^2 A}{AE - B^+ B^-}, \tag{10.10}$$

with

$$\begin{aligned} A &:= 1 - e^{K-M}, \\ B^{\pm} &:= [aM + (1-a)K]e^{\pm K} \\ &\quad - (1-a)Ke^{\pm(K-M)} - aM, \\ E &:= a^2M^2(1 - K - e^{-K}) \\ &\quad + a(1-a)KM(1-e^{M})(1-e^{-K}) \\ &\quad + (1-a)^2K^2(1 + M - e^{M}). \end{aligned}$$

For $p < 1/2$, there is a positive current for forces smaller than the "stopping force" F_{stop} (the one that leads to the cancellation of the velocity), so a work is done against the load for $F_{\text{ext}} \in (0, F_{\text{stop}})$. For $p = 1/2$, the stopping force is zero, because no positive flux is obtained even in the absence of the external load. Our noisy control acts instantaneously, *i.e.* in a time scale much faster than the characteristic times of the system $[(aL)^2/(2D)$ for the diffusion time and $\gamma(1-a)^2L^2/V_0$ for the characteristic time of the drift induced by the potential]. Thus, for $p = 1/2$ the potential $V(x)$ is randomly switched on and off very fast and the particle just feels the average potential. This implies that the effective potential in absence of the load, namely $V(x)/2$ (see fig. 10.1), is not tilted, giving a zero flux for the $p = 1/2$ case for zero load. Therefore, in order to get work the noise level of the channel should be $p \in [0, 1/2)$ and the value of F_{stop} is obtained equating eq. (10.10) to zero,

$$F_{\text{stop}} = \frac{V_0}{L}(1 - 2p). \tag{10.11}$$

Substituting eq. (10.10) in eq. (10.8) we get the analytical expression for the power output in the one-particle ratchet. The dependence with the load is plotted in fig. 10.2 for noise levels $p = 0$, $p = 1/4$, and $p = 1/2$. The positive regions correspond to the system doing work against the external force. The load F^*_{ext} that maximizes the power output lies between 0 and F_{stop} and it is given by the condition

$$\frac{\partial P}{\partial F_{\text{ext}}}(F^*_{\text{ext}}) = 0. \tag{10.12}$$

In general, it is a function of the noise level of the binary symmetric channel and it also depends on the physical parameters of the potential, V_0 and a. The condition (10.12) gives a transcendental equation for F^*_{ext} that can be numerically solved in order to obtain the maximum power output,

$$P_{\max} = P(F^*_{\text{ext}}). \tag{10.13}$$

This equation gives the dependence of the maximum power with the noise level p, which is related with the information I through eq. (10.5). This

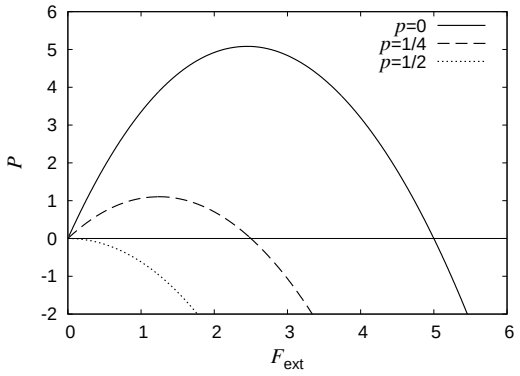

Figure 10.2: Power output versus the load for $V_0 = 5$ and $a = 1/3$ in the one particle case [eqs. (10.8) and (10.10)]. Units: $L = 1$, $D = 1$, $k_B T = 1$.

last equation requires to compute b, which can be obtained integrating over the space interval $[0, aL]$ the stationary distribution of the Fokker-Planck equation for the effective potential (10.9),

$$b = \langle \dot{x} \rangle \left(\frac{a}{K}\right)^2 \left\{ \left(1 - e^{-K}\right) \left[1 + \frac{1 - e^{-K} + (1-a)(1-e^{-M})K/(aM)}{e^{-K} - e^{-M}} \right] - K \right\} \tag{10.14}$$

(units $L = 1$, $D = 1$, $k_B T = 1$). Therefore, the combination of eqs. (10.5), and (10.12-10.14) permits to obtain the (implicit) exact dependence of the maximum power developed by the Brownian motor as a function of the information gathered by the controller (see fig. 10.3).

We analyze now the regime of small potentials in the one particle case. For small potentials ($V_0 \lesssim k_B T$) the value of the external force that maximizes the power is also small [remember eq. (10.11) and the fact that $F^*_{\rm ext} < F_{\rm stop}$]. In this regime, the velocity (10.10) reduces to $\langle \dot{x} \rangle \simeq D(M - K)$, or, recovering units,

$$\langle \dot{x} \rangle \simeq (1 - 2p)\frac{V_0}{\gamma L} - \frac{F_{\rm ext}}{\gamma}. \tag{10.15}$$

We see that there are two contributions to the velocity: the current effect due to the white thermal noise and the control through the binary channel, $(1 - 2p)V_0/(\gamma L)$, and the net drift due to the load, $-F_{\rm ext}/\gamma$. We highlight that for small potentials (and loads) these two effects appear uncoupled, and the result is independent of the asymmetry of the potential. This independency of the asymmetry for small potentials can be understood realizing that in this case the effective potential is well approximated by a flat potential with the same average slope, *i.e.*, $V_{\rm eff}(x) \simeq [-V_0(1 - 2p)/L + F_{\rm ext}]x$.

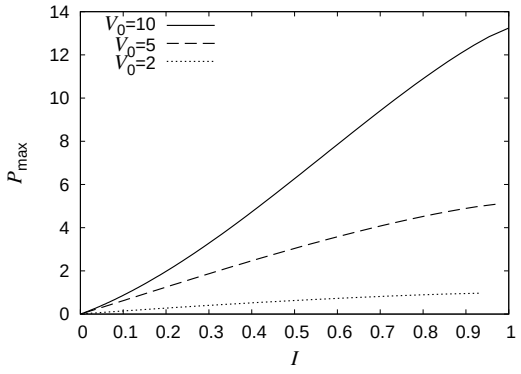

Figure 10.3: Maximum power output in the one particle case as a function of the information used. The curves are for heights of the potential $V_0 = 2, 5, 10$ and asymmetry parameter $a = 1/3$. Units: $L = 1$, $D = 1$, $k_B T = 1$.

Applying eq. (10.12) to the power output computed using eq. (10.15) we obtain

$$F^*_{\rm ext} = \frac{V_0}{2L}(1-2p) = \frac{F_{\rm stop}}{2}, \tag{10.16}$$

and then the power output is

$$P_{\rm max} = \frac{F^{*2}_{\rm ext}}{\gamma} = \frac{V_0^2}{4\gamma L^2}(1-2p)^2. \tag{10.17}$$

On the other hand, for small potential heights $b \simeq a$, and using eq. (10.7) we get

$$P_{\rm max} \simeq R_1 I, \tag{10.18}$$

with R_1 a constant that depends on the physical parameters of the system,

$$R_1 = \frac{V_0^2 \ln 2}{8\gamma L^2 a(1-a)}. \tag{10.19}$$

Notice that the dependence on the asymmetry a does appear here because it determines the relation between p and I [eq. (10.7)], as $b \simeq a$ for small potentials.

Therefore, eq. (10.17) indicates that for small potential heights and small values of the information (*i.e.*, $p \sim 1/2$) the maximum power is approximately directly proportional to the information gathered. In addition, we have numerically checked that eq. (10.18) gives an upper bound of the maximum power for any potential height V_0 and for any value of the information I.

A better approximation for the dependence of the maximum power output with the information can be found using the result of inverting eq. (10.6) up to fourth order,

$$P_{\rm max} \simeq S_1(-1+\sqrt{1+S_2 I}), \tag{10.20}$$

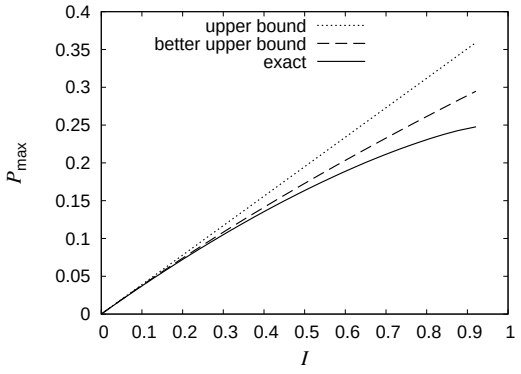

Figure 10.4: Maximum power output in the one particle case as a function of the information for $V_0 = 1$ and $a = 1/3$, and comparison with the upper bound (10.18) and the better upper bound (10.20). Units: $L = 1$, $D = 1$, $k_B T = 1$.

with

$$S_1 = \frac{3V_0^2}{4\gamma L^2}\frac{1-(1-2a)^2}{1-(1-2a)^4};\; S_2 = \frac{4}{3}\frac{1-(1-2a)^4}{[1-(1-2a)^2]^2}\ln 2, \tag{10.21}$$

which is also an upper bound of $P_{\max}$ for any potential and information values. In fig. 10.4 these upper bounds [eqs. (10.18) and (10.20)] are compared with the exact result for $V_0 = k_B T$.

10.4 Few particles

Let us now study a collective ratchet composed of a few particles and show that the results are similar to those in the one particle case. Summing and averaging the Langevin equations (10.2), the average velocity of the center-of-mass in the stationary state can be written as

$$\gamma\langle \dot{x}_{\rm cm}\rangle = \langle \alpha_{\rm eff}(f) f\rangle - F_{\rm ext}. \tag{10.22}$$

An approximate solution can be found assuming, as in [9, 11], that: (i) the position of the particles are statistically independent, and (ii) the probability of finding a particle in a negative force interval (for example $[0, aL]$) is a. These assumptions are verified for small potentials and small loads even in the presence of noise, and they imply that the probability distribution for f is approximately Gaussian,

$$\rho(f) \simeq \frac{1}{\sqrt{2\pi\Sigma^2}}\, e^{-f^2/(2\Sigma^2)}, \tag{10.23}$$

with Σ the amplitude of the fluctuations of the net force, given by $\Sigma = \frac{V_0}{L\sqrt{a(1-a)N}}$ (see ref. [9]). Following [11], we get for the center-of-mass velocity

$$\langle \dot{x}_{\rm cm} \rangle \simeq \frac{\Sigma}{\gamma\sqrt{2\pi}}(1-2p) - \frac{F_{\rm ext}}{\gamma}. \tag{10.24}$$

This result is the sum of the center-of-mass velocity without the external load [11] plus the drift $-F_{\rm ext}/\gamma$ due to the external load. We see that, like in the one particle case, these two effects are decoupled for small potential heights. The expression (10.24) agrees with the results of numerical simulations of the stochastic evolution equations (10.2).

Applying eqs. (10.8) and (10.12), it can be shown that the maximum power is reached for

$$F^*_{\rm ext} = \frac{V_0}{L\sqrt{8\pi a(1-a)N}}(1-2p) \tag{10.25}$$

and takes the value

$$P_{\rm max} = \frac{V_0^2}{\gamma L^2 8\pi a(1-a)N}(1-2p)^2, \tag{10.26}$$

or simply $P_{\rm max} = F^{*2}_{\rm ext}/\gamma$. Therefore, we also have in the regime of few particles (and small potentials) that the maximum power is at first approximation directly proportional to the information,

$$P_{\rm max} \simeq R_N I. \tag{10.27}$$

In the previous expression, the constant R_N depends only on the physical parameters of the system, in particular the number of particles N,

$$R_N = \frac{V_0^2 \ln 2}{\gamma L^2 16\pi a(1-a)b(1-b)N}, \tag{10.28}$$

where b can be calculated for small potentials and loads,

$$b = \sum_{n>aN}^{N} \binom{N}{n} a^n (1-a)^{N-n}, \tag{10.29}$$

using the same assumptions that lead to the Gaussian approximation for $\rho(f)$. We have checked numerically that eq. (10.27) is an upper bound for the maximum power output in the few particles case. Again, as in the one-particle ratchet, a linear upper bound has been found for the maximum power output that the system can get using a certain amount of information I.

10.5 Correlation

The previous expression of the different physical magnitudes of the system in terms of the noise level p can be recast in terms of a correlation C that we introduce in this section. The main underlying idea is that the presence of noise in the control induces a decorrelation between the relevant magnitudes of the control policy. In the instant maximization of the center-of-mass protocol [9] the switching of the potential only depends on the sign of the net force, namely $\mathrm{sgn}f$, and the presence of noise in the control implies that the controller does not use the actual value $\mathrm{sgn}f$ but a value $\mathrm{sgn}\tilde{f}$. The correlation between these quantities,

$$C = \langle \mathrm{sgn}f \ \mathrm{sgn}\tilde{f} \rangle, \tag{10.30}$$

can be written as

$$C = P_{++} + P_{--} - P_{+-} - P_{-+}, \tag{10.31}$$

where P_{+-} is the join probability of having $\mathrm{sgn}f = +1$ while the controller receives $\mathrm{sgn}\tilde{f} = -1$, and analogously for the other joint probabilities. As in our system $\mathrm{sgn}\tilde{f}$ is different from $\mathrm{sgn}f$ with probability p (the noise level) these joint probabilities can be easily computed by noting that $P_{-+} = bp$, $P_{--} = b(1-p)$, $P_{+-} = (1-b)p$ and $P_{++} = (1-b)(1-p)$, with b the probability of $\mathrm{sgn}f$ being -1. Therefore, the correlation can be parameterized in terms of the noise level p as

$$C = 1 - 2p. \tag{10.32}$$

In other words, the effect of the noise is to decrease the correlation C, which has its maximum value ($C = 1$) for zero noise and its minimum ($C = 0$) for a completely noisy policy, $p = 1/2$.

Finally, using eq. (10.32), the relations derived in previous sections can be restated in terms of the correlation. For example, eqs. (10.17) and (10.26) reads

$$P_{\max} = \frac{V_0^2 C^2}{4\gamma L^2}, \tag{10.33}$$

(one particle case), and

$$P_{\max} = \frac{V_0^2 C^2}{\gamma L^2 8\pi a(1-a)N}, \tag{10.34}$$

(few particles case).

This reformulation helps to understand the physical meaning of the relations derived in the previous sections giving a complementary view. In addition, it indicates that the noisy control considered can give an effective description of other feedback ratchets with an imperfect operation of the feedback control. For instance, this effective description has been shown to

be valid in time-delayed feedback ratchets consisting of few particles [14], where $f = f(t)$, $\tilde{f} = f(t-\tau)$ (with τ being the time-delay), and the correlation can be computed just from the time series of the net force $f(t)$.

10.6 Comparison with open-loop protocols

The instantaneous maximization of the center-of-mass velocity is the optimal protocol to maximize the power output in the one particle case for a noiseless channel ($p = 0$). Thus, we also expect this protocol to give a power output close to the maximum possible value in the few particles case and in the presence of noise with a memoryless protocol (note that protocols with memory can perform error corrections). Therefore, we expect eq. (10.18) and eq. (10.27) to be upper bounds of the maximum power output that can be obtained with a memoryless closed-loop protocol that uses an amount of information I about the system.

In addition, the maximum power output obtained with open-loop protocols is much smaller than that obtained with efficient closed-loop protocols. For instance, for the saw-tooth potential with parameters $V_0 = 5k_BT$ and $a = 1/3$, the periodic protocol with optimum periods $\mathcal{T}_{\rm on} \simeq 0.06L^2/D$ and $\mathcal{T}_{\rm off} \simeq 0.04L^2/D$ gives a small maximum power $P_{\rm max}^{\rm open} \simeq 0.04V_0^2/(\gamma L^2)$, which is reached for a load $F_{\rm ext}^* \simeq 0.25V_0/L$. In contrast, the closed-loop one-particle ratchet yields a maximum power $P_{\rm max}^{\rm closed} \simeq 5.1V_0^2/(\gamma L^2)$ for $F_{\rm ext}^* \simeq 2.4V_0/L$ when it works without noise in the channel. Therefore, the linear eqs. (10.18) and (10.27) are also good estimates of the maximum improvement that can be attained changing from the optimal open-loop control to a closed-loop protocol, *i.e.,*

$$P_{\rm max}^{\rm closed} - P_{\rm max}^{\rm open} \leq RI, \tag{10.35}$$

where R is a constant depending on the system's characteristics; see eqs. (10.19) and (10.28).

10.7 Concluding remarks

In this article we have analyzed the relation between the information about the state of the system used by the controller and the power output in a feedback controlled ratchet. We have obtained exact analytic results for one-particle ratchets, and also approximate simple expressions for the maximum power output in both one-particle and few-particle ratchets. Moreover, we have found that the increase of the maximum power output when we change from the optimal open-loop protocol to a closed-loop protocol has an upper bound proportional to the information used by the controller. Also an upper bound proportional to the information was found in [15] for the entropy reduction in a general closed-loop controlled system. The result obtained in

the present paper for the maximum power output is the analog upper bound of the one found in [11] for the flux, but with the important difference that the upper bound for the flux was proportional to the square root of the information.

Acknowledgments

This work has been financially supported by grants BFM2003-02547/FISI, FIS2005-24376-E and FIS2006-05895 from MEC (Spain), and by the ESF Programme STOCHDYN. M.F. acknowledges support from UCM (Spain) through grant "Beca Complutense".

Bibliography

[1] P. Reimann, Phys. Rep. **361**, 57 (2002)

[2] H. Linke, Appl. Phys. A **75**, 167 (2002); P. Hänggi, F. Marchesoni and F. Nori, Ann. Phys. **14**, 51 (2005)

[3] M. Bier, Biosystems **88**, 301 (2007)

[4] V. Serreli, C.-F. Lee, E. R. Ray and D. Leigh, Nature (London) **445**, 523 (2007); E. A. Kay, D. A. Leigh and F. Zerbetto, Angew. Chem. Int. Ed. 46, 72 (2007)

[5] J. M. R. Parrondo and B. J. Cisneros, Appl. Phys. A **75**, 179 (2002); H. Linke, M. T. Downton and M. J. Zuckermann, Chaos **15**, 026111 (2005)

[6] R. D. Astumian and M. Bier, Phys. Rev. Lett. **72**, 1766 (1994)

[7] M. O. Magnasco, Phys. Rev. Lett. **71**, 1477 (1993); H. Kamegawa, T. Hondou and F. Takagi, Phys. Rev. Lett. **80**, 5251 (1998); L. Machura, M. Kostur, P. Talkner, J. Łuczka, F. Marchesoni and P. Hänggi, Phys. Rev. E **70**, 061105 (2004)

[8] A. Ajdari and J. Prost, C. R. Acad. Sci. Paris II **315**, 1635 (1993); D. Suzuki and T. Munakata, Phys. Rev. E **68**, 021906 (2003)

[9] F. J. Cao, L. Dinis and J. M. R. Parrondo, Phys. Rev. Lett. **93**, 040603 (2004)

[10] L. Dinis, J. M. R. Parrondo and F. J. Cao, Europhys. Lett. **71**, 536 (2005); M. Feito and F. J. Cao, Phys. Rev. E **74**, 041109 (2006)

[11] F. J. Cao, M. Feito and H. Touchette, *Information and flux in a feedback controlled Brownian ratchet*, arXiv:cond-mat/0703492 preprint (2007)

[12] K. Sekimoto, J. Phys. Soc. Jpn. **66**, 1234 (1997); J. M. R Parrondo, J. M. Blanco, F. J. Cao and R. Brito, Europhys. Lett. **43**, 248 (1998); A. Parmeggiani, F. Jülicher, A. Ajdari and J. Prost, Phys. Rev. E **60**, 2127 (1999)

[13] T. M. Cover and J. A. Thomas, *Elements of Information Theory* (John Wiley, New York, 1991)

[14] M. Feito and F. J. Cao, *Time-Delayed Feedback control of a flashing ratchet*, arXiv:0706.1496 preprint (2007)

[15] H. Touchette and S. Lloyd, Phys. Rev. Lett. **84**, 1156 (2000); H. Touchette and S. Lloyd, Physica A **331**, 140 (2004)

Chapter 11

Thermodynamics of feedback controlled systems

PHYSICAL REVIEW E **79**, 041118 (2009)
Thermodynamics of feedback controlled systems

F. J. Cao[1,2] and M. Feito[1]

[1] *Departamento de Física Atómica, Molecular y Nuclear, Universidad Complutense de Madrid, Avenida Complutense s/n, 28040 Madrid, Spain.*
[2] *LERMA, Observatoire de Paris, Laboratoire Associé au CNRS UMR 8112, 61, Avenue de l'Observatoire, 75014 Paris, France.*

We compute the entropy reduction in feedback controlled systems due to the repeated operation of the controller. This was the lacking ingredient to establish the thermodynamics of these systems, and in particular of Maxwell's demons. We illustrate some of the consequences of our general results by deriving the maximum work that can be extracted from isothermal feedback controlled systems. As a case example, we finally study a simple system that performs an isothermal information-fueled particle pumping.

PACS numbers: 89.70.Cf, 05.20.-y

11.1 Introduction

Controllers are ubiquitous in science and technology with a number of purposes such as stabilizing unstable dynamics or increasing the performance [1]. Furthermore, many real systems in nature can be modeled as a system plus a controller. A controller is an external agent whose action is to modify the evolution of the system with a purpose. *Feedback or closed-loop* controllers use information about the state of the system. The feedback is the process performed by the controller of measuring the system, deciding on the action given the measurement output, and acting on the system. On the contrary, an open-loop controller operates on the system blindly, i.e., without information of its state. Although it is intuitively clear that the information about the state of the system can be used to improve the performance, there are still open questions on the connections between feedback control theory and information theory (see Ref. [1]). In particular, the understanding of the thermodynamics of feedback control is still incomplete. Much of the progress in the solution of this problem has come from the study of Maxwell's demon [2]. This is a being that gathers information about a system and is able to decrease the entropy of the system without performing work on it. The seminal work of Szilard [3] contains the basic ingredients of the trade off between information theory and thermodynamics, which is precisely stated in Landauer's principle: The erasure of 1 bit of information at temperature T implies an energetic cost of at least $k_B T \ln 2$ [4]. Bennett [5]

pointed out that Landauer's principle is the key to preserving the second law of thermodynamics in feedback systems, as the controller must erase its memory after each cycle to allow the whole system to truly operate cyclically. How to achieve the shorter description for the memory record of the controller in order to minimize the energetic erasure cost was established by Zurek [6] by using an algorithmic complexity approach. On the other hand, Lloyd used in [7] a different point of view —that of the feedback controlled system. From this approach the effect of the interaction of the controller with the system is to reduce the entropy of the system, due to the additional determination of the macrostate of the system through the information obtained from it. More recently, Touchette and Lloyd [8] have computed the maximum additional reduction in entropy attainable in one control action when a feedback control is used instead of an open-loop control.

In this paper we also consider the point of view of the feedback controlled system. The thermodynamics of the interactions of the system with the controller and the environment are well studied for the heat and work exchanges. However, a complete understanding of the entropy reduction in the system due to its interaction with the feedback controller is still lacking. We solve here this problem and show how to compute this entropy reduction after one or several control steps. This result allows us to establish the thermodynamics of feedback controlled systems without assuming Landauer's principle. Several concepts and quantities defined in information theory [9] emerge naturally as one computes this entropy reduction. For the definition of the entropy we will use $k_B = 1$ and natural logarithms. This implies that the information quantities that naturally appear will be in nats ($\ln 2$ nats $= 1$ bit).

In the next section we compute the entropy reduction in a general feedback controlled system due to the repeated operation of the controller. The result allows us to establish the thermodynamics of feedback controlled systems. In Sec. 11.3, we illustrate some of the consequences of our general result by deriving the maximum work that can be extracted from isothermal feedback controlled systems. In Sec. 11.4, we show the applicability and usability of the results in a simple dynamical system, a Markovian particle pump that is able to extract useful work from the entropy reduction due to the information used by an external feedback controller. Finally, we summarize the results of the paper in Sec. 11.5.

11.2 Entropy reduction in feedback controlled systems

Let us call $X_k := X(t_k)$ the macrostate of a general dynamical system at the kth control step of the controller (at time t_k). In a feedback controlled system the control step involves several operations by the controller:

measuring the system, deciding the control action to take given the measurement output, and acting on the system following the selected control action. Therefore, the control action is the modification of the evolution of the system made by the external agent that we shall call the controller. The controller can perform several control actions on the system. By $C_1 = c$ we denote that, at the first control step, the controller has chosen to perform the action labeled by c. (It is *not* a specification of the state of the controller.) As the control actions are decided at their respective control steps, C_k represents only the decision taken at the kth control step.

Initially the entropy of the system is S_0, which is fixed by the probabilities $p_{X_0}(x)$ of each possible microstate x at time $t = 0$. Subsequently, the system evolves with an entropy change from S_0 to S_1^b, which is the entropy just *before* the first control step. It is given by the statistical entropy

$$S_1^b = -\sum_{x\in\mathscr{X}} p_{X_1}(x) \ln p_{X_1}(x) =: H(X_1), \tag{11.1}$$

with $\mathscr{X}$ as the set of possible microstates of the system. At time t_1 the controller measures the state of the system. The result of this measurement determines, at least partially, the action the controller will take. The additional information on the system provided by the measure further determines the system macrostate [7], i.e., it defines a submacrostate that contains only microstates compatible with the measured value. However, from the point of view of the system, each set of measurement outputs that leads to the same control action can be considered as defining a single submacrostate of the system, because the controller in its action on the system ignores the differences inside these sets. Thus, if the measurement implies a control action $C_1 = c$, the entropy of the system decreases to

$$H(X_1|C_1 = c) := -\sum_{x\in\mathscr{X}} p_{X_1|C_1}(x|c) \ln p_{X_1|C_1}(x|c). \tag{11.2}$$

Therefore, the average entropy *after* the first control step can be obtained by averaging over the set $\mathscr{C}$ of all possible control actions,

$$S_1^a = \sum_{c\in\mathscr{C}} p_{C_1}(c) H(X_1|C_1 = c) =: H(X_1|C_1). \tag{11.3}$$

Hence the average variation in the entropy at the first step is

$$\Delta S_1 = S_1^a - S_1^b = H(X_1|C_1) - H(X_1) =: -I(X_1; C_1), \tag{11.4}$$

i.e., it is the (minus) mutual information [9] between X_1 and C_1.

Let us describe one more step. Each of the previous $|\mathscr{C}|$ submacrostates of the system with entropy $H(X_1|C_1 = c)$ evolves to give an entropy $H(X_2|C_1 = c)$ just before the second control step. Following the second control step, each

one of these submacrostates of the system give $|\mathscr{C}|$ more submacrostates. The entropy of the system given that $C_1 = c$ and $C_2 = c'$ is $H(X_2|C_2 = c', C_1 = c)$. Therefore, the average entropy of the system after the second step is

$$\begin{aligned} S_2^a &= \sum_{c,c' \in \mathscr{C}} p_{C_2 C_1}(c', c) H(X_2|C_2 = c', C_1 = c) \\ &= H(X_2|C_2, C_1), \end{aligned} \tag{11.5}$$

and the average variation in the entropy at this second control step is $\Delta S_2 = S_2^a - S_2^b = H(X_2|C_2, C_1) - H(X_2|C_1) = -I(X_2; C_2|C_1)$. This conditioning of the mutual information shows that the entropy of the system is only reduced by the new information.

Analogously we get for the average entropy reduction in the kth step $\Delta S_k = -I(X_k; C_k|\mathbf{C}^{k-1})$, where $\mathbf{C}^{k-1}$ stands for $C_{k-1}, C_{k-2}, \ldots, C_1$. Using the properties of mutual information [9], this average entropy reduction can be written as

$$\begin{aligned} \Delta S_k &= -I(X_k; C_k|\mathbf{C}^{k-1}) = -I(C_k; X_k|\mathbf{C}^{k-1}) \\ &= -H(C_k|\mathbf{C}^{k-1}) + H(C_k|\mathbf{C}^{k-1}, X_k). \end{aligned} \tag{11.6}$$

Finally, we find that the *total average entropy reduction due to the information used* in M control steps is $\Delta S_{\text{info}} = \sum_{k=1}^{M} \Delta S_k$, i.e.,

$$\Delta S_{\text{info}} = -\sum_{k=1}^{M} I(C_k; X_k|\mathbf{C}^{k-1}). \tag{11.7}$$

This general result indicates that this entropy reduction can be computed in terms of the joint probabilities for the state of the system and the control actions history. Using Eq. (11.6) and the chain rule for H (see Ref. [9]), we rewrite the last equation as

$$\Delta S_{\text{info}} = -H(\mathbf{C}^M) + \sum_{k=1}^{M} H(C_k|\mathbf{C}^{k-1}, X_k). \tag{11.8}$$

Equation (11.7), or equivalently Eq. (11.8), is a central result of this paper. As a consistency check, note that for open-loop controlled systems the controller acts independently of the state of the system and it gets no information of it. Thus, $H(C_k|\mathbf{C}^{k-1}, X_k) = H(C_k|\mathbf{C}^{k-1})$, which gives $\Delta S_{\text{info}} = 0$ after applying the chain rule in Eq. (11.8), as expected. Note also that the mutual information in Eq. (11.7) between the system and the control actions is conditioned by the past control actions. This reflects that the correlations between measurements limit the attainable entropy reduction. Therefore, the entropy reduction in M consecutive measurements is equal or lower than in M independent measurements.

11.2.1 Deterministic feedback controllers

A relevant class of closed-loop controllers is *deterministic feedback controllers*. For them the control action is determined without uncertainty by the state of the system and the control actions history. Therefore

$$H(C_k|\mathbf{C}^{k-1}, X_k) = 0, \tag{11.9}$$

and the entropy reduction in Eq. (11.8) simplifies to $\Delta S_{\text{info}} = -H(\mathbf{C}^M)$, which can be computed by just using the joint probability $p_{C_1,\ldots,C_M}(c_1,\ldots,c_M)$. Consequently, the average entropy reduction after a large number of control actions is given by the entropy rate $\bar{H}(\mathscr{C})$ of the stochastic process describing the control actions:

$$\lim_{M\to\infty} \frac{\Delta S_{\text{info}}}{M} = \lim_{M\to\infty} \frac{-H(\mathbf{C}^M)}{M} =: -\bar{H}(\mathscr{C}). \tag{11.10}$$

For a system and control dynamics without explicit dependencies in time, this average entropy reduction coincides with the asymptotic entropy reduction in one step [9], that is, $\lim_{M\to\infty} \Delta S_{\text{info}}/M = \lim_{M\to\infty} \Delta S_M$.

11.2.2 Non-deterministic feedback controllers

Feedback controllers satisfying Eq. (11.9) are error free. On the other hand, controllers affected by some *source of error* are common in real systems. In this case the decorrelation between the control actions and the state of the system reduces the attainable entropy reduction; see Eq. (11.8). For instance, consider a feedback controller with two possible actions, say "on" and "off", for which the system state and the previous control actions history determine which one of the actions is taken with probability $1-\epsilon$. For this system, $H(C_k|\mathbf{C}^{k-1}, X_k) = H_b(\epsilon)$, with $H_b(\epsilon)$ as the binary entropy function $H_b(\epsilon) := -\epsilon\ln\epsilon - (1-\epsilon)\ln(1-\epsilon)$, and Eq. (11.8) gives

$$\lim_{M\to\infty} \frac{\Delta S_{\text{info}}}{M} = -\bar{H}(\mathscr{C}) + H_b(\epsilon). \tag{11.11}$$

This shows that errors in the control operation limit the attainable entropy reduction.

11.2.3 Discussion

The new relation (11.7) sets the entropy reduction in the controlled system due to the information used by the external agent that operates on it. The reformulation of this relation as Eq. (11.8) allows us to understand the average entropy reduction per control step as two competing contributions: a negative term accounting for the entropy rate of the control actions, and a positive term accounting for the decorrelation between the controller actions

and the state of the system. This decorrelation can arise, for instance, from errors in the operation of the controller [see Eq. (11.11)]. These new relations, Eqs. (11.7) and (11.8), also show how the past control action history must be taken into account to avoid redundancy in the computation of the entropy reduction. They are consistent with the Zurek's computational interpretation of the controller as a memory record whose blocks occupied by past measurements must be compressed before the erasure process [6,10]. On the other hand, when only one control step is considered, Eq. (11.7) reduces to Eq. (11.4), which gives the well-known Landauer's energetic cost due to information [2], $k_B T I(X_1; C_1)$ (recovering units), also found for quantum systems [11].

The statement of the entropy reduction in terms of the control actions is an important point of this paper. It allows one to give a reachable bound for the efficiency. (If the controller performs the same action for two different measured values, the bound found for the efficiency considering the entropy reduction in terms of the measure could be nonreachable.) Note also that the overall reduction in the entropy of the system due to feedback control is expressed in terms of physical quantities and it can be computed without knowledge of internal details of the controller. In addition, this approach also allows one to compute the maximum entropy reduction attainable with a nondeterministic feedback control, Eq. (11.11), giving a reachable bound.

The entropy reduction in the system due to the information used by the controller is a fundamental ingredient in the thermodynamics of feedback controlled systems. It is the key to improving the performance in these systems compared with their open-loop counterparts. Once this entropy reduction is understood and we know how to compute it [Eqs. (11.7) or (11.8)], the thermodynamics of feedback controlled systems is complete. In particular, we show in the next section how to compute thermodynamic relations for an *isothermal feedback controlled system*.

11.3 Application: Isothermal feedback controlled systems

We study in this section the implications of the previous results for the case of an isothermal feedback controlled system.

A general isothermal feedback controlled system is a system that is coupled to a feedback controller, to a thermal bath of temperature T, and to another external system on which it does work. When the system is operated cyclically, the initial state is recovered after a cycle, and the variations in internal energy and entropy of the system in the cycle are zero. During such a cycle the system releases a quantity of heat Q to the thermal bath and does work W on the external system. The transfer of the internal energy of the controller ΔU_{cont} to the system is given by the first law of

thermodynamics,

$$\Delta U_{\rm cont} + Q + W = 0. \tag{11.12}$$

On the other hand, the second law of thermodynamics gives

$$T\Delta S_{\rm cont} + Q \geq 0, \tag{11.13}$$

with $\Delta S_{\rm cont}$ as the entropy increase in the controller. Combining both relations we get the inequality

$$W \leq -\Delta U_{\rm cont} + T\Delta S_{\rm cont} = -\Delta F_{\rm cont}, \tag{11.14}$$

where $\Delta F_{\rm cont}$ is the variation in the Helmholtz free energy of the controller in the cycle. From this relation it is natural to define the efficiency of a feedback controlled system as

$$\eta = \frac{W}{-\Delta F_{\rm cont}}. \tag{11.15}$$

In addition, if the controller only interacts with the system and without heat transfer, we have $\Delta S_{\rm cont} \geq -\Delta S_{\rm info}$, i.e., the increase in entropy of the controller should be greater than or equal to the reduction in the entropy of the system due to the actions of the controller. This implies that the maximum efficiency that can be attained with an isothermal feedback controlled system is

$$\eta = \frac{W}{-\Delta U_{\rm cont} - T\Delta S_{\rm info}}, \tag{11.16}$$

where W is the work extracted from the system, $-\Delta U_{\rm cont}$ is the work done by the controller on the system, and $\Delta S_{\rm info}$ is the entropy reduction in the system due to the information-dependent operation of the controller, which can be computed with Eq. (11.7).

11.4 Example: Markovian particle pump

We shall illustrate how to apply our results in a simple dynamical system, a *Markovian particle pump*, which is able to extract useful work from the entropy reduction due to the information about the system used by an external feedback controller. Consider a particle in a one-dimensional lattice that is in contact with a thermal bath at temperature T. An external controller can activate reflecting barriers separated by a distance L with n lattice sites between two consecutive barriers; see Fig. 11.1. For the discussion of this example we will consider units of $k_B T = 1$ and $L = 1$. In the absence of external forces, the particle jumps to the left or to the right site with the same probability, $1/2$, at each time step. Now let us have a force f pointing in the negative direction. The probability of jumping to the right decreases and becomes $\alpha := 1/(1 + e^{f/n})$, as follows from detailed balance. We aim

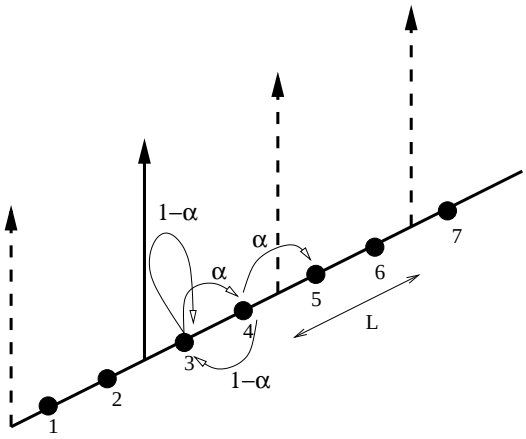

Figure 11.1: Illustration of the Markovian particle pump with $n = 2$ lattice sites between barriers. This is a simple feedback controlled system that extracts useful work from the entropy reduction due to the information about the system used by the external feedback controller.

to move the particle to the right (against the force). For this purpose the controller measures the particle location and consecutively raises from left to right the reflecting barriers to trap the particle further and further to the right. The next barrier to the right is raised when the measurement indicates that the particle has crossed to the righthand side. This implies that when the particle moves to the left until the raised barrier location it finds a reflecting boundary condition, while the particle has no bounds to its displacements to the right.

This defines a deterministic feedback control that pumps the particle by using information about the location of the jumping particle. We stress that a blind open-loop control strategy for the lifting of the barriers cannot achieve direct flux against the load. In addition, our closed-loop controller does not introduce any extra energy in the system. Thus, the entropy reduction in the system thanks to the information-gathering operation is the only responsible for the pumping. In particular, we highlight that a naive definition of efficiency as $\eta = W/(-\Delta U_{\rm cont})$ is meaningless for engines that work due to an information-dependent operation. Our general results allow us to compute the maximum possible efficiency of this pump as a case example, not only in the quasistatic regime (large time intervals between two operations of the controller) but also when it is operated non-quasistatically (for instance every time step).

Let us first compute the maximum efficiency attainable when the controller operates every time step. We consider the particle initially at the origin with the reflecting barrier to the left raised. At time t_k the controller takes the value $C_k = 1$ when the next right barrier is raised or $C_k = 0$ if

the barrier remains off. As the feedback control in this example satisfies the deterministic condition (11.9), the average entropy reduction per step is given by Eq. (11.10). Furthermore, in order to simplify the computation of the entropy rate, it is useful to change to a description in terms of a new stochastic process $\tilde{C}$, with $\tilde{C}_s$ defined as the number of steps between the raise of the barrier $s-1$ and that of the barrier s (first passage time). For example the event $(C_1,\ldots,C_7)=(0,0,0,1,0,0,1)$ corresponds to the event $(\tilde{C}_1,\tilde{C}_2)=(4,3)$. It is clear that we can establish a one-to-one correspondence between C and $\tilde{C}$, as both represent univocally the control actions history. Calling $\langle\tau\rangle$ as the average first passage time through the next barrier position, we have that Eq. (11.10) reads

$$\lim_{t\to\infty}\frac{T\Delta S_{\rm info}}{t}=\lim_{t\to\infty}\frac{-H(\mathbf{C}^t)}{t}=\lim_{s\to\infty}\frac{-H(\tilde{\mathbf{C}}^s)}{s\langle\tau\rangle}. \tag{11.17}$$

[That is, $\bar{H}(\mathscr{C})=\bar{H}(\tilde{\mathscr{C}})/\langle\tau\rangle$.] As the new tilde variables are independent and identically distributed we have $H(\tilde{\mathbf{C}}^s)=sH(\tilde{C}_1)$. Thus,

$$\lim_{t\to\infty}\frac{T\Delta S_{\rm info}}{t}=\frac{-H(\tilde{C}_1)}{\langle\tau\rangle}=\frac{\sum_{k=1}^{\infty}p_\tau(k)\ln p_\tau(k)}{\sum_{k=1}^{\infty}kp_\tau(k)}, \tag{11.18}$$

where $p_\tau(k)$ is the probability mass function of the first passage time being $\tau=k$. This asymptotic value, Eq. (11.18), is reached in a characteristic time $\langle\tau\rangle$. The probability $p_\tau(k)$ can be obtained from the transition probabilities between the states of the jumping particle.

On the other hand, the average potential increase is $W=f/\langle\tau\rangle$. Therefore, the maximum efficiency attainable at this nonquasistatic regime is obtained from Eq. (11.16) that reads

$$\eta_{\rm nq}=\frac{f}{H(\tilde{C}_1)}. \tag{11.19}$$

11.4.1 One lattice site between consecutive barriers

For instance, for the case with a single lattice site between two barriers $p_\tau(k)=\alpha(1-\alpha)^{k-1}$, implying $H(\tilde{C}_1)=H_b(\alpha)/\alpha$ and $\langle\tau\rangle=1/\alpha$. Thus, the average entropy reduction per step is $H_b(\alpha)$, and the average potential increase is $W=f/\langle\tau\rangle=\alpha f$. Finally, the maximum efficiency attainable at this nonquasistatic regime is $\eta_{\rm nq}=\alpha f/H_b(\alpha)$. This result for the model with a single site between two consecutive barriers can also be obtained without using Eq. (11.18). For this simple case operation steps at different times are independent and $T\Delta S_k=-H(C_k)$ with $p_{C_k}(1)=\alpha$. This gives an entropy reduction per step $H_b(\alpha)$. On the other hand, the average potential energy gain per step is αf because the particle gains an energy f with probability α. In view of these considerations we recover $\eta_{\rm nq}=\alpha f/H_b(\alpha)$.

11.4.2 Several lattice sites between consecutive barriers

As α is the probability of jumping to the right, the probability of the first passage time being $\tau = k$ is obtained from the probability $p_{X_{k-1}}(n)$ of finding the particle at site n (just to the left to the first barrier) at instant time $k-1$ as $p_\tau(k) = \alpha p_{X_{k-1}}(n)$. To evaluate this probability we only need to know the transition probabilities of jumping between the different spatial positions (see Fig. 11.1). We shall call Π as the matrix such that its (i,j)th entry is the probability $p_{j\to i}$ of jumping from the j site to the i site. Then, for the particle pump with n sites between barriers, Π is the $n\times n$ tridiagonal matrix

$$\Pi = \begin{pmatrix} 1-\alpha & 1-\alpha & & & & \\ \alpha & 0 & \ddots & & & \\ & \alpha & \ddots & 1-\alpha & & \\ & & \ddots & 0 & 1-\alpha \\ & & & \alpha & 0 \end{pmatrix}. \tag{11.20}$$

Assuming that the particle is initially situated at the origin, the probability $p_{X_{k-1}}(n)$ is given by the $(n,1)$th element of the $(k-1)$th power of Π. Hence,

$$p_\tau(k) = \alpha \Pi^{k-1}(n,1). \tag{11.21}$$

For instance, for $n=1$ we recover $p_\tau(k) = \alpha(1-\alpha)^{k-1}$, with $\alpha = 1/(1+e^f)$. For $n=2$ we get, after some straightforward calculus, $p_\tau(k) = a(b_+^{k-1} - b_-^{k-1})$, where $a := \alpha^2/\sqrt{1+2\alpha-3\alpha^2}$ and $b_\pm := (1-\alpha \pm \sqrt{1+2\alpha-3\alpha^2})/2$, with $\alpha = 1/(1+e^{f/2})$.

Once the probabilities $p_\tau(k)$ are obtained, the entropy reduction and the efficiency can be computed with Eqs. (11.18) and (11.19) respectively. We plot in Fig. 11.2 this entropy reduction $\lim_{t\to\infty} T\Delta S_{\rm info}/t$ for the particle pump with $n=5$ lattice sites between barriers, together with the time dependence of the average entropy reduction per time step obtained by means of computer simulations of the dynamics in the maximum measurement regime. As expected, this time evolution tends to the theoretical asymptotic value in a characteristic time of order $\langle\tau\rangle = \sum_{k=1}^{\infty} k p_\tau(k)$.

The numerical results in Fig. 11.2 have been obtained evolving the particle distribution according to the known transition probabilities. The entropy reduction in each measurement is given by the entropy difference between the particle distributions before and after the measurement. After the measurement we keep one of the two possible particle distributions chosen randomly with the probability of the corresponding measurement output, and we evolve this particle distribution until the next measurement. Following this procedure we have performed several realizations of the control actions history, and thereafter we have performed an average over realizations to obtain the average entropy per time step as a function of time. For these

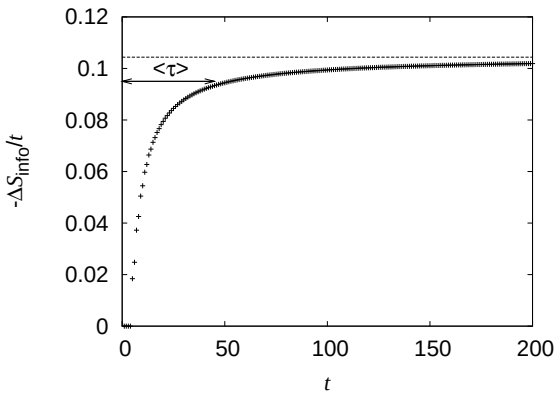

Figure 11.2: Average entropy reduction per time step as a function of time for the particle pump with $n = 5$ lattice sites between barriers: numerical simulations (+ signs) and asymptotic value (dashed line). The asymptotic value is approached in a characteristic time of the order of the mean first passage time $\langle\tau\rangle$. Force $f = 1$. Units $k_BT = 1$ and $L = 1$.

simulations we have considered $n = 5$ lattice sites and force $f = 1$ (in units of $k_BT = 1$ and $L = 1$) or equivalently $\alpha = 1/(1 + e^{1/5}) \approx 0.45$.

11.4.3 Quasistatic regime

To conclude the analysis of the illustrating example, the Markovian particle pump, we shall compute its maximum efficiency in the quasistatic regime. Consider again the particle initially situated at the origin. As the time between measurements is large enough, the system has reached equilibrium when the controller measures at a time $t \gg 1$. Hence $p_{X_t}(m) = (1 - e^{-f/n})e^{-fm/n}$ and the jumping particle is at the righthand side of the next barrier with probability $\sum_{m>n} p_{X_t}(m) = e^{-f}$. On the other hand, when the barrier is raised the system gains a potential energy f. Thus, the entropy reduction due to information is $H_b(e^{-f})$, while the potential energy gained in one step is fe^{-f}. Therefore the maximum efficiency for the quasistatic operation of the Markovian particle pump is $\eta_{\rm q} = fe^{-f}/H_b(e^{-f})$. We note that $0 < \eta_{\rm nq} < \eta_{\rm q} < 1$, as expected.

In order to compare with results in Fig. 11.2 note that for the same parameter values a measurement step in the quasistatic regime reduces the entropy on average an amount $H_b(e^{-1}) \approx 0.66$. However, a measurement step in the quasistatic regime requires many evolution time steps resulting in a very low entropy reduction per time step.

11.5 Conclusions

In this paper we have addressed the thermodynamics of closed-loop controlled systems, focusing on what characterizes them, namely, the use of information. Our results show explicitly how to calculate the entropy reduction due to information, Eq. (11.7) or (11.8). Therefore, they allow one to compute the thermodynamic quantities and their relations for feedback controlled systems. In particular, we have calculated the thermodynamic relations for isothermal feedback controlled systems, Eqs. (11.12)–(11.14), and also the maximum efficiency attainable, Eqs. (11.15) and (11.16). As a case example, we have shown how to apply our general results to a simple system that performs an isothermal information-fueled particle pumping, for both a maximum measurement regime and a quasistatic regime. The results presented in this paper allow one to study the thermodynamics of many other feedback controlled systems. It will be particularly interesting to obtain the thermodynamics of feedback flashing ratchets that have been studied theoretically [12], and recently realized experimentally [13].

Acknowledgments

We are grateful to Martin Bier for a critical reading of the paper. We acknowledge financial support from MCYT (Spain) through the Research Project No. FIS2006-05895, from the ESF Programme STOCHDYN, and from UCM and CM (Spain) through Grant No. CCG07-UCM/ESP-2925.

Bibliography

[1] J. Bechhoefer, Rev. Mod. Phys. **77**, 783 (2005).

[2] H. S. Leff and A. F. Rex (eds.), *Maxwell's Demon 2: Entropy, Classical and Quantum Information, Computing* (Institute of Physics, Bristol, 2003).

[3] L. Szilard, Z. Phys. **53**, 840 (1929).

[4] R. Landauer, IBM J. Res. Dev. **5**(3), 183 (1961).

[5] C. H. Bennett, Int. J. Theor. Phys. **21**, 905 (1982).

[6] W. H. Zurek, Phys. Rev. A **40**, 4731 (1989); Nature **341**, 119 (1989).

[7] S. Lloyd, Phys. Rev. A **39**, 5378 (1989).

[8] H. Touchette and S. Lloyd, Phys. Rev. Lett. **84**, 1156 (2000); Physica A **331**, 140 (2004).

[9] T. M. Cover and J. A. Thomas, *Elements of Information Theory* (John Wiley, New York, 1991).

[10] C. M. Caves, Phys. Rev. Lett. **64**, 2111 (1990); Phys. Rev. E **47**, 4010 (1993). C. M. Caves, W. G. Unruh, W. H. Zurek, Phys. Rev. Lett. **65**, 1387 (1990).

[11] T. Sagawa, M. Ueda, Phys. Rev. Lett. **100**, 080403 (2008); H. T. Quan, Y. D. Wang, Y. X. Liu, C. P. Sun, F. Nori, Phys. Rev. Lett. **97**, 180402 (2006).

[12] F. J. Cao, L. Dinis and J. M. R. Parrondo, Phys. Rev. Lett. **93**, 040603 (2004). E. M. Craig, N. J. Kuwada, B. J. López, H. Linke, Ann. Phys. **17**, 115 (2008). L. Dinis, J. M. R. Parrondo, and F. J. Cao, Europhys. Lett. **71**, 536 (2005). M. Feito and F. J. Cao, Phys. Rev. E **74**, 041109 (2006). M. Bier, BioSystems **88**, 301 (2007). M. Feito and F. J. Cao, Phys. Rev. E **76**, 061113 (2007). E. M. Craig, B. R. Long, J. M. R. Parrondo, and H. Linke, Europhys. Lett. **81**, 10002 (2008). F. J. Cao, M. Feito, and H. Touchette, Physica A **388**, 113 (2009). M. Feito and F. J. Cao, Eur. Phys. J. B **59**, 63 (2007).

[13] B. J. López, N. J. Kuwada, E. M. Craig, B. R. Long, and H. Linke, Phys. Rev. Lett **101**, 220601 (2008).

Parte III

Discusión, conclusiones y cuestiones abiertas

Esta Parte III de la tesis contiene dos capítulos. En el primero de ellos, capítulo 12, presentamos una discusión global que integra los capítulos anteriores e incide sobre los resultados principales que hemos obtenido así como sobre sus implicaciones. En el último capítulo, capítulo 13, presentamos las conclusiones de la tesis y destacamos los objetivos alcanzados y también algunas cuestiones abiertas y posibles trabajos futuros.

Capítulo 12

Discusión

En esta tesis hemos presentado nuestros resultados originales [1–8] sobre ratchets con control retroalimentado y sistemas generales con control retroalimentado. Las ratchets, y específicamente las ratchets de ciclo cerrado, han demostrado ser relevantes por sus implicaciones fundamentales para la física estadística fuera del equilibrio y también por sus aplicaciones en biología y nanotecnología; véanse, por ejemplo, los artículos de revisión [9–11]. Las ratchets retroalimentadas han sido recientemente sugeridas como un mecanismo capaz de explicar el movimiento de pasos de la kinesina de doble cabeza [12] y están también presentes en otros motores moleculares activados químicamente [13–15]. Por lo tanto, nuestros resultados, que implican un entendimiento más profundo de estos sistemas, son importantes tanto desde una perspectiva teórica como por sus posibles aplicaciones en biología y nanotecnología.

Hemos adoptado un enfoque teórico a las ratches brownianas retroalimentadas combinando métodos analíticos y numéricos y la discusión de sus implicaciones [1–6, 8]. También hemos resuelto algunos problemas abiertos sobre sistemas generales con retroalimentación [7, 16, 17]. En concreto, los capítulos 5, 6, 7, 8, 9 y 10 han tratado con ratchets retroalimentadas y corresponden, respectivamente, a nuestros trabajos [1–4, 6, 8]. La Parte II de la tesis se culmina con el capítulo 11, donde se han estudiado sistemas con control retroalimentado de manera general, y corresponde a nuestro artículo [7].

La primera cuestión que uno se plantea sobre las ratches retroalimentadas es si proporcionan alguna ventaja sobre sus correspondientes versiones de ciclo abierto. La respuesta es afirmativa. Gracias al uso de la información sobre el sistema, las ratchets retroalimentadas o de ciclo cerrado pueden diseñarse para dar mayores rendimientos que las ratchets de ciclo abierto. En la presente tesis hemos investigado la dinámica y el rendimiento de diferentes políticas de retroalimentación, e.g. el llamado protocolo de umbrales (capítulo 5). Hemos obtenido resultados analíticos y numéricos para las principales magnitudes de estas ratchets retroalimentadas y hemos discutido diferentes regímenes dependiendo del número de partículas del sistema. En particular, para el protocolo de umbrales hemos mostrado que la ratchet retroalimentada colectiva compuesta por un número cualquiera de partículas puede alcanzar valores para el flujo iguales o mayores que los valores de la ratchet de ciclo abierto óptima.

El estudio de las ratchets retroalimentadas nos ayuda a ganar conocimiento en los fenómenos no lineales y fuera del equilibrio. En este sentido, hemos obtenido efectos imprevistos y sorprendentes cuando se aplica una fuerza periódica al sistema con control retroalimentado. Esta rocking ratchet retroalimentada ha revelado una dinámica rica que exhibe un régimen vibracional y efectos de tipo resonante. Además este sistema es también importante por sí mismo puesto que da el máximo flujo que se ha alcanzado en un dispositivo ratchet sin un sesgo a priori, tal y como hemos mostrado

anteriormente (capítulo 8).

Hemos resuelto otra cuestión importante, la viabilidad de implementar experimentalmente ratchets con protocolos de ciclo cerrado. Este es un punto crucial para realmente sacar partido de los beneficios en el rendimiento de las ratchets de control retroalimentado. En los dispositivos reales la medida del estado del sistema y la acción de control no son instantáneas. Por el contrario, siempre hay un retardo temporal debido a limitaciones físicas en la velocidad de transmisión y procesamiento de la información. Hemos estudiado los efectos de un retardo temporal en el mecanismo de control retroalimentado para mostrar que los protocolos de ciclo cerrado continuan mejorando a los de ciclo abierto para una y varias partículas siempre que los retardos sean menores que los tiempos característicos de la dinámica del sistema (capítulos 6 y 7). Hemos encontrado y explicado dos efectos adicionales sorprendentes relativos a la ratchet retroalimentada con retardo compuesta por muchas partículas. Primero, que la presencia de retardo puede aumentar el rendimiento sobre la ratchet retroalimentada sin retardo (capítulo 6), y segundo, se pueden inducir inversiones de corriente en las ratchet colectivas variando el retardo temporal cuando la asimetría del potencial ratchet y el protocolo con retroalimentación favorecen transportes en direcciones opuestas (capítulo 7). Además, la presencia del retardo lleva a la aparición de regímenes dinámicos con distintas soluciones cuasiperiódicas (multiestabilidad). Para muchas partículas y retardos grandes la dinámica del protocolo de maximización instantánea con retardo es similar a la dinámica de la solución para el protocolo de umbrales que tiene el mismo quasiperiodo característico.

Aparte de retardos temporales, en los dispositivos reales pueden aparecer otros ruidos. Hemos estudiado el rendimiento del sistema bajo la presencia de ruido en el mecanismo de retroalimentación (capítulos 9 y 10). Los resultados analíticos que hemos encontrado para el flujo han sido usados para comprobar la viabilidad de una realización experimental de las ratchets retroalimentadas antes de su implementación [10]. Recientemente se ha realizado experimentalmente una ratchet con control retroalimentado usando una trampa óptica [18]; los resultados de este experimento muestran un buen acuerdo con nuestros cálculos teóricos.

Para comprender completamente las ratchets de control retroalimentado es necesario un estudio específico centrado en lo que las distingue de sus análogas de ciclo abierto, es decir, el uso de la información. Para ello hemos calculado las relaciones entre la información recogida por el controlador por paso y el rendimiento de las flashing ratchets retroalimentadas (capítulos 9 y 10). Hemos obtenido estas relaciones para una ratchet con el protocolo de ciclo cerrado óptimo para una partícula y su generalización a varias partículas. Estas relaciones muestran que el aumento máximo que puede obtenerse en el flujo al pasar del protocolo de ciclo abierto óptimo a un protocolo de ciclo cerrado está acotado por una cantidad proporcional a la raíz cuadrada

de la información recibida en cada paso (capítulo 9). Por otra parte, hemos estimado que el aumento máximo que puede obtenerse en la potencia de salida tiene una cota superior proporcional a la información por paso (capítulo 10). Estas cotas nos indican las limitaciones en el aumento de rendimiento que hay dada una cantidad de información. Además, constituyen un ejemplo del tipo de relaciones que puede proporcionar una teoría general sobre las conexiones entre la información y el control retroalimentado.

También hemos comparado el rendimiento entre las ratchets colectivas con control retroalimentado compuestas por muchas partículas y sus versiones de ciclo abierto. Tanto para la ratchet retroalimentada con el protocolo de umbrales como para la ratchet retroalimentada con balanceo (rocking) hemos mostrado que sus flujos máximos tienden a valores constantes conforme aumenta el número de partículas N. Estos valores independientes de N coinciden con los valores máximos que se obtienen en las correspondientes ratchets de ciclo abierto, i.e., el protocolo periódico óptimo para el protocolo de umbrales, y la flashing ratchet con balanceo para la ratchet retroalimentada con balanceo. Ambas coincidencias se pueden entender teniendo en cuenta que los protocolos de ciclo cerrado considerados sólo usan un bit de información del sistema, lo que no es suficiente para obtener una ventaja significativa de la retroalimentación debido al gran número de grados de libertad para un gran número de partículas. Por lo tanto, estos protocolos con retroalimentación no pueden mejorar significativamente a sus análogos de ciclo abierto para un número elevado de partículas.

Hay escalas de tiempo características comunes para estas ratchets colectivas que dan lugar al mismo flujo máximo para el caso de muchas partículas. Para la flashing ratchet de ciclo abierto el flujo máximo se alcanza cuando el tiempo con el potencial apagado es del orden del tiempo característico que lleva difundir la distancia aL de la parte creciente del potencial, $\mathcal{T}_{\text{off}} \sim a^2L^2/(2D)$, y cuando el tiempo con el potencial encendido es del orden del tiempo característico que lleva deslizarse por la parte decreciente del potencial, $\mathcal{T}_{\text{on}} \sim \gamma(1-a)^2L^2/V_0$. Aquí a es el parámetro de asimetría del potencial ratchet, L es el periodo espacial, V_0 la altura del potencial, D el coeficiente de difusión y γ el coeficiente de fricción. Para el protocolo de ciclo cerrado de umbrales los umbrales óptimos en el caso de muchas partículas son aquellos que hacen que el potencial esté encendido típicamente un tiempo $\mathcal{T}_{\text{on}}$ y apagado típicamente un tiempo $\mathcal{T}_{\text{off}}$, lo que conduce a soluciones con un cuasiperiodo $\mathcal{T} = \mathcal{T}_{\text{on}} + \mathcal{T}_{\text{off}}$ (capítulo 5). Además, para el protocolo de maximización instantánea con retardo en el control observamos que para el régimen de muchas partículas el flujo máximo se obtiene para un retardo no nulo, y que el retardo óptimo es $\tau = \mathcal{T}$ que estabiliza una solución de cuasiperiodo $\mathcal{T}$ (capítulos 6 y 7). Tambien la frecuencia óptima de forzado en la ratchet retroalimentada con balanceo para muchas partículas resulta ser $\Omega = 2\pi/\mathcal{T}$, que consigue estabilizar soluciones de cuasiperiodo $\mathcal{T}$ (capítulo 8). Por lo tanto, estas escalas de tiempo, $\mathcal{T}_{\text{on}}$ y $\mathcal{T}_{\text{off}}$, son las escalas

de tiempo características de relajación y difusión de las ratchets colectivas con muchas partículas y determinan los valores óptimos para los parámetros de distintos protocolos.

Para ahondar en la relación entre información y rendimiento hemos estudiado sistemas con control retroalimentado generales (no sólo restringidos a flashing ratchets retroalimentadas); vid. capítulo 11. Los sistemas con control retroalimentado se diseñan habitualmente con la finalidad de incrementar el rendimiento del sistema por medio de la información sobre el estado del sistema recogida por el controlador. Por lo tanto, la cuestión natural que surge es cuánto se puede aumentar el rendimiento con una cierta cantidad de información, o dicho de otra forma, cuáles son los límites a este aumento del rendimiento. En última instancia, esta cuestión está relacionada con el establecimiento de la termodinámica de los sistemas con control retroalimentado. El caso de una sola operación del controlador se ha estudiado extensamente en el contexto de los demonios de Maxwell y en teoría de la computación [17], y las cantidades termodinámicas fundamentales se conocen bien. Sin embargo, el caso de operaciones repetidas presenta nuevos ingredientes, que nosotros hemos tratado en el capítulo 11. Para operaciones del controlador repetidas y que están descorrelacionadas, el sistema se comporta como si estuviese sujeto a una sucesión de operaciones independientes unas de otras y, por consiguiente, los resultados previos bien conocidos se pueden aplicar sin mayor dificultad. Sin embargo, para operaciones del controlador repetidas y que están correlacionadas aparecen nuevos puntos clave fundamentales que hemos discutido en detalle. Hemos mostrado que la reducción de entropía debida a la información viene dada por la información mutua entre el sistema y el estado del controlador condicionada a la historia pasada de la evolución del controlador. Este cálculo de la reducción de entropía era el ingrediente que faltaba para establecer la termodinámica de los sistemas con control retroalimentado. En particular, ello nos ha permitido calcular la eficiencia máxima de un sistema retroalimentado isotermo. Nuestros resultados allanan el camino para obtener las relaciones termodinámicas para otros sistemas con control retroaliementado, en particular para las ratchet brownianas retroalimentadas. Discutiremos éste y otros problemas abiertos en el capítulo 13.

En resumen, en esta tesis hemos resuelto cuestiones esenciales relativas a las ratchets brownianas retroalimentadas y a los sistemas generales con control retroalimentado. Hemos analizado la dinámica y el rendimiento de ratchet con control retroalimentado, y también cómo la presencia de ruidos y de retardos temporales puede afectarles. El uso de conceptos de teoría de la información nos ha permitido alcanzar una profunda comprensión de las ratchets y de sistemas más generales que son controlados con retroalimentación.

Bibliografía

[1] M. Feito and F. J. Cao, Phys. Rev. E **74**, 041109 (2006).

[2] M. Feito and F. J. Cao, Eur. Phys. J. B **59**, 63 (2007).

[3] M. Feito and F. J. Cao, Phys. Rev. E **76**, 061113 (2007).

[4] M. Feito and F. J. Cao, Physica A **387**, 4553 (2008).

[5] M. Feito and F. J. Cao, J. Stat. Mech. P01031 (2009).

[6] F. J. Cao, M. Feito, and H. Touchette, Physica A **388**, 113 (2009).

[7] F. J. Cao and M. Feito, Phys. Rev. E **79**, 041118 (2009).

[8] M. Feito, J. P. Baltanás, and F. J. Cao, *Rocking feedback ratchets*, arXiv:0902.3941 (2009).

[9] P. Reimann, Phys. Rep. **361**, 57 (2002).

[10] E.M. Craig, N.J. Kuwada, B.J. López, and H. Linke, Ann. Phys. **17**, 115 (2008).

[11] P. Hänggi and F. Marchesoni, Rev. Mod. Phys. **81**, 387 (2009).

[12] M. Bier, Biosystems **88**, 301 (2007).

[13] H. X. Zhou and Y. D. Chen, Phys. Rev. Lett., **77**, 194 (1996).

[14] R. D. Astumian and I. Derényi, Eur. Biophys. J **27**, 474 (1998).

[15] M. Álvarez-Pérez, S. M. Goldup, D. A. Leigh, and A. M. Z. Slawin, J. Am. Chem. Soc. **130**, 1836 (2008).

[16] J. Bechhoefer, Rev. Mod. Phys. **77**, 783 (2005).

[17] H. S. Leff and A. F. Rex (eds.), *Maxwell's Demon 2: Entropy, Classical and Quantum Information, Computing* (Institute of Physics, Bristol, 2003).

[18] B. J. López, N. J. Kuwada, E. M. Craig, B. R. Long, and H. Linke, Phys. Rev. Lett **101**, 220601 (2008).

Capítulo 13

Conclusiones y cuestiones abiertas

Esta tesis contiene nuestros resultados [1–8] sobre ratchets brownianas retroalimentadas y sistemas generales con control retroalimentado. En ella hemos alcanzado con éxito los objetivos propuestos y descritos en la sección 4.3.

El primer objetivo era investigar las ratchets retroalimentadas centrándonos en su capacidad para dar un mayor rendimiento que las ratchets de ciclo abierto. Para alcanzar este objetivo hemos propuesto y estudiado protocolos de control que presentan un incremento significativo en el flujo y la potencia de salida máxima. Estas ratchets de ciclo cerrado han revelado una dinámica rica con sorprendentes efectos tales como multiestabilidad, régimen vibracional, comportamientos de tipo resonante y otros efectos colectivos que conducen a un mejor entendimiento de los fenómenos no lineales y de fuera del equilibrio en física estadística.

El segundo objetivo de la tesis era dilucidar la viabilidad de dispositivos reales capaces de implementar ratchets retroalimentadas con un alto rendimiento. Hemos mostrado la viabilidad de estos dispositivos teniendo para ello en cuenta la presencia de retardos temporales y otros ruidos indeseados que pueden aparecer en un control realista. Nuestras predicciones se han visto confirmadas con la reciente realización experimental de una flashing ratchet con control retroalimentado por parte de un grupo experimental [9], lo que además ha verificado la ventaja en el rendimiento de las ratchets de ciclo cerrado sobre sus análogas de ciclo abierto.

Nuestro tercer objetivo era cuantificar el rendimiento de las ratchets retroalimentadas en términos de la información por paso usada en el control. Hemos logrado este propósito estableciendo expresiones explícitas para el flujo y la potencia máxima en función de la información. Nuestros resultados nos permiten comparar las ratchets de ciclo abierto y cerrado basándonos en la información, que es el punto clave que las diferencia.

Finalmente, hemos abordado el cuarto objetivo de investigar la termodinámica de sistemas generales retroalimentados computando la reducción de entropía alcanzable gracias a la información usada en el caso de que el controlador opere repetidamente sobre el sistema. Hemos mostrado de forma explícita cómo calcular esta reducción de entropía y, consiguientemente, cómo establecer la termodinámica de los sistemas con control retroalimentado.

El presente trabajo proporciona respuesta a cuestiones sobre la dinámica y el rendimiento de las ratchets brownianas retroalimentadas y de los sistemas generales con control retroalimentado, y aclara la relación de sus rendimientos y la termodinámica con magnitudes y conceptos de la teoría de la información. Sin embargo, quedan todavía por resolver algunas cuestiones que permanecen abiertas. Vamos a discutirlas.

Hemos visto que la introducción de políticas de retroalimentación adecuadas en flashing ratchets colectivas mejora el rendimiento del sistema para un número finito de partículas. En concreto, el protocolo de maximización

instantánea [10] es el protocolo óptimo para ratchets de una sola partícula, tal y como hemos demostrado en [5]. Sin embargo, esta estrategia 'avariciosa' no es óptima para la versión colectiva de la ratchet con $N > 1$ partículas. Hacemos notar aquí que en los llamados juegos pradójicos también se ha visto que esta clase de maximización a corto alcance no siempre es óptima [11, 12]. Por otra parte, en el límite de infinitas partículas no puede obtenerse ninguna ventaja sobre las estrategias de ciclo abierto. Nuestros resultados también muestran que el protocolo de umbrales [1, 13] con umbrales adecuados es óptimo para $N = 1$ y $N \to \infty$, y da valores altos del flujo para números intermedios de partículas. Es interesante señalar que una optimización exacta en el marco de un sistema discreto tipo ratchet ha revelado que el protocolo óptimo es de hecho una especie de operación de umbrales [12]. A pesar de los avances que representan estas respuestas parciales, el problema fundamental —cuál es el protocolo óptimo para una flashing ratchet colectiva retroalimentada— no se ha resuelto. No hay ningún estudio sistemático sobre la maximización del flujo en estos sistemas que use técnicas propias de la teoría de control óptimo como por ejemplo la versión estocástica del principio del máximo de Pontryagin o la programación dinámica de Bellman [14]. Por otra parte, subrayamos que añadiendo una perturbación externa a la flashing ratchet retroalimentada puede aumentarse el flujo del sistema, como ocurre, por ejemplo, cuando balanceamos una flashing ratchet retroalimentada con amplitud y frecuencia adecuadas [8]. Finalmente, apuntamos a que a día de hoy tampoco hay estudios sobre los efectos de inercia en ratchets con retroalimentación. Estas investigaciones ampliarían la comprensión de las ratchets con control retroalimentado.

Otras cuestiones abiertas conciernen al establecimiento de límitaciones al rendimiento de sistemas generales con control retroalimentado a la luz de la teoría de la información. Hemos estudiado sistemas con retroalimentación desde la perspectiva del sistema que es controlado, y hemos cuantificado la reducción de entropía máxima que se puede obtener con una actuación repetida del controlador retroalimentado [7]. Aunque hemos establecido de esta manera la termodinámica de los sitemas con control retroalimentado [7], vid. capítulo 11, hay aún cuestiones por resolver. Por ejemplo, las conexiones precisas entre estos resultados recientes y el enfoque basado en la complejidad algorítmica adoptado por Zurek [15, 16], que estudió la actuación repetida del controlador desde la perspectiva del sistema más el controlador. El enfoque de Zurek proporciona cuál es el mínimo coste energético para borrar un dispositivo de memoria que almacena las medidas procesadas por el controlador. Se expresa en términos de la complejidad algorítmica de la secuencia almacenada, que está relacionada con el espacio de memoria que ocuparía la secuencia una vez que ya ha sido comprimida de forma óptima. Este coste energético mínimo establece restricciones termodinámicas que conducen a la máxima reducción de entropía para el sistema. Otra cuestión abierta es la aplicación y extensión de nuestros resultados para encontrar limitaciones a

otras medidas del rendimiento de los sistemas con control retroalimentado.

La aplicación de los resultados del capítulo 11 a flashing ratchets retroalimentadas no se ha hecho todavía. Esto permitiría calcular la reducción máxima de entropía que se puede alcanzar en flashing ratchets con retroalimentación y establecer la termodinámica de estos sistemas relevantes tanto teórica como tecnológicamente. Previamente, en los capítulos 9 y 10, hemos encontrado cotas para el incremento del rendimiento —medido por el flujo [6] y la potencia de salida [2]— gracias a la información usada por el controlador. Estas relaciones se expresaron en función de la información por actuación. Sin embargo, como reexpresarlas en función de la cantidad total de información por unidad de tiempo, i.e., computando sólo la información no redundante por unidad de tiempo, sigue siendo una cuestión abierta. Esta reformulación es la clave para poner esos resultados en relación con los encontrados para la reducción de entropía en sistemas generales con control retroalimentado [7].

Para concluir, subrayamos que los sistemas con control retroalimentado, y específicamente las ratchet brownianas retroalimentadas, constituyen actualmente un campo con implicaciones notables para la estadística física fundamental y su relación con la teoría de la información, y también con aplicaciones en biología y nanotecnología. Nuestros resultados originales [1–8] profundizan en el conocimiento de estos sistemas y están despertando un interés creciente entre los físicos tanto teóricos como experimentales [9,17–28]. En esta tesis no sólo hemos resuelto cuestiones fundamentales en este campo, sino que además hemos planteado nuevos y apasionantes problemas abiertos que deseamos abordar en el futuro.

Bibliografía

[1] M. Feito and F. J. Cao, Phys. Rev. E **74**, 041109 (2006).

[2] M. Feito and F. J. Cao, Eur. Phys. J. B **59**, 63 (2007).

[3] M. Feito and F. J. Cao, Phys. Rev. E **76**, 061113 (2007).

[4] M. Feito and F. J. Cao, Physica A **387**, 4553 (2008).

[5] M. Feito and F. J. Cao, J. Stat. Mech. P01031 (2009).

[6] F. J. Cao, M. Feito, and H. Touchette, Physica A **388**, 113 (2009).

[7] F. J. Cao and M. Feito, Phys. Rev. E **79**, 041118 (2009).

[8] M. Feito, J. P. Baltanás, and F. J. Cao, *Rocking feedback ratchets*, arXiv:0902.3941 (2009).

[9] B. J. López, N. J. Kuwada, E. M. Craig, B. R. Long, and H. Linke, Phys. Rev. Lett **101**, 220601 (2008).

[10] F. J. Cao, L. Dinis, and J. M. R. Parrondo, Phys. Rev. Lett. **93**, 040603 (2004).

[11] L. Dinis and J. M. R. Parrondo, Europhys. Lett. **63**, 319 (2003).

[12] B. Cleuren and C. Van der Broeck, Phys. Rev. E **70**, 067104 (2004).

[13] L. Dinis, J. M. R. Parrondo, and F. J. Cao, Europhys. Lett. **71**, 536 (2005).

[14] J. Yong and X. Y. Zhou, *Stochastic Controls: Hamiltonian systems and HJB equations* (Springer, New York, 1999).

[15] W. H. Zurek, Phys. Rev. A **40**, 4731 (1989).

[16] W. H. Zurek, Nature **341**, 119 (1989).

[17] E.M. Craig, N.J. Kuwada, B.J. López, and H. Linke, Ann. Phys. **17**, 115 (2008).

[18] E. M. Craig, B. R. Long, J. M. R. Parrondo, and H. Linke, Europhys. Lett. **81**, 10002 (2008).

[19] W. Son, J. Ryu, D. Hwang, S. Lee, Y. Park, and C. Kim, Phys. Rev. E **77**, 066213 (2008).

[20] M. Santillán and M. C. Mackey, Phys. Rev. E **78**, 061122 (2008).

[21] J. Cai and D. Mei, Mod. Phys. Lett. B **22**, 2759 (2008).

[22] S. Guo, G. Feng, X. Liao, and Q. Liu, Chaos **18**, 043104 (2008).

[23] J. L. Mateos and F. L. Alatriste, Chaos **18**, 043125 (2008).

[24] T. Giao and J. Chen, J. Phys. A: Math. Theor. **42**, 065002 (2009).

[25] D. Henning, Phys. Rev. E **79**, 041114 (2009).

[26] D. Henning, L. Schimansky-Geier, and P. Hänggi, Phys. Rev. E **79**, 041117 (2009).

[27] S. Yanchuk and P. Perlikowski, Phys. Rev. E **79**, 046221 (2009).

[28] P. Hänggi and F. Marchesoni, Rev. Mod. Phys. **81**, 387 (2009).